TORSIONAL BEHAVIOUR OF SINGLE CELL BOX GIRDER BRIDGES

by

Adel R.M. Fam

Master of Engineering

July, 1969

Department of Civil Engineering
and
Applied Mechanics
McGill University
Montreal

TORSIONAL BEHAVIOUR OF SINGLE CELL BOX GIRDER BRIDGES

THESIS
submitted to the Faculty
of
Graduate Studies and Research

by
Adel R.M. Fam, B. Eng.,

In partial fulfilment of the requirements
for the degree of
Master of Engineering

July, 1969.

Department of Civil Engineering
and
Applied Mechanics
McGill University
Montreal

ABSTRACT

The effect of the parameters involved in the torsional analysis of box girder bridges is investigated in this thesis. The study is limited to single span orthotropic steel bridges, with one cell of rectangular shape. Several theoretical solutions are presented and discussed.

A suitably accurate finite element program is formulated for the analysis of box bridges. The program is developed by modifying an existing shell program. The modifications are focused on introducing the effect of artificial orthotropy and on automating the preparation of a large amount of the input information. Another program is developed to interpret the computer output automatically.

The programs are checked and used to study the torsional behaviour of several chosen bridge examples. The study is presented and discussed in such a way as to provide aids for bridge design. It demonstrates the importance of torsional bending stresses which have been ignored in the design.

ACKNOWLEDGEMENT

The writer wishes to express his gratitude to his director, Professor C.J. Turkstra, for his guidance and helpful suggestions given in the course of this work. He also wishes to express his deepest appreciation to Professor R.G. Redwood for his direction and comments in the pursuit of this investigation.

The advice of Dr. P.R. Taylor - Dominion Bridge Ltd., - who gave willingly of his time, the help of A.A. Mufti and B.L. Mehrotra are gratefully acknowledged.

The numerical results were obtained by using IBM 360-75 computer system of McGill University.

Financial support of this investigation was provided by The National Research Council of Canada, NRC Grant A-2786.

LIST OF CONTENTS

LIST OF TABLES

LIST OF FIGURES

NOTATIONS

Symbol	Meaning
A	Area enclosed by the center lines of the box walls.
A_x	Average depth of the stiffeners in x direction.
A_y	Average depth of the stiffeners in y direction.
B	Bending stiffness of a flat plate = $\frac{E \cdot f^3}{12(1-\nu^2)}$
B_x	$B + b_x$
B_y	$B + b_y$
B_{xy}	Torsional rigidity of the stiffeners in the x direction per unit length.
B_{yx}	Torsional rigidity of the stiffeners in the y direction per unit length.
b	Width of box girder.
b_x	Moment of inertia of the stiffeners within a unit length in the y direction about their centroidal axis.
b_y	Moment of inertia of the stiffeners within a unit length in the x direction about their centroidal axis.
$\underline{\bar{D}}$	Total elasticity matrix (including coupling terms) relating the resultant forces and strains.
D	$\frac{E}{1-\nu^2} \cdot f$
D_x	$D + E \cdot A_x$
D_y	$D + E \cdot A_y$
$\underline{\bar{D}}_b$	Direct bending elasticity submatrix in the $\underline{\bar{D}}$ matrix.
$\underline{\bar{D}}_p$	Direct in-plane elasticity submatrix in the $\underline{\bar{D}}$ matrix.
$\underline{\bar{D}}_{pb}$ $\underline{\bar{D}}_{bp}$	Coupling submatrices in the $\underline{\bar{D}}$ matrix.
$\underline{D}_b$	Elasticity matrix for bending stresses in the base program.

$\underline{D}_p$	Elasticity matrix for the in-plane stresses in the base program.
$\underline{\grave{D}}_p$	Modified elasticity matrix relating the in-plane stresses and strains.
$\underline{\hat{D}}_p$	In-plane elasticity matrix used in the modified program to develop the stiffness matrix of the element.
d	Depth of girder.
E	Young's modulus.
E_x	Young's modulus in the x direction (natural orthotropic sheet).
E_y	Young's modulus in the y direction (natural orthotropic sheet).
e	Load eccentricity.
e_x	Adjusted centroid in the x direction (orthotropic plate).
e_y	Adjusted centroid in the y direction (orthotropic plate).
e_x^*	Distance between centroid of stiffeners in the x direction and the middle of the deck plate.
e_y^*	Distance between centroid of the stiffeners in the y direction and the middle of the deck plate.
$\underline{F}$	Matrix of the resultant forces and moments.
$\underline{F}_p$	Matrix of in-plane forces.
$\underline{F}_b$	Matrix of bending moments.
f	Thickness of the plate in an orthotropic plate element.
f_1	Average thickness of the orthotropic plate in the x direction.
f_2	Average thickness of the orthotropic plate in the y direction.
f_x	Average thickness of the stiffeners in the x direction per unit length in the y direction.
f_y	Average thickness of the stiffeners in the y direction per unit length in the x direction.

G	Modulus of rigidity.
G_{xy}	Torsional stiffness of a natural orthotropic plate.
h	Normal distance from the center of twist to the tangent at a given point on the perimeter.
I	Moment of inertia of the section about the neutral axis.
J	Torsional constant of an eccentrically stiffened orthotropic plate.
K	Torsion parameter for $\grave{\sigma}_L = I/[A^2 (L/b)^{2/3}]$.
K_x	Curvature in the y direction.
K_y	Curvature in the x direction.
L	Beam length.
M	Twisting moment.
$\underline{M}$	Matrix for bending moments.
M_x	Total resultant bending moment about the y axis.
M_y	Total resultant bending moment about the x axis.
M_{xy}	Total resultant twisting moment.
m_x	Resultant moment about y axis due to a unit strain.
m_y	Resultant moment about x axis due to a unit strain.
m_{xy}	Resultant twisting moment due to a unit strain.
N_x	Total resultant axial force in the x direction.
N_y	Total resultant axial force in the y direction.
N_{xy}	Total shear force in the x-y plane.
n_x	Resultant axial force in x direction due to a unit strain.
n_y	Resultant axial force in y direction due to a unit strain.

n_{xy}	Resultant shearing force in the x-y plane due to a unit strain.
q	Shear flow at the point considered.
s	Tangential co-ordinate of a point along the circumference of a section.
t	Wall thickness.
u	Axial displacement of a point in a section in pure shear theory.
v	Tangential displacement of a point in a section in pure shear theory.
x	Co-ordinate of a point along the x axis.
y	Co-ordinate of a point along the y axis.
z	Co-ordinate of a point along the z axis.
Ω	Double the area enclosed by the centerline of thin-walled section.
ϕ	Angle of twist.
ϕ'	Rate of twist.
α	Shape ratio = width/depth.
ν	Poisson's ratio (isotropic sheet).
ν_x	Poisson's ratio in the x direction (natural orthotropic plate).
ν_y	Poisson's ratio in the y direction (natural orthotropic plate).
τ	Shear stress.
γ	Shear strain.
σ_w	Warping stress.
σ_B	Bending stress.
σ_{Bc}	Maximum axial stress of a beam in flexure due to concentrated load at midspan.
σ_{Bu}	Maximum axial stress of a beam in flexure due to uniformly distributed load.
σ_L'	Maximum longitudinal torsion bending stress due to line load of unit eccentricity.

σ_L	Maximum longitudinal torsion bending stress due to the loading in the studied examples.
σ_{Lm}	In-plane corner longitudinal torsion bending stress in an orthotropic plate.
σ_{Lp}	Total longitudinal corner stress at the outer fiber of the plate in an orthotropic plate.
σ_{Ls}	Total longitudinal corner stress at the free edge of the stiffener in an orthotropic plate.
$\hat{\sigma}_T$	Maximum transverse torsion bending stress due to line load of unit eccentricity.
σ_T	Maximum transverse torsion bending stress due to the loading in the studied examples.
σ_{Tm}	In-plane corner transverse torsion bending stress in an orthotropic plate.
σ_{Tp}	Total transverse corner stress at the outer fiber of the plate in an orthotropic plate.
σ_{Ts}	Total transverse corner stress at the free edge of the stiffener in an orthotropic plate.
σ_x	Axial stress in the x direction.
σ_y	Axial stress in the y direction.
σ_z	Axial stress in the z direction.
σ_{yb}	Bending stress at the corner in the y direction.
σ_{zb}	Bending stress at the corner in the z direction.
σ_{xb}	Bending stress at the corner in the x direction.
σ_o	Reference stress.
σ_{xm}	Membrane stress at the corner in the x direction.
ϵ_x	Axial strain in the x direction.
ϵ_y	Axial strain in the y direction.
ϵ_{xy}	Engineering shear strain.
$\underline{\epsilon}$	Matrix for the in-plane and bending strains.
$\underline{\epsilon}_p$	Matrix of in-plane strains.
$\underline{\epsilon}_b$	Matrix of bending strains.

δ_{ji}	Relative warping displacements of opposite sides of the slit in cell j due to unit shear flows in cell i.
δ_y	Corner displacement in the y direction of a box section due to torsion.
δ_{y_o}	The deformation δ_y at midspan.
δ_z	Corner displacement in the z direction due to torsion.

1. INTRODUCTION

1.1 GENERAL

During the past decade, the introduction of box girders in bridges has revolutionized the design of steel and reinforced concrete highway bridges. The development of this type of construction, and its practical application have received much attention in Europe - primarily in Germany - where there exists a large proportion of the total number of these bridges.

A box girder bridge (Fig. 1.1) consists of top and bottom flanges connected by webs to form a cellular structure. This structure may be formed by a single-cell or multi-cell units of rectangular or trapezoidal shapes. The bridge may be made entirely of reinforced concrete or of steel and in some box bridges the deck is made of reinforced concrete while the webs and bottom flange are of steel.

Due to the difficulty in understanding the actual behaviour of a box girder bridge, because of its high indeterminacy, and because of the very limited work that has been done on the subject, design methods are generally based on empirical methods.

In these methods a typical I shaped member, consisting of a web and top and bottom flanges, equal in width to the web spacing, is taken from the structure and is analyzed as an independent beam. The dead load for which such a beam is designed is its own dead weight, plus that portion of the deck carried by the beam, plus the weight of curbs, railings and wearing surface, divided by the number of beams supporting the deck. As for wheel loads placed on the bridge, empirical formulae based on the web spacing are used to determine the load distribution to the independent longitudinal beams. Beams are then designed to resist the maximum longitudinal and shear stresses developed due to all cases of loading.

One of the most important structural characteristics of box-shaped cross sections is its high torsional rigidity, which leads to nearly uniform transverse distribution of longitudinal flange stresses for eccentrically distributed loads.

An eccentric load can be replaced by a symmetrical pair which produces pure bending, and a skew symmetrical pair which produces twisting (Fig. 1.2). The degree of uniformity in transverse distribution of symmetrical loads, depends mainly on the phenomenon of shear lag; however, for skew symmetrical loads it depends also on the torsional deformation of the box which is characterized by:

(i) Distortion and rotation of the cross-section (Fig. 1.3a) which is resisted by frame action of the walls of the closed section and the diaphragms.

(ii) Warping deformation (Fig. 1.3b) which is mainly restrained by the supports.

A complex distribution of longitudinal and transverse stresses, which attain their maximum values at the corners, is introduced in the actual bridge girder due to the above mentioned deformations. Those which are shear stresses are added to the stresses calculated from the conventional methods of design, which neglect the effect of this deformation. Other stresses (secondary transverse and longitudinal stresses) are completely ignored in conventional design. Although the magnitude of these secondary stresses might be small in some cases, yet they are quite important in bridge design, as they undergo full reversal as lanes on alternate side of the bridge are loaded, and fatigue failure could occur at places where they have maximum values.

1.2 OBJECTIVE

The torsional deformation of the cross-section of box girder bridges depends upon many parameters, and the object of this investigation is to define such parameters and review the various methods available to study the behaviour of box girders under torsion. Another object of this work is to develop a suitably accurate finite element computer program capable of considering all the factors that play an important role in the behaviour of box girder bridges. Based upon the finite element method of analysis, a study is made to provide a clear view of the interaction between important parameters such as shape, length and end

conditions. The results are then presented in a way to provide design aids for box girder bridges.

1.3 SCOPE OF PRESENT INVESTIGATION

The box girders studied in this thesis are of a constant cross section. They are single span and composed of one cell of rectangular shape. The end conditions are either simply supported or fixed. Simply supported indicates that the section at the support is free to warp in the longitudinal direction but not free to rotate in its plane. A fixed end indicates that the section is not free to move or rotate in any direction. The diaphragms are always provided at the ends of the boxes and at midspan. Diaphragms are assumed very stiff in their plane and highly flexible in bending out of their plane. Only steel orthotropic bridges are considered in this investigation although any kind of bridge can be considered using the method of analysis presented.

The loading condition is one of uniformly distributed torsional line load applied at top and bottom corner nodes of the box section (Fig. 1.4). The study considers only elastic behaviour of box girder bridges. A summary of the cases considered is shown in Table I.

All the programming in this work was in FORTRAN IV language for use on an IBM 360-75 digital computer.

2. THE TORSION PROBLEM

2.1 INTRODUCTION

The exact solution of the torsion problem for a general case of a beam of non-uniform cross section and varying end conditions is not yet available in the literature. However, in 1856 a well known simple theory was developed by St. Venant for the special case of uniform twist of circular shafts. In this theory, the only stresses developed in the shaft are the pure shear stresses. Since that time, designers have thought that torsion problems can either be solved by St. Venant theory (pure shear), or, if they violated St. Venant assumptions, they had to look for a suitable theory to estimate the induced secondary or torsional bending stresses. However, in the latter case the designer might find it more convenient to redesign the structure to satisfy approximately the St. Venant assumptions and to convince himself that the only significant stresses were those of St. Venant pure shear stresses, and that the secondary stresses were small and could be safely neglected.

2.2 PURE TORSION

This section will be limited to an outline of the assumptions and conclusions of St. Venant's theory in relation to its application to thin walled closed sections.

Pure torsion takes place in beams with thin walled cross sections when the beam is twisted by end torques and the only stresses developed are the shear stresses on each transverse cross section. The shear is considered uniform over the thickness of the wall and the product of the shear stress and the thickness at every point is a constant called the shear flow.

In order to ensure pure torsion, certain assumptions must be made:

(i) Members are straight.

(ii) The cross section of the beam is constant.

(iii) The beam cross sections are stiffened by closely spaced rigid diaphragms to ensure that the cross sections do not distort in their plane.

(iv) Both ends of the beam are completely free to warp.

2.2.1 FORMULAS OF PURE TORSION IN THIN WALLED CLOSED SECTIONS

If the shear flow in a thin walled section (Fig. 2.1) is q and the twisting moment is M, using the above assumptions, it follows that

$$q = \tau \cdot t \qquad (2.1)$$

where τ = shear stress and t is the wall thickness.

By equilibrium conditions it can be shown that

$$M = \tau \cdot t \cdot \Omega \tag{2.2}$$

where Ω is double the area enclosed by the centerline of the wall.

The shear strain γ is given by

$$\gamma = \frac{\tau}{G} = \frac{\partial u}{\partial s} + \frac{\partial v}{\partial z} \tag{2.3}$$

where G is the modulus of rigidity, and u and v are the axial and tangential displacements respectively. From assumption (iii) above it follows that

$$v = h \cdot \Phi \tag{2.4}$$

where h is the distance from the center of twist to the tangent at the given point, and Φ is the angle of twist. It follows from equation (2.3) that

$$\frac{\partial u}{\partial s} = \frac{\tau}{G} - h \cdot \Phi' \tag{2.5}$$

where $\Phi' = \frac{\partial \Phi}{\partial z}$

Integrating (2.5) over the whole perimeter, it can be shown that

$$\Phi' = \frac{q}{G \cdot \tau} \cdot \int \frac{ds}{t} \tag{2.6}$$

2.2.2 MULTICELL THIN WALLED SECTION IN PURE TORSION

The above relations can be extended to the case of multi-

cell thin walled section. In this case, the problem is statically indeterminate of degree (n-1), where n is the number of cells. However, by following the same procedure as above for each cell and noting that the section does not distort in its plane, i.e., the angle of twist is the same for all cells, the following formulas can be derived:

From equilibrium condition

$$M = \sum_{j=1}^{n} q_j \cdot \Omega_j \tag{2.7}$$

And since ϕ' is the same for each cell, it follows that

$$\phi' = \frac{1}{G\Omega_j}\left[q_j \cdot \oint_{sj} \frac{ds}{t} - \sum_{r=1}^{m} \left(q_r \cdot \int_{sjr} \frac{ds}{t} \right) \right] \tag{2.8}$$

Where the subscript on the integral indicates the path over which the integration is to be performed, and m is the number of cells immediately adjacent to the cell j.

By introducing the concept of flexibility coefficients (Ref. 1) - which is the angle of twist of the cell due to unit shear flow - equation (2.8) can be written in a matrix form

$$\begin{bmatrix} \delta_{11} & \delta_{12} & \delta_{13} \cdots\cdots & \delta_{1n} \\ \delta_{21} & \delta_{22} \cdots\cdots\cdots & & \delta_{2n} \\ \delta_{n1} \cdots\cdots\cdots\cdots & & & \delta_{nn} \end{bmatrix} \begin{bmatrix} q_1 \\ q_2 \\ q_n \end{bmatrix} = \phi' \cdot \begin{bmatrix} \Omega_1 \\ \Omega_2 \\ \Omega_n \end{bmatrix} \tag{2.8a}$$

where $\delta_{ji} = -\frac{1}{G} \int_{sji} \frac{ds}{t}$ and $\delta_{jj} = \frac{1}{G} \cdot \oint_{sj} \frac{ds}{t}$

or $$[\delta]\{q\} = \phi' \cdot \{\Omega\} \qquad (2.8)b$$

and hence $$\{q\} = \phi'[\delta]^{-1}\{\Omega\} \qquad (2.9)$$

Equation (2.9) gives the shear flow q in each cell in terms of ϕ', and by substituting these values of q in equation (2.7) we get ϕ'. Substituting back in euqation (2.9) the shear flow and thence the shear stress in each cell can be obtained.

2.3 TORSION BENDING

The theory of St. Venant and its resulting formulas are perfectly valid only for a beam of circular cross section. However, within the scope of this investigation, it can be said that the application of the formulas of pure shear (Sec. 2.2) can be accepted only when one can practically ignore additional stresses caused by either warping or distortion of the cross section.

In many practical problems (box bridges, craneway girders, water gates) it becomes impossible to guarantee free warping or a constant shape for beam cross sections. In these cases equation (2.4) is not valid any more, and a complex distribution of longitudinal and transverse stresses are developed, and the application of St. Venant theory may lead to serious errors.

The presence of the longitudinal and transverse stresses infers that part of the work done by the twisting moment is used up in developing them, and only the remainder will develop shear stresses associated with St. Venant twist. Hence it can be

postulated that a total twisting moment is the sum of a pure St. Venant twist and some additional torsion causing bending, or rather, restrained warping of the section. This torsional part is known as torsion bending.

Several theories have been developed to estimate these torsional bending stresses. These theories will be described and discussed in the next Chapter.

3. REVIEW OF PREVIOUS WORK

3.1 INTRODUCTION

Many investigators during the past thirty years have attempted to develop a solution for the torsional bending problem. Since, at the beginning, the problem was frequently encountered in aircraft structures (wings and fuselages), most of the theoretical and experimental work that has been done was primarily for the specific purpose of the analysis of aircraft structures. In these investigations the procedure of the analysis was based on the assumption that due to the presence of transverse stiffeners or bulkheads, no transverse distortion of the beam cross section occurred. Hence the torsional bending stresses were caused mainly by warping restraints. These types of theories are described in the next section.

However, during the past decade, the development of box girders in bridge construction has rapidly increased and since, in general, a box girder bridge system does experience transverse distortion as well as warping restraints, the above mentioned

procedure cannot be used for this problem. Therefore, researchers started to investigate the problem for the case of boxes of deformable cross sections. However, owing to the high degree of indeterminacy of the problem and the mathematical difficulties involved, most of the theoretical solutions for the problem have been restricted by one or more conditions.

Recently, with the advent of fast digital computers with large storage capacity, some approaches which were theoretically established before and which required an enormous amount of computation have become practicable. These approaches, such as the finite difference method, folded plate method, finite element and others, might be considered in fact the most versatile of those presently available, since they can treat cases having a large range of variables.

In Section 3.3 a description of the work done on the problem with deformable cross sections will be presented with special emphasis on recent work applicable to bridge structures.

3.2 WORK DONE FOR NON-DEFORMABLE CROSS SECTIONS

Most of the work done on the problem of torsion bending of box beams with closely spaced rigid diaphragms has been done primarily for analysing aircraft structures. The first work in that field was done in 1934 by Ebner (Ref. 2) for the case of bisymmetrical box beams. A general solution for stiffened beams of arbitrary cross section was developed later, in 1938, by Ebner and Köller (Ref. 3). The main step in their analysis was in

idealizing the structure to consist of both longitudinal stiffeners which carry axial stresses only and connecting thin webs which carry shear stresses only.

The first attempt to develop a theory valid for arbitrary closed thin walled cross sections without the limitations of aircraft structures was developed by Umansky (Ref. 4) and by Karman and Christensen (Ref. 5). In both methods the effect of secondary shear on the shear strain distribution was neglected. They assumed an arbitrary rate of twist "ϕ'" existing along the span of the beam, and the distribution of shear and axial components of strain were then determined as a function of "ϕ'". These components were calculated according to pure torsion theory. After calculating the strains the stresses were obtained from fundamental stress-strain relations. Thence from the conditions of equilibrium of axial stresses the magnitude of the secondary shear could be obtained. A method was proposed which reduced the mathematical calculations to a sequence of graphical integrations, analogous to that used in dealing with transversely loaded beams. The results of carrying out calculations for four examples of open and closed sections with different loading and end conditions indicated the following:

(i) In closed sections, unlike open sections, the secondary shearing stresses are considerably greater than primary shearing stresses.

(ii) In the case of a cantilever beam with a concentrated torque at an intermediate point, the results showed that although there was no resulting torque in the overhanging part, normal and

shear stresses existed.

(iii) In the case of a beam with one end fixed and the other free to warp but not to rotate, and loaded by uniform torque along the span, the reaction moment at the fixed end was greater than the other end, while the elementary theory gives both the same.

Later, in 1946, Karman and Chien (Ref. 6) developed the first "exact" analysis for torsion of thin walled sections of uniform thickness. Their theory was based on two assumptions; first that the bending stiffness of the wall of the cross section could be neglected, and second that the deformation of any section was due to rigid rotation of the cross section plus warping displacement in the longitudinal direction. They developed a differential equation for the warping function and its solution in detail. The differential equation for the case of a polygonal section was reduced to the Laplace equation (valid at every point except the corners) together with some transition conditions at the corners. Karman and Chien proved that the secondary shear stress had an important effect on the stress distribution. This was demonstrated by the marked increase of axial stresses at the corners and at the fixed end of a doubly symmetrical cantilevered beam loaded by end torque. The torsional behaviour of this particular case was worked in detail and curves were drawn (Fig. 3.1) showing the rate of twist at various distances from the restrained end and for different sizes of rectangular thin walled section. It should be noted that the rate of twist "ϕ'" approaches a constant as the shape of the section approaches a square. Also curves were obtained (Fig. 3.2)

for different sizes of rectangular sections showing the circumferential distribution of axial stresses at the restrained end. In Fig. (3.3) the maximum stress, which was found to be at the corners, is plotted against various sizes of the rectangular thin walled section. Figures (3.2) and (3.3) show that the curvature of the stress distribution along the section increases rapidly near the corners especially for shallower sections, and that the maximum stresses decrease nonlinearly when the shape of the section approaches a square.

An exact solution for arbitrary section was given by Adadurov (Ref. 7) but no numerical results were obtained. Another exact analysis was given by Benscotter (Ref. 8).

Although the exact theories give satisfactory results providing their assumptions are valid, yet they require an extensive amount of computational work. Hence an approximate solution having sufficient accuracy for engineering design was desirable.

An approximate solution was developed by Umansky (Ref. 9) in his second paper on the problem of torsion bending. This was followed by an analogous solution by Benscotter (Ref. 10). Both approximate solutions were based on the assumption that the axial displacements leading to axial stresses had the same transverse distribution at a section of an arbitrary beam as would occur in St. Venant torsion of a uniform beam with that section. Another approximate solution of the problem, based on the same above assumption but furnishing a somewhat different degree of accuracy was presented by Dshanelidze and Panovko (Ref. 11). A similar

solution was given recently by Heilig (Ref. 12).

In 1963, Dabrowski (Ref. 13) suggested the use of these approximate theories in civil engineering design where the required accuracy of analysis is not as demanding as in aircraft engineering. He carried out a comparison between the two approximate theories, namely of Umansky (or Benscotter) and Panovko. The two theories were applied to find the maximum axial stress at the fixed end of a sufficiently long cantilever beam twisted by a torque at the free end. The beam had a rectangular cross section and was of uniform thickness. The results are shown in Fig. (3.4) for different width to depth ratios of the section. It can be seen that the first theory (Umansky) furnishes somewhat greater values of axial stresses, being on the safe side. It should be mentioned that both theories give zero axial stress for a square section. Also, another comparison has been carried out between the exact solution (Karman - Chien), the refined approximate (Umansky - Benscotter) and the ordinary approximate (Karman - Christensen) solutions. The same example mentioned before was used in the comparison. The results are shown in Fig. (3.5). It should be noted that both the exact and refined approximate solutions yield, as should be, zero stress for a square section whereas the ordinary approximate solution wrongly indicates a finite value. The latter also gives exaggerated values of axial stresses for a/b ratios up to 4, that is for most box sections in bridge structures. On the other hand, the refined approximate theory furnishes corner stresses below those of exact theory,

being on the unsafe side.

Using the formulas of the refined approximate theory derived by Dabrowsky for the values of the maximum torsion bending stress in an eccentrically loaded simply supported beam, the writer inspected the effect of shape ratio on the increase of axial stresses due to eccentricity of load on box girder bridges. The results presented in Figures (3.6) and (3.7) show the transverse influence lines of the maximum axial stress (σ_w) at midspan, for the cases of concentrated and uniformly distributed load. The stresses are made dimensionless by dividing by the bending stress (σ_{bu} or σ_{bc}) at midspan. The practical range of width to length ratios, for box girder bridges, has been chosen for the case of uniformly distributed load. It can be seen that the stress increase is greater in the case of concentrated load and for the worst practical conditions this increase may reach approximately 50%. However, the corresponding increase for uniformly distributed loads is about 20%.

3.3 WORK DONE FOR DEFORMABLE CROSS SECTION

A considerable body of the early literature was devoted to problems in aircraft field. The most important of this is the work of Reissner (Ref. 14) and Ebner (Ref. 15). The idealization mentioned in Section 3.2 for aircraft structures was also the basis of this work. Ebner showed how doubly symmetrical boxes could be solved by the method of influence coefficients (δ_{ik}). His method is based on the principle of virtual forces and is applicable to problems of two dimensional elasticity. Argyris

(Ref. 16) extended Ebner's work and developed a matrix formulation of the stiffness of the structure but it was based on the principle of virtual displacements or the total potential energy method. He was the first to use the finite element in a stiffness form for solving complex problems in aircraft structures.

The first work done to approach the requirements of bridge structures using the work of Ebner and Argyris was done by Resenger in 1959 (Ref. 17) and was extended by Richmond in 1966. Richmond in his first paper (Ref. 18) suggested an approximate solution for the problem of twisting of a simply supported rectangular box girder with no restraint against warping. Distortion was only prevented at end cross sections by end diaphragms, and was resisted by a continuous medium along the span. He assumed that deflections could be considered as a result of bending stresses in the separate walls, which could be computed by engineering bending theory. Another approximate solution by the displacement method was given in the same paper for the case of boxes with concentrated diaphragms. In this case the beam was divided into bays each containing two diaphragms. An expression was found for the displacements and the internal forces at any section in terms of the diaphragm displacements. Then, by satisfying the equilibrium conditions just before and after each diaphragm, a set of simultaneous equations was formed which when solved gave the unknown displacements of the diaphragms.

Richmond, in his second paper (Ref. 19) extended his work on rectangular sections to include trapezoidal sections and

presented numerical values for several simple box girders systems with different widths of bottom flange. Studying these examples, it was concluded that the top flange stresses could be significantly reduced by reducing the bottom flange width. It was also noticed that the torsion bending stresses decrease with the increase of the enclosed area and depend on the position and properties of the diaphragms.

Attention has been focused recently on the folded plate method as a convenient tool for analysing box girder bridges which have simple supports at the two ends, since a harmonic analysis using Fourier series can be used to analyze structures for both concentrated and distributed loads on the bridge. The bridge is treated as a series of rectangular plates interconnected along the longitudinal joints. In the formulation of the analysis, the properties of each plate can be obtained using either ordinary methods or elasticity methods.

The ordinary methods assume that the membrane stresses can be calculated by elementary beam theory and that plate bending is defined by means of transverse one-way slab action. This means that the following quantities are neglected: the longitudinal bending moment, the torsional moment in the plate elements, the transverse axial elongation and the in-plane shearing deformations of the plate elements. Examples of these ordinary methods are the theories of Wlassow (Ref. 20) and of Björklund (Ref. 21). A study of the accuracy of these theories is presented in Section 4.4.4.

The elasticity methods utilize plane stress elasticity theory and the classical two-way thin plate bending theory to determine the membrane stresses and slab moments in each plate. This means that all the quantities neglected in the ordinary methods are considered. However, these methods are restricted to a one span simply supported folded flat isotropic plates. The methods belonging to this group are presented by Goldberg and Leve (Ref. 22) and by De Fries and Scordelis (Ref. 23).

An approximate analysis based on an analogy with the theory of beams on elastic foundation was developed by Wright, Abdel-Samad and Robinson (Ref. 24) for multicell box girders of deformable cross section. A basic assumption in this method was that the distortions were accompanied by sufficient warping to annul the average shear strains in the plates forming the cross section. The method, however, provided an analytical procedure which accounted for deformation of the cross section, for the effects of rigid or deformable interior diaphragms, longitudinally and transversely stiffened plate elements, non-prismatic sections, continuity over intermediate supports and for arbitrary end support conditions.

Recently, Abdel-Samad (Ref. 25) extended Wlassow's theory to consider multicell composite box girders with intermediate diaphragms and with transverse or longitudinal stiffeners. Results were presented for different types of single cell box girders. A parameter study was given for a single cell square box with walls of uniform thickness and under uniform torsional load. Several multicell box girders under torsion loads were also presented.

The effect of introducing diaphragms was studied extensively. The number and location of diaphragms were varied and the effect of their stiffnesses was investigated. The following are the most important results and conclusions that can be extracted from this study to serve the present investigation:

(i) The intermediate diaphragms are effective in reducing stresses and deflections. The results of the study made on the effect of diaphragm location on the longitudinal stress (σ_L) and transverse stress (σ_T) at midspan of a simply supported girder under uniform and concentrated torsional load at midspan are presented by the writer in Fig. (3.8). The terms σ_{BC} and σ_{BU} indicate the maximum axial stresses produced by the two equal midspan concentrated loads and two equal uniform line load at the edges of the box respectively. It can be seen that the stresses decrease as the nearest diaphragm approaches the load. A diaphragm located below the load reduces the distortion stresses almost to zero. Also, for the case of uniform torsional load, two diaphragms at third points reduce stresses and deflections to small values.

(ii) For the same girder mentioned above (but with diaphragms only at the ends) a study was made to investigate the effect of loading and end conditions on the maximum longitudinal and transverse stresses. The study is presented by the writer in Figures (3.9) and (3.10). In the case of a concentrated load it can be seen that end fixity does influence the response quantities when the load is near the end, and the longitudinal axial stresses produced at the end become higher as the load approaches the end. The end stresses must, of course, drop to zero when the load is at

the end. The transverse bending stresses are decreased for loads close to the ends.

(iii) The stiffening action of diaphragms is insensitive to practical variations in the stiffness of the diaphragms.

4. FINITE ELEMENT ANALYSIS

After reviewing the various methods available for studying torsional behaviour of box girders, and noting the restrictions made upon each method by the nature of the problem in box girder bridges, it was concluded that one should seek a solution by a method which takes into consideration the effect of torsional bending, shear lag and end restraints. The actual rib spacing and rib stiffnesses should also be accounted for in a realistic fashion. It is also desirable to avoid the assumption of closely spaced rigid diaphragms and to consider the variation of dimensions and materials of the bridge elements.

This is indeed a sizable task; however, the great development in the finite element method and modern high speed digital computers, offer considerable hope that these objectives can be maintained all at the same time with a considerable amount of accuracy.

4.1 INTRODUCTION TO FINITE ELEMENT TECHNIQUE

Many researchers have contributed to the development of

the finite element technique in structural analysis. This is evidenced by the extensive bibliographies on the subject given elsewhere (Ref. 26), (Ref. 27), (Ref. 28). Briefly this method can be applied to the analysis of any structure by means of the following four phases:

(i) Structure idealization by replacing the structure by an assemblage of individual structural elements connected to each other at selected nodal points.

(ii) Representation of the elastic and geometric properties by evaluating the stiffness properties of the individual elements. The stiffness properties of the complete assemblage are then derived by superposition of those element stiffnesses.

(iii) Imposing the desired support conditions, by making the proper changes to the corresponding rows and columns of the structure stiffness matrix.

(iv) Representation of the loading characteristic of the structure in a matrix form; then by applying matrix algebra to the stiffness matrix, all the components of the nodal displacements and thence stresses in the elements can be obtained.

The above topics are discussed in the following Sections with reference to the analysis of box girder bridges as three dimensional structures.

4.2 THE STRUCTURE AND ITS SIMULATION

Two approaches have been tried by the writer to simulate box girder bridges:

4.2.1 EQUIVALENT GRIDWORK AND PLANE STRESS TRIANGULAR ELEMENT

In this approach the structure was considered as a three dimensional frame of one dimensional beam members connected together at nodal points so as to provide all six degrees of freedom, and three nodal point, triangular, plane stress finite elements were introduced as an extra constraint between the nodal points (Fig. 4.1). The beam members were assigned an axial stiffness to simulate the axial stiffness of the stiffeners in the beam direction. They also were assigned bending and torsional stiffnesses of the stiffeners plus that of the two dimensional plate elements. The triangular plate element was assigned six degrees of freedom, two at each nodal point in the plane of the element.

The computer program developed by A.J. Carr (Ref. 29) was used for the above idealization.

4.2.2 EQUIVALENT ORTHOTROPIC PLATE

In this method each wall of the box was subdivided into a number of discrete finite orthotropic triangular elements interconnected at nodal points (Fig. 4.2). Six degrees of freedom were provided at each nodal point. The orthotropic plate elements were assigned membrane and bending stiffness to simulate the axial and bending stiffness of the plate with the stiffeners placed in two orthogonal directions and on one side of the plate.

It was later decided to base the study of this investigation

on the second method of idealization, Sec. 4.2.2, and to use the program developed by B.L. Mehrotra and A.A. Mufti (Ref. 30). Modifications were necessary to account for the artificial orthotropy and additional programs were developed to provide automatic preparation of data and automatic analysis of results for the specific type of box girder bridges considered in this thesis.

4.3 COMPUTER PROGRAM

4.3.1 INTRODUCTION

The three dimensional plate structure program developed in Reference (30) in 1968 was the base upon which the writer built up the program for analysing single cell orthotropic box girder bridges. Since that time the base program has been used in the investigation of the behaviour of many different and diverse structures. The results have been compared in many cases to other finite element programs in relation to exact or experimental values. Perhaps the most interesting case considered in checking the base program was that of the analysis of an isotropic spine bridge. In this case, a comparison was made with another finite element program together with experimental results, and the results presented in Ref. (31) show very good agreement. In conclusion, the testing of the base program in the analysis of two dimensional and three dimensional structures has proved the reliability of such a program especially in cases of three dimensional structures where the membrane stresses dominate. Further verifications

related to the type of problem considered herein and also designed to test the modification are described later.

In developing the final program, the policy of the writer was first, to account for the variables introduced in the analysis in a realistic manner and second, to reduce to a minimum the effort in using the program for solving a particular problem. Also it was kept in mind that the new programming logic should be independent from the base program whenever possible, the reason for this was to facilitate locating the errors in the process of debugging the program, and to make it possible to use the program for any other particular structure by making relatively simple alterations.

The usefulness of the base program was limited to structural elements of isotropic or of natural orthotropic materials. However, that is not the case in steel orthotropic bridges. Therefore, assumptions have been made in the next section to idealize the structural behaviour of an orthotropic plate element of the bridges. The relation between stress and strain is summed up in a matrix form called the elasticity matrix. According to the above mentioned assumptions, the elasticity matrix used in the base program has been replaced by a new one which is described in Section 4.4.4 and which is based on the study presented in Section 4.4.3. Consequently, a few modifications were necessary in the stress and strain matrices of the base program since the stresses and strains, which the writer was concerned with, are those of the top of the plate and of the bottom fiber of the stiffeners. These modifications are

described in Sections 4.3.4.1 and 4.3.4.2.

As in any finite element program, a huge amount of information needs to be supplied by data cards. The amount of time and effort in preparing such data, and the probable human error and consequently the significant loss in computer time, may certainly be considered as a disadvantage which may outweigh the advantages of such a powerful method of analysis. Therefore, it was found necessary to write several programs to reduce this number of data cards. These programs are described in detail in Sections 4.3.6 and 4.3.7.

It was also expected that if all the interpretation was done by hand for such a large amount of output of the computer analysis, then a considerable amount of time and effort would be needed. Also the accuracy of the results would be questionable, and the extrapolation of the stresses at points other than those obtained by the program would be somewhat arbitrary. Therefore an interpretation program has been developed for the particular case of box girders considered in this investigation. An explanation of this program can be found in Section 4.3.8.

All the above programs, except the interpretation program, have been integrated with the main modified program after being tested separately. A check has been made to assure the functioning of the integrated programs through the total program.

A plan for testing the accuracy of the final program

has been developed so that it can be used with confidence in the analysis of box girder bridges. This plan is described in Section 4.4.

A detailed description of the final programs and the method of using them and their limitations can be found in Ref. (32.).

4.3.2 ASSUMPTIONS

The structural system of steel box girder bridges is composed of plates with stiffeners placed at one side in both longitudinal and transverse directions. This is commonly described as an orthotropic plate with eccentric stiffeners. A typical orthotropic plate element with eccentric stiffeners is shown in Fig. (4.3). The equations governing the behaviour of an orthotropic plate in this finite element program are based on the following assumptions:

(i) The orthotropic plate acts as a monolitic unit, i.e., there is no relative movement between the deck plate and the stiffeners.

(ii) Within an element, the stiffeners are equally and closely spaced in each direction. They are orthogonal and they consist of uniform cross section with weak torsional resistance.

(iii) The deck plate is of constant thickness over each element and has the same isotropic elastic material of the stiffeners.

(iv) The horizontal strain in case of bending is zero at the adjusted centroid of the cross section in each direction.

The adjusted centroids in the x and y directions are located at distances e_x and e_y respectively, below the middle surface of the deck plate.

From the above it follows that the adjusted centroids can be defined as follows:

$$e_x = \frac{1}{D_x} \int E(z) \cdot z \cdot dA_x$$

$$= \frac{e_x^* \cdot A_x}{A_x + \frac{f}{(1 - \nu^2)}} \qquad (4.1)$$

$$e_y = \frac{1}{D_y} \int E(z) \cdot z \cdot dA_y$$

$$= \frac{e_y^* \cdot A_y}{A_y + \frac{f}{(1 - \nu^2)}} \qquad (4.2)$$

where:

$D_x = D + E \cdot A_x$

$D_y = D + E \cdot A_y$

$D = \frac{E}{1 - \nu^2} \cdot f$

e_x^* = distance between centroid of stiffeners in the x direction and middle of the deck plate.

e_y^* = distance between centroid of the stiffeners in the y direction and middle of the deck plate.

f = thickness of the deck plate.

A_x = average depth of the stiffeners in x direction.

A_y = average depth of the stiffeners in y direction.

E = modulus of elasticity.

ν = poisson's ratio.

(v) Plane surfaces initially perpendicular to the middle surface of the deck plate remain plane and perpendicular to the middle surface during bending.

(vi) The torsional stiffness of the stiffener may be estimated by neglecting any restraint due to warping.

(vii) The angle of twist per unit length of the stiffener is the same as the middle surface of the plate.

4.3.3 ANALYSIS OF ORTHOTROPIC PLATE ELEMENT WITH ECCENTRIC STIFFENERS

Based on the assumptions in section 4.3.2 the writer was able to make use of the method of effective stiffness developed by E. Giencke (Ref. 33) and which was introduced later in a modified form by Klöppel (Ref. 34). The method is more effective in the case of orthotropic plates with torsionally soft stiffeners.

In this method, a unit strain is applied to the orthotropic plate element along one of the six degrees of freedom. The resulting forces and moments corresponding to each of the six degrees of freedom are obtained based on the assumptions given in section 4.3.2. This procedure is repeated for each of the 6 degrees of freedom. The behaviour of the orthotropic plate in each of these cases is fully explained by Figures 4.4 through 4.9.

The following terms will appear in the derivation of the final expression for the elasticity matrix, and they are defined at this stage for convenience.

$$D = \frac{E}{1-\nu^2} \cdot f$$

$$D_x = D + E \cdot A_x$$

$$D_y = D + E \cdot A_y$$

$$B = \frac{E \cdot f^3}{12\,(1-\nu^2)}$$

b_x = moment of inertia of the stiffeners within a unit length in the y direction about their centroidal axis.

b_y = moment of inertia of the stiffeners within a unit length in the x direction about their centroidal axis.

$$B_x = B + E \cdot b_x$$

$$B_y = B + E \cdot b_y$$

$$B_{xy} = \frac{1}{6} \int Gt^2 \, df_x$$

= torsional rigidity of the stiffeners in the x direction per unit length.

$$B_{yx} = \frac{1}{6} \int Gt^2 \, df_y$$

= torsional rigidity of the stiffeners in the y direction per unit length.

n_x = resultant axial force in x direction.

n_y = resultant axial force in y direction.

n_{xy} = resultant shearing force.

m_x = resultant moment about y axis.

m_y = resultant moment about x axis.

m_{xy} = resultant twisting moment.

The moments are assumed to be applied at their adjusted centroids.

The cases discussed will now be individually studied.

(i) For the axial strain in the x direction $\epsilon_x = 1$ (Fig. 4.4) the forces and moments are:

$$n_x = \int \sigma_x \cdot dA_x = D_x$$

$$n_y = \int \sigma_y \cdot dA_y = \nu \cdot D$$

$$n_{xy} = 0$$

$$m_x = \int \sigma_y \cdot z \cdot dA_y = -\nu \cdot e_y \cdot D$$

$$m_y = \int \sigma_x \cdot z \cdot dA_x = 0$$

$$m_{xy} = 0$$

(ii) For the axial strain in the y direction $\epsilon_y = 1$ (Fig. 4.5) we similarly obtain:

$$n_x = \nu \cdot D \qquad m_x = 0$$

$$n_y = D_y \qquad m_y = -\nu \cdot e_x \cdot D$$

$$n_{xy} = 0 \qquad m_{xy} = 0$$

(iii) For the shear strain in the x, y plane $\epsilon_{xy} = 1$ we obtain the following forces and moments. Note that the stiffeners do not resist any shear stresses since their bending stiffness about vertical planes is very small. Accordingly we get the distribution of stresses shown in the fig. (4.6).

$n_x = 0$ $\qquad$ $m_x = 0$

$n_y = 0$ $\qquad$ $m_y = 0$

$n_{xy} = \frac{D}{2}(1-\nu)$ $\qquad$ $m_{xy} = (1-\nu)(e_x + e_y) \cdot D$

(iv) For the curvature $k_x = -\frac{\delta^2 w}{\delta y^2} = 1$ (Fig. 4.7)

$n_x = \nu \cdot e_y \cdot D$ $\qquad$ $m_x = B_y$

$n_y = 0$ $\qquad$ $m_y = \nu \cdot (e_x \cdot e_y \cdot D + B)$

$n_{xy} = 0$ $\qquad$ $m_{xy} = 0$

(v) For the curvature $k_y = -\frac{\delta^2 w}{\delta x^2} = 1$ (Fig. 4.8)

$n_x = 0$ $\qquad$ $m_x = \nu\ (e_x \cdot e_y \cdot D + B)$

$n_y = \nu \cdot e_x \cdot D$ $\qquad$ $m_y = B_x$

$n_{xy} = 0$ $\qquad$ $m_{xy} = 0$

(vi) The torsional strain is defined in the elasticity matrix by $2\frac{\delta^2 w}{\delta x \delta y}$

For $2\frac{\delta^2 w}{\delta x \delta y} = 1$ (Fig. 4.9) we get

$n_x = 0$ $\qquad$ $m_x = 0$

$n_y = 0$ $\qquad$ $m_y = 0$

$$n_{xy} = -(1-\nu)(e_x+e_y)\frac{D}{4} \qquad m_{xy} = -\tfrac{1}{2}(B_{xy}+B_{yx})-B(1-\nu) - \frac{D}{4}(1-\nu)(e_x+e_y)^2$$

The previous relations between strains and resultant forces can be summed up into the following matrices:

$$\left\{F\right\} = \left[\bar{D}\right] \left\{\epsilon\right\} \tag{4.3}$$

where

$\underline{F}$ is the matrix representing the resultant forces and moments, $\underline{\bar{D}}$ is the elasticity matrix and $\underline{\epsilon}$ is the strain matrix. These matrices can be divided into submatrices to separate the terms corresponding to in-plane and out-of-plane deformations, and equation (4.3) will have the form

$$\begin{Bmatrix} \underline{F}_p \\ F_b \end{Bmatrix} = \left[\begin{array}{c:c} \underline{\bar{D}}_p & \underline{\bar{D}}_{pb} \\ \hdashline \underline{\bar{D}}_{bp} & \underline{\bar{D}}_b \end{array}\right] \begin{Bmatrix} \underline{\epsilon}_p \\ \epsilon_b \end{Bmatrix} \tag{4.4}$$

a subscript "p" indicates plane and a subscript "b" indicates bending. Equation (4.4) is shown below in detail.

$$
\begin{bmatrix} N_x \\ N_y \\ N_{xy} \\ \hline M_x \\ M_y \\ M_{xy} \end{bmatrix}
=
\left[\begin{array}{ccc:ccc}
D_x & \nu \cdot D & 0 & \nu \cdot e_y \cdot D & 0 & 0 \\
\nu \cdot D & D_y & 0 & 0 & \nu \cdot e_x \cdot D & 0 \\
0 & 0 & (1-\nu)\frac{D}{2} & 0 & 0 & -(1-\nu)(e_x+e_y)\frac{D}{4} \\
\hdashline
-\nu \cdot e_y \cdot D & 0 & 0 & B_y & \nu(e_x \cdot e_y \cdot D+B) & 0 \\
0 & -\nu \cdot e_x \cdot D & 0 & \nu(e_x \cdot e_y \cdot D+B) & B_x & 0 \\
0 & 0 & (1-\nu)(e_x+e_y)D & 0 & 0 & \begin{array}{l} -\frac{D}{4}(1-\nu)(e_x+e_y)^2 \\ -(1-\nu) \cdot B \\ -\frac{1}{2}(B_{xy}+B_{yx}) \end{array}
\end{array}\right]
\begin{bmatrix} \epsilon_x \\ \epsilon_y \\ \epsilon_{xy} \\ \hline -\frac{\partial^2 w}{\partial y^2} \\ -\frac{\partial^2 w}{\partial x^2} \\ 2\frac{\partial^2 w}{\partial x \partial y} \end{bmatrix}
$$

DETAILS OF EQUATION (4.4)

4.3.4 MODIFICATIONS INTRODUCED IN THE BASE PROGRAM

The elasticity matrices used in the base program were for an isotropic or natural orthotropic plate element. These matrices should be replaced by the elasticity matrix ($\bar{\underline{D}}$) derived in the preceding section.

The base program was built up by combining a plane stress program and a bending stress program. In formulating the overall structure stiffness matrix the logic was as follows:

(i) The 3x3 elasticity matrix $\underline{D}_b$ was developed for each element and then used in forming the strain, stress and stiffness matrices for the element in bending.

(ii) The 3x3 elasticity matrix $\underline{D}_p$ was developed for each element and then used in forming the strain, stress and stiffness matrices for the element in plane stress.

(iii) The bending and plane stress stiffness matrices were joined together later in formulation of the overall structure stiffness matrix.

The introduction of the 9x9 elasticity matrix ($\bar{\underline{D}}$) derived in sec. 4.3.3 infers that a change should be made in the method of formulating the element stiffness matrix. Such a change implies modifications in the size of matrices and in the "DO" loops used in the program. This inherently means a major change in the whole logic of programming.

In view of the above explanation, it was decided to neglect the coupling terms in the submatrices $\bar{\underline{D}}_{pb}$ and $\bar{\underline{D}}_{bp}$ of the 9x9 elasticity matrix ($\bar{\underline{D}}$), and to consider only the terms

in the direct plane and bending submatrices $\underline{\bar{D}}_p$ and $\underline{\bar{D}}_b$ respectively. The terms in these direct plane and bending submatrices have been used to replace the corresponding terms in the elasticity matrices of the plane stress and bending stress parts of the base program respectively. The writer found that although the coupling terms in the submatrices $\underline{\bar{D}}_{pb}$ and $\underline{\bar{D}}_{bp}$ have been neglected, a relatively high degree of accuracy can be obtained by using the program. This will be seen later in Section 4.4.

4.3.4.1 ELASTICITY MATRIX FOR IN-PLANE STRESSES

The elasticity matrix used in the base program for the plane stress part relates the stress to the strain in the plane of the plate. However, the derived elasticity matrix $\underline{\bar{D}}_p$ relates the resultant in-plane forces to the in-plane strains. The function of the elasticity matrix in the two cases is shown below for convenience.

(i) In the base program

$$\begin{bmatrix} \sigma_x \\ \sigma_y \\ \tau_{xy} \end{bmatrix} = \begin{bmatrix} \frac{E_x}{1-\nu_x\nu_y} & \frac{\nu_y \cdot E_x}{1-\nu_x\nu_y} & 0 \\ \frac{\nu_x \cdot E_y}{1-\nu_x\nu_y} & \frac{E_y}{1-\nu_x\nu_y} & 0 \\ 0 & 0 & G \end{bmatrix} \begin{bmatrix} \epsilon_x \\ \epsilon_y \\ \epsilon_{xy} \end{bmatrix} \qquad (4.5)$$

or $\underline{\sigma} = \underline{D}_p \cdot \underline{\epsilon}_p$

where E_x, E_y, ν_x, ν_y, G are the elastic constants of the orthotropic material.

(ii) In the developed elasticity matrix

$$\begin{bmatrix} N_x \\ N_y \\ N_{xy} \end{bmatrix} = \begin{bmatrix} D_x & \nu \cdot D & 0 \\ \nu \cdot D & D_y & 0 \\ 0 & 0 & \frac{(1-\nu)}{2} D \end{bmatrix} \begin{bmatrix} \epsilon_x \\ \epsilon_y \\ \epsilon_{xy} \end{bmatrix} \quad (4.6)$$

or $\underline{F}_p = \underline{\overline{D}}_p \cdot \underline{\epsilon}_p$ (4.6)a

It follows from assumption (ii) section 4.3.2 that the average axial stress in the x or the y direction is equal to the resultant force in that direction divided by the sum of the area of the plate and the stiffeners in the perpendicular direction. It can also be concluded that the plate is carrying all the in-plane shear forces. Hence, the relation between the stresses and strains can be obtained by modifying the $\underline{\overline{D}}_p$ matrix to $\underline{\grave{D}}_p$ and we get

$$\underline{\sigma} = \underline{\grave{D}}_p \cdot \underline{\epsilon}_p \quad (4.7)$$

or

$$\begin{bmatrix} \sigma_x \\ \sigma_y \\ \tau_{xy} \end{bmatrix} = \begin{bmatrix} \frac{D_x}{f_1} & \frac{\nu \cdot D}{f_1} & 0 \\ \frac{\nu \cdot D}{f_2} & \frac{D_y}{f_2} & 0 \\ 0 & 0 & \frac{(1-\nu)}{2} \cdot \frac{D}{f} \end{bmatrix} \begin{bmatrix} \epsilon_x \\ \epsilon_y \\ \epsilon_{xy} \end{bmatrix} \quad (4.7)a$$

where:

f_1 = average thickness of the plate and the stiffeners in the x direction per unit length in the y direction

$= f + f_x$

f_x = average thickness of the stiffeners in the x direction per unit length in the y direction.

f_2 = average thickness of the plate and the stiffeners in the y direction per unit length in the x direction

$= f + f_y$

f_y = average thickness of the stiffeners in the y direction per unit length in the x direction.

However, in the calculation of the strain energy in the process of deriving the stiffness matrix, the resultant forces were obtained in the base program by simply multiplying the stress vector by a multiplier equal to the thickness of the orthotropic plate. Since this is not the same in artificial orthotropic plates, as can be seen from equations (4.6) and (4.7)a, the writer introduced an imaginary thickness equal to f_1 to be used as a multiplier. Accordingly, the elasticity matrix which was used in deriving the stiffness matrix of the element, was given the imaginary form:

$$\underline{D}''_p = \begin{bmatrix} \frac{D_x}{f_1} & \frac{\nu \cdot D}{f_1} & 0 \\ \frac{\nu \cdot D}{f_1} & \frac{D_y}{f_1} & 0 \\ 0 & 0 & \frac{(1-\nu)\ D}{2\ f_1} \end{bmatrix} \qquad (4.8)$$

In order to obtain the stresses, the method used in the base program was simply to post multiply the elasticity matrix by the final strain vector ϵ_x, ϵ_y, ϵ_{xy} . However when this was adopted on the above matrix ($\underline{D}''_p$) the stresses obtained σ_x, σ_y,

τ_{xy} have to be multiplied by the factors 1, f_1/f_2 and f_1/f respectively in order to obtain the real stresses. This modification has been introduced in the stress matrix of the subroutine "FEMP" of the base program.

4.3.4.2 ELASTICITY MATRIX FOR BENDING STRESSES

The elasticity matrix in the base program relates the moments and curvatures as follows:

$$\begin{bmatrix} M_x \\ M_y \\ M_{xy} \end{bmatrix} = \begin{bmatrix} \frac{E_x \cdot f^3}{12(1-\nu_x \nu_y)} & \frac{\nu_y \cdot E_x \cdot f^3}{12(1-\nu_x \nu_y)} & 0 \\ \frac{\nu_x \cdot E_y \cdot f^3}{12(1-\nu_x \nu_y)} & \frac{E_y \cdot f^3}{12(1-\nu_x \nu_y)} & 0 \\ 0 & 0 & -\frac{G f^3}{6} \end{bmatrix} \begin{bmatrix} -\frac{\partial^2 w}{\partial x^2} \\ -\frac{\partial^2 w}{\partial y^2} \\ 2\frac{\partial^2 w}{\partial x \partial y} \end{bmatrix} \qquad (4.9)$$

or $\underline{M} = \underline{D}_b \cdot \underline{\epsilon}_b \qquad (4.9)a$

There was no difficulty in replacing the above matrix $\underline{D}_b$ by the new derived matrix $\underline{\bar{D}}_b$.

As for the normal stresses and strains due to bending, the writer was interested, within the scope of this investigation, in their values at the top of the plate and at the free edge of the stiffeners. On the other hand, the shear stresses and strains were only significant, as far as the study of the overall torsional behaviour is concerned, in the plate and not in

the stiffeners. Therefore, the shear stresses were calculated in the bending part of the program at the top of the plate only.

The strains have been assumed equal to zero at the adjusted centroids in the x and y directions. They are also assumed to vary linearly across the depth of the orthotropic plate. Thus the normal strains ϵ_x, ϵ_y, could be described in terms of the calculated curvatures $\frac{\delta^2 w}{\delta x^2}$ and $\frac{\delta^2 w}{\delta y^2}$ and of the distance z of the point considered from the adjusted centroid.

$$\epsilon_x = z \cdot \frac{\delta^2 w}{\delta x^2} \tag{4.10}$$

$$\epsilon_y = z \cdot \frac{\delta^2 w}{\delta y^2} \tag{4.11}$$

Similarly the normal stresses can be found in terms of the obtained resultant internal moments per unit length, and the bending stiffness of the plate and the stiffeners.

For stresses in the plate

$$\sigma_x = \frac{E}{1-\nu^2} \cdot z \cdot \frac{M_x}{B_y} \tag{4.12}$$

$$\sigma_y = \frac{E}{1-\nu^2} \cdot z \cdot \frac{M_y}{B_x} \tag{4.13}$$

For stresses in the stiffeners

$$\sigma_x = E \cdot z \cdot \frac{M_x}{B_y} \tag{4.14}$$

$$\sigma_y = E \cdot z \cdot \frac{M_y}{B_x} \tag{4.15}$$

The shear strain ϵ_{xy} at top of the plate is

$$\epsilon_{xy} = \frac{\partial^2 w}{\partial x \partial y} (e_x + e_y + f) \qquad (4.16)$$

Also the shear stress τ_{xy} is given by

$$\tau_{xy} = \frac{M_{xy} \cdot f}{J} \qquad (4.17)$$

where J is the torsional constant of the plate and the stiffeners and is given by

$$J = \frac{1}{G} \left[\tfrac{1}{2}(B_{xy} + B_{yx}) + B \cdot (1-\nu) + \frac{D}{4} (1-\nu)(e_x + e_y)^2 \right] \qquad (4.18)$$

Since the base program was concerned with the strains and stresses at the top and bottom of a plate with uniform thickness, modifications were then necessary to account for these stress and strains at the top of the plate and at the free edge of the stiffeners. The modifications were achieved by substituting the co-ordinate (z) of the point concerned in the above equations and making the corresponding changes at their appropriate positions in the subroutine "FEMB" of the base program.

4.3.5 STRUCTURE IDEALIZATION PROGRAM

Perhaps the most critical, and at the same time tedious work for the user of a finite element program, is the data preparation for an idealized large structure. Initially the nodal points have to be selected and numbered. The co-ordinates of each nodal point are defined w.r.t. the structural axis, then the elements are numbered, and the nodes at the boundaries of each element are defined. Also the material properties and

thickness of each element must be specified.

The difficulty in preparing such a large amount of data without error has been overcome by developing a computer program to first idealize the bridge and then to calculate all the above mentioned data.

A unique form to idealize a single span, single cell box girder bridge with diaphragms has been chosen (Fig. 4.10). The bridge has been subdivided by imaginary lines or surfaces parallel to the structural axes. The intersections of these lines locate the positions of nodal points enclosing the finite elements. The program allows for two sizes of subdivisions in each of the three directions of the structure. This will enable the user to increase the number of elements at locations where the stresses increase rapidly, and where a coarse mesh size would not reflect the actual behaviour. The diaphragms are always defined by one of the vertical subdividing surfaces. A pattern for diaphragm subdivision (Fig. 4.11) has been chosen, such as to give the best orientation of finite elements with the least number of nodal points. This was important because the main program is limited to a maximum of 20 nodes in each subdivision of the structure.

Another subprogram has been developed to number the elements of the idealized structure. The nodal points (I, J, K) of each element are numbered in an anticlockwise direction and the thickness of the element and its material property is given an indicative number.

The above mentioned programs can either idealize the total span of the bridge, or only half of it if the structure has symmetry of form and loading.

To give an example of the great benefit of these programs, the data cards prepared without the aid of the programs which were needed for example No. 1 (Fig. 5.1) numbered 306, and with the help of these programs the same amount of information is generated by the use of only 5 cards.

4.3.6 ORTHOTROPIC PROPERTIES PROGRAM

In order to reduce the effort in preparing the data and to speed up the process of debugging the program, the policy has been to minimize the changes required in the original variables which were used through the base program.

The elasticity matrices were specified in the base program by the natural elastic constants of the orthotropic plate. The constants used were E_x, E_y, ν_x, ν_y, G for the plane stress part, and E_x, E_y, ν_x, ν_y, G_{xy} for the bending part. As these constants had appeared in many places in the program, and because of the above mentioned reasoning, a program has been developed to calculate these same elastic constants in terms of the geometry and material of the elements which constitute the eccentrically stiffened plate. This was easily achieved by the manipulation of the equalities which were obtained simply by comparing each term in the original and the new elasticity

matrices.

Another object of this program is to calculate the factors which were used in the modification of the stress and strain matrices of both plane and bending parts of the program.

The geometry of the stiffeners which can already be considered in this program are shown in (Fig. 4.12 a, b & c). However, it should be mentioned that for case "c" the torsional rigidity of the stiffeners is treated as if they had a cut in their perimeters and not as closed cells.

A detailed description of this program can be found in (Ref. 52).

4.3.7 INTERPRETATION PROGRAM

It was found by practice that it takes about 40 to 50 hours of hand work to interpret the results of one problem of the size used in this investigation. Even so, the accuracy of the calculation is limited, and fitting and extrapolation from the curves are a little arbitrary. Therefore, a program was developed to manipulate the very large output of the finite element program, and to take care of most of the tedious work in interpreting the results. The program could be extended to represent the results graphically by means of an automatic plotter.

The results of the deformations at all nodal points and the stresses at the C.G. of each element are obtained from the

main program punched on cards. These cards are then loaded with the interpretation program into the computer.

The process of interpretation in the developed program can be explained in the following points:

(i) Sorting out the stresses corresponding to each of the top flange, bottom flange and webs.

(ii) Averaging the membrane and bending stresses of each two adjacent elements in the crosswise direction.

(iii) Calculating the stresses at the top of the plate and the free edge of the stiffeners due to the combined action of plane and bending stresses.

(iv) At cross-sections along the span of the bridge - defined by the plane containing the averaged stress points - a curve is fitted to each of the obtained average stress. The method used in fitting the curves was to find the highest possible polynomial yielding the least mean square error. The details of the method are described in (Ref. 55). The degree and constants of the polynomial which fit the points are printed out in the program.

(v) The values of the maximum stresses at the corners of the box could not be obtained directly from the finite element program. However, they were obtained in the interpretation program by substituting the co-ordinates of the corner points in the equation of the corresponding fit polynomial.

(vi) The calculated corner stresses are divided by the reference value of the stress to give the non-dimensional stress

parameter which is used in plotting the final curves. The reference stress used in the examples of this investigation will be defined later in Sec. 5.4.

(vii) The calculated results, namely the average stresses, corner stresses and the non-dimensional stress parameter are tabulated for each wall of the box separately.

A detail list of the program and the method of using it can be found in (Ref. 32).

A macro-flow chart showing the integration of all the programs used in the present investigation is shown in Appendix (A).

4.4 VERIFICATION OF THE PROGRAM VALIDITY

4.4.1 INTRODUCTION

Several kinds of checking were needed to ensure that the program was free from programming as well as logical errors.

The first check was to ensure the correct functioning of the new programs which were joined to the main program after introducing the modifications to the elasticity, stress and strain matrices. This was easily achieved by checking each program individually before and after being joined to the main program.

For the individual programs, a variety of problems

were chosen to check each part of the program alone. Each problem was carefully prepared by hand and then checked against the computer results.

As for the total behaviour of the program; the problem of a box girder of isotropic material (Fig. 4.13) was used in the checking procedure. The data for the problems were carefully prepared by hand and then loaded together with the original base program into the computer. The same problem was solved using the final modified program. The results of the two runs were found to be exactly identical.

The developed program can now be said to be operational.

The accuracy of the base program for isotropic structures has been previously proved, by the solution of many examples to be reliable. However, for orthotropic structures, the example of a two dimensional natural orthotropic square plate was the only one which was tried by the authors of the base program. Therefore, there was a need to study the accuracy of the final program for two and three dimensional structures with artificial orthotropic elements of the type used in bridges. There was also a need to check the accuracy of the program in solving problems where bending or in-plane stresses dominate. This will automatically check separately the modifications introduced in the bending and plane parts of the program. However, since the object of this investigation is to study the torsional behaviour of box girders, it was felt advisable to check the accuracy of the pro-

gram for such a particular problem.

The above mentioned requirements for checking the program have been satisfied through the study of the following particular problems.

4.4.2 ORTHOTROPIC BRIDGE DECK PROBLEM

In many highway bridges, the deck is constructed by a set of rectangular orthotropic plate panels supported on the main girders and the cross beams. In this section one of these panels has been chosen to check the accuracy of the program for bending. The panel is loaded with a wheel load of 1 kip at the centre. The orthotropic plate is made of structural steel having $E = 30 \times 10^6$ psi and $\nu = 0.30$.

The problem has been solved before by several exact or approximate methods (Ref. 36, Ref. 37). A solution by the finite element method was obtained using the developed program to check its accuracy in problems where bending stresses dominate. In the above solutions the load is assumed to be uniformly distributed over a square area of side = 15 in. It should be mentioned that the panel is assumed in all the above solutions to be supported on unyielding supports. However, for the complete solution, one should superimpose on the results obtained from this solution the results of another solution in which the deck plate is considered acting as an upper flange of the girders.

The geometry of the orthotropic panel together with the nodal points and the arrangement of the finite elements that were adopted in the finite element program are shown in Fig. (4.20). A quarter of the panel was analysed, making use of symmetry, as this has reduced the size of the system to be handled thus reducing the effort in producing the data deck and saving valuable computer time.

Figures (4.21), (4.22), (4.23) show the complete set of influence surfaces for the vertical deflection and the stresses σ_x and σ_y at the top of the deck plate.

Table 2 gives the values of the deflection and stresses at the center of the plate obtained by five different methods. The percentage error shown in this table is based on taking the exact single series solution by Clifton (Ref. 36) as a base for the calculation.

By comparing the results of the finite element analysis against the other methods of analysis, we can see that the results are in good agreement with the exact theory if compared to other theories. However, one would expect even better results if the case considered was for a uniform load rather than concentrated load, and if the point of comparison was not that point of high stress concentration.

4.4.3 SHEAR LAG IN BOX GIRDER BRIDGES

The shear lag phenomenon in thin wall cross sections is

known to reflect the stress diffusion in the plane of the walls of the section. One of the methods used to define the extent of shear lag in box girders due to bending action is to define the width of the flange which when uniformly stressed with the maximum stress would carry the same longitudinal in-plane load. This method is known as the effective width concept.

The problem of shear lag has been examined in Ref. (38) with particular reference to single cell box girder bridges. One of the most critical cases in shear lag problem which was considered in this reference is for a 2 ft. span aluminum box girder model with the top and bottom flanges heavily stiffened in the longitudinal direction. The results obtained from the experiment on the model together with the results predicted by three other theoretical methods of analysis have been compared with those results obtained by using the three-dimensional finite element program developed in the present investigation. The results of the different methods of analysis which are grouped in the curves shown in Appendix (B) of the present thesis, prove the reliability of using the developed program for the analysis of three-dimensional orthotropic structures especially in problems where the in-plane stresses dominate.

4.4.4 TORSIONAL BEHAVIOUR OF ISOTROPIC BOX-LIKE GIRDER

The problem of torsional bending has been thoroughly investigated in Chapter 3. A very reliable experimental study for the torsional behaviour of a single span, single cell box girder,

has been presented by G. Florin (Ref. 39). The box consists of walls of uniform thickness and is provided with a diaphragm at each end. The end diaphragms are allowed to warp but not to rotate. The results of his experiment were compared with those results obtained by two methods of analysis namely; theory of Wlassow (Ref. 20) and theory of Björklund (Ref. 21). The assumptions of these theories were given in Sec. 3.3.

In this section a study similar to that presented by G. Florin will be obtained using the finite element program. The results are then compared with the above mentioned theoretical analysis and checked against the experimental results.

In order to develop the confidence in the present investigation and to give some sense to the deviations between different results, it is felt advisable to mention the important details of the experiment.

4.4.4.1 MODEL EXPERIMENT

The dimensions of the box model and the load arrangement are shown in Fig. (4.13). The model is made from plexiglass which has been tested to show linear proportionality between stress and strain in the low range of stresses within which the test was performed. The material constants were found to be $E = 305.0\ kg/mm^2$ and $\nu = 0.38$. The material has been chosen from a large stock after being checked for homogeneity and uniformity of the thickness. The edges of the box walls had been machined to guarantee that they fit together to form the

right dimensions when glued together.

In order to be able to measure the stresses inside the box, the end diaphragm was substituted by a ring made of the same material and has a very small thickness. These rings were glued to the ends in such a way as to provide no restraint against warping while the boundary conditions could be satisfied by the edges of the ring itself. To avoid inevitable creeping of the material, small loads and special loading devices were used, also very careful measuring techniques were adopted.

The deformations δ_y, δ_z of the cross section (Fig. 4.14) were measured at the corners A, B, C, D and at six cross sections along the span. The strains in the x, y and at 45° angle between, were measured from the inside and the outside of the box. From the strain measurements the longitudinal stress σ_x and the transverse stress σ_y or σ_z were calculated at top and bottom of the plate. Using these stresses the membrane stresses could be evaluated, and then from the stress distribution in each cross section the stresses at the corner points were obtained by extrapolation.

4.4.4.2 EXPLANATION OF THE RESULTS

Figures (4.15) through (4.16) show the variation of the deformations and the extreme stresses at the corners along half the span of the box girder. These relations were obtained using each of the previously mentioned theoretical methods of analysis together with the experimental results. The curves were made

dimensionless by using δ_{y_o}, σ_o and L as reference values for the deformations, stresses and distances along the span where; δ_{y_o} = the deformation δ_y at the middle of the beam, and $\sigma_o = \sigma_{yb} = \sigma_{zb}$ and is equal to the transverse bending stresses at the corners of the middle span section. All reference values were taken from the experimental results.

The study made on the above mentioned curves can be summarized into the following points:

(a) Deformations

From Fig. (4.15) and Fig. (4.16) it is seen that theory of Wlassow provides values which are 16% too high for the deformation δ_y and 10% too high for the deformation δ_z while the finite element analysis gives values which are 6% too high for δ_y and 3% too high for δ_z. The slight flattening of the slope of the experimental curves near to the end support can be attributed to the slight fixity of the beam as a result of applying the end restraints to the ring and not to the beam itself.

(b) Stresses

(i) In Fig. (4.17) the longitudinal bending stress is shown. The deviation in the maximum stress is about 8% lower in the finite element analysis than the experiment. This stress is assumed zero in Wlassow and in Björklund theories since the bending stiffness of the walls is neglected in their analysis.

However, this longitudinal stress amounts to 38% of the maximum induced secondary stresses due to torsional bending. It also amounts to 68% of the longitudinal membrane stress at the same point.

(ii) The membrane longitudinal stress σ_{xm} is shown in Fig. (4.19). Theory of Wlassow gives values which are 16% too high but theory of Björklund gives less deviation with a maximum value of 13% too high. However, in the finite element analysis the deviation was varying in sign and reaches a maximum near the center which is only 5% higher than the experimental value.

It should be mentioned that the longitudinal membrane stresses are expected to be slightly less in the experiment than the ideal theoretical simply supported beam, this is due to the slight fixation at the ends. This can be foreseen since for a completely fixed beam the longitudinal stress is 30% less than simply supported beam. However, in the experiment, it will decrease with a small fraction of the above mentioned 30% since the degree of fixation is small. Hence the 5% deviation of the finite element would be less if the above correction could be introduced to the experimental values.

An interesting observation on the longitudinal membrane stresses is that they are almost zero in the quarter of the span near the supports and then they start to increase rapidly to a maximum at the point of the applied torsional moment.

(iii) The variation of the transverse bending stress

along half the span is shown in Fig. (4.18). The deviations of the stress are 14% too high in theory of Björklund and 12% too high in theory of Wlassow while the finite element analysis gives values less than the experimental values with a maximum deviation of 10% of the maximum value at the center.

The transverse membrane stresses were excluded from the study since they were small and did not exceed 1% of the reference stress σ_o .

5. ANALYTICAL STUDY OF TORSION BENDING PROBLEM IN BOX GIRDER BRIDGES

5.1 GENERAL REMARKS

The finite element computer program described in the preceding chapter provides a powerful means for the analysis of box girder bridges since it accounts rationally for all the parameters governing the response of box girders to loadings tending to deform their cross sections.

In this chapter the finite element program will be used to estimate for some chosen examples of single cell steel box girder bridges the longitudinal and transverse stresses which arise from torsional deformations.

It has been concluded from Chapter 3 that the principal parameters governing the response of box girders to torsional loadings are: (1) The dimensions and elastic properties of the bridge elements (2) End conditions, (3) Number and location of the diaphragms and (4) the type of loading. The procedure

presented in the rest of the present investigation is aimed at supplementing the methods described in Chapter 3 by providing a clear view of interactions between proportions, loading, end conditions and response, and thus helping the designer work efficiently toward a satisfactory design.

5.2 STUDY OF THE LIMITS OF VARIABLES

In this section an exposition of the variables which are involved in the design of box girder bridges and which affect its torsional behaviour will be presented. Some of these variables will be excluded from the present investigation either because their effect on torsional behaviour has been studied extensively before (e.g. diaphragm action), or because those variables are mainly governed in the design by considerations which are independent of the torsional behaviour of the box (e.g. longitudinal stiffeners in top flange, web stiffeners ..). However, these variables will be accounted for, in the examples studied here, in a realistic fashion and according to the design specifications.

In order to ascertain the range of variables used in designing existing box girder bridges, a review was made by the State Bridge Department in California - (Ref. 40) - of over 200 simple span box girder bridges constructed during the past ten years in California. The available data indicated the following:

(1) Spans

A large proportion of the existing bridges are in the

50 to 90 ft. span range. For bridges without diaphragms this is particularly true, and for spans above 85 ft., all bridges have at least one interior diaphragm.

(2) Overall Width

The overall widths are a direct function of the number of bridge lanes.

(3) Depth-Span Ratio

The majority of existing bridges have a depth-span ratio in the 0.05 to 0.065 range.

In the following, the limitations on the variables are discussed in view of the above mentioned ranges and by considering the nature of the rest of the variables in the design and their significance in torsion bending problem.

(i) Length

Most single span box girder bridges have the length close to 80 ft., thus it was found advisable to inspect the torsional behaviour of this majority by choosing the 80 ft. length. However, the effect of torsional bending stresses may be more significant for long spans, therefore a 200 ft. span length has been chosen to form an idea of the problem for this case.

(ii) Width

Since the scope of this investigation has been limited

to single cell box bridges, the two widths of 12 ft. and 24 ft. are considered sufficient to cover the possible variation in the number of lanes that may practically exist on a single cell single span bridge.

(iii) Depth

In view of the range of length - depth ratio mentioned before and of the chosen spans in (i) it has been decided to consider the depths of 8 ft. and 12 ft. for the 200 ft. span and 4 ft. and 6 ft. for the 80 ft. span.

(iv) Orthotropic Plate Deck

The top flange of a box girder bridge consists of a plate with longitudinal stiffeners supported on transverse cross beams which run between the webs of the box. The spacing of longitudinal stiffeners is usually taken as about one foot for open rib stiffeners and two feet for closed cell ones. However, since it has been noted before that the computer program is best suited for stiffeners of weak torsional resistance, open ribs of the type shown in Fig. (4.12.a) have been chosen with one foot spacings.

The cross beams are also chosen with open cross section (Fig. 4.12.b) and spaced with the minimum allowable spacings of 5 ft. (see Ref. 41, p. 149) to ensure uniform transverse distribution of deck plate stiffness.

Fixing the spacings of the stiffeners as indicated above implies that the longitudinal stiffeners will be the same for all bridges and that the cross beams will be the same for cross sections having the same width.

However, the plate on top of the stiffeners is so proportioned as to resist the sum of the local stresses caused by concentrated wheel loads and the longitudinal stresses obtained by considering the deck plate acting as an upper flange of the girder. This latter will influence the thickness when considering the different spans and number of lanes.

(v) Bottom Flange

The bottom flange is made of unstiffened plate which is proportioned to resist the longitudinal stresses obtained by considering it as a bottom flange of the box girder.

(vi) Web Plate

The web plates are chosen to be transversely stiffened with rectangular plate stiffeners. The proportion and spacing are obtained according to AASHO specifications (Ref. 42, clauses 1.7.71 and 1.7.72).

(vii) Loading

Although a more qualitatively significant effect of torsional bending stresses may be expected if the torsional

loading is concentrated rather than distributed, it has been decided that it is more realistic to consider distributed torsion line load since it has a larger contribution to the total stresses induced in eccentrically loaded design conditions. Also it has been decided to apply the torsional line load at the four joints of the box to assure good representation of the torsional moment, and to omit consideration of the local bending stresses in the top flange if the loads are acting other than at the corners.

(viii) End Conditions

Two types of end conditions are considered in this investigation; (1) simply supported ends, (2) fixed ends. It is expected that the behaviour of a continuous box girder where the ends of intermediate spans are partially restrained, can be roughly understood by logical interpolation of the results of these two cases.

(ix) Computer Output

Because of the large amount of information which can be provided by the computer, it has been decided to concentrate the study of the results on those stresses which are most important in terms of the design of box girder bridges. Thus - in general- only corner longitudinal and transverse stresses and their distribution along the span are discussed and presented in this investigation.

5.3 CHOSEN CASES FOR ANALYTICAL STUDY

5.3.1 GENERAL REMARKS

The cases studied included two spans, 80 ft. or 200 ft. Three plate diaphragms were provided in each case, two at the ends and one at the middle. They were given 1½ inches thickness to ensure sufficient stiffness in their plane. The cross sectional details for each case were obtained according to the design example mentioned in the next section, and they are shown in Figures (5.1) through (5.5).

In all cases, two concentrated skew symmetric line loads were considered. The line load was represented by applying 500 lbs at top and bottom corner nodes of the finite element idealization. The end conditions were either simply supported or fixed.

It should be noted that only half the span was analysed because of symmetry. The structure idealization was such that the longitudinal divisions were six equal divisions for half the girder. However, the deck plate, bottom flange and the webs were each transversely divided into four divisions.

Table (1) shows a list of the cases considered in this investigation.

5.3.2 DESIGN EXAMPLE

The procedure used in the design of the cases considered

is illustrated by the design example given in Appendix (C) for a 200 feet span box bridge having two lanes and simply supported at the two ends. The cross section is of a single cell of width 24 feet and depth of 8 feet. Standard AASHO H 20-44 loading (Ref. 42) and ASTM A-36 steel are used in this design.

5.4 INTERPRETATION OF COMPUTER RESULTS

The results obtained from the interpretation program are for the percentage ratio of the extremal torsion bending stresses at the corners to the reference stress (σ_r). This reference stress is taken as the uniform compressive stress at the top fiber of the deck plate. This stress is obtained by treating the girder as simply supported, and acted upon by two symmetrical line loads equal to those used in applying the torque but both acting in the same direction (See Fig. 1.2).

For each example, the variations of the longitudinal and transverse stresses along half the span are plotted in dimensionless forms for the critical sections (AD), (AB), (BA) and (BC), (See Appendix C, Fig. C.3). It has been found that the shape of these curves is similar provided the end conditions are the same. For the cases of simply supported and fixed ends the curves follow the pattern given in Figures (5.6) through (5.9) and in Figures (5.10) through (5.13) respectively. In these curves, the horizontal ordinate represents a point at distance X of the span L, and the vertical ordinate represents the above mentioned percentage stress ratio which is identified

on the curves by (σ) with two subscripts; the first is "T" or "L" which indicates the transverse or longitudinal direction respectively, and the second is either "m", "p" or "s" which indicates whether the stress is the membrane stress or total stress at outside fiber of the plate or at the inside free edge of the stiffeners respectively. It should be noted that the difference between the total and membrane stress curves gives the contribution of the bending action to the total stress.

The variation of the stresses across any wall of the cross section, for a torsional load, has been found to be non-linear at the majority of the cross sections along the span (and particularly for in-plane stresses). The stresses are maximum at the corners and have opposite signs at adjacent corners.

Tables (3-a, b, c, d) show for each example the maximum positive and negative total stresses with their locations and the maximum contribution of bending and in-plane stresses to the total stresses. These values represent in fact the most important information that can be extracted from stress distribution curves.

5.4.1 CASES OF SIMPLY SUPPORTED ENDS

These cases are represented by examples (1) to (5). The values of the variables considered were 80' and 200' for length (L), 4', 6', 8' and 12' for depth (d), and 12' and 24' for width (b).

From the curves shown in Figures (5.5) through (5.9) and Tables (3-a, b, c, d) the following observations can be made.

(a) Longitudinal Stresses

(i) The longitudinal stresses start with zero value at the support and increase to the first peak value at a distance ranging from 0.2 to 0.23 of the span length. Then the stresses reverse their sign at a distance of about 0.4 L from each end and reach another peak with opposite sign at the midspan diaphragm. The value of the peak longitudinal stresses at the midspan is always greater than the value of the first peak. This is important in design since midspan stress controls design for simply supported girders.

(ii) The in-plane longitudinal stresses are always larger than the bending stresses and they dominate the shapes of the total stress distribution curves particularly at sections (AD), (AB) and (BA). At these sections the ratio of the maximum in-plane stress to the maximum bending stress ranges roughly from 12 to 60. However, this ratio is quite low at section (BC) of the top flange because it is heavily stiffened in the longitudinal direction; the ratio at that section ranges approximately from 1.5 to 2.0 for short spans (80 ft.) and from 3.4 to 6.3 for long spans (200 ft.). It should be noted here that these longitudinal bending stresses have been neglected in all the methods that have been suggested so far for the torsional analysis of box bridges.

(iii) The maximum longitudinal stress induced (σ_L) is always at section (AD) where the ratio σ_L / σ_o ranges from 60% in example (3) to 27% in example (1). Also it has been observed that this ratio is always larger for the examples with the short span (80 ft.).

(b) Transverse Stresses

(i) The in-plane transverse stress (σ_{Tm}) starts with zero value at the support and increases to a first peak at a distance ranging from 0.18 L to 0.22 L, and then reverses its sign at a distance ranging from 0.35 L to 0.45 L and reaches another peak of opposite sign at the midspan diaphragm. The maximum ratio σ_{Tm} / σ_o in a cross section is generally small and ranges from 1% to 14%.

(ii) The transverse bending stress has a large effect on the total transverse stresses induced in the plate and the stiffeners. The bending stress is almost zero at the ends and at midspan, where the diaphragms are rigid enough in their plane to keep the curvature of the walls of the cross section almost close to zero. However, the bending stress reaches a maximum at a distance 0.42 L where it adds to the first peak of the in-plane stress σ_{Tm} . The ratio of the maximum transverse bending stress to the maximum in-plane stress is very small except at section (BA) where it ranges from 2.85 in example (3) to 23.5 in example (4). The percentage ratio of the maximum bending stress to σ_o ranges from 40% in example (5) to 70% in example (4).

(iii) The most critical total transverse stress (σ_T) is induced at the edge of the vertical web stiffeners at section (BA). The ratio of σ_T / σ_o ranges from 66% in example (4) to 25% in example (3).

It should be mentioned here that although these transverse stresses are sizable, bridge specifications do not consider any transverse stresses in any phase of the design.

5.4.2 CASES OF FIXED ENDS

These cases are represented by examples (6) through (8). The values of the variables considered were 80' and 200' for length (L), 4', 8' and 12' for depth (d) and 12' and 24' for width (b).

From the curves shown in Figures (5.10) through (5.13) and Tables (3-a, b, c, d) the following observations can be made:

(a) Longitudinal Stresses

(i) The longitudinal stresses start with a maximum at the support, reverse the sign at a distance 0.125 L from the ends, increase to a peak at about 0.3 L and then reverse the sign again at a distance 0.075 L from the midspan diaphragm where the stresses reach another peak.

(ii) The value of the maximum longitudinal stress (σ_L) for a box with fixed supports is almost equal to the maximum longitudinal stress at midspan if the box is simply supported.

(iii) The maximum longitudinal stress (σ_L) at mid-span of simply supported girder is reduced 50% by fixing the supports.

(iv) As in the case of simply supported ends the in-plane longitudinal stresses dominate the shape of the total stress distribution curves. However, the ratio of the maximum in-plane stress to the maximum bending stress ranges in the fixed end examples from 25 to 38 at sections (AD), (AB) and (BA) and from 1.12 to 13.5 for section (BC).

(v) For the maximum longitudinal stress (σ_L) the percentage ratio σ_L / σ_o ranges from 28% in examples 6 and 7 to 38% in example 8.

(b) Transverse Stresses

(i) The in-plane transverse stress (σ_{Tm}) starts with a maximum value ($\frac{\sigma_{Tm}}{\sigma_o} < 13\%$) at the fixed end, decreases rapidly and changes sign at 0.075 L from the ends and then remains almost flat with a very small value ($\frac{\sigma_{Tm}}{\sigma_o} < 4\%$). At a distance 0.05 L from the midspan it changes sign once more to reach another peak of very small magnitude ($\frac{\sigma_{Tm}}{\sigma_o} < 3\%$).

(ii) The shapes of the transverse bending stress curves and the sections at which it is maximum are still the same as described in cases of simple supports. However, the magnitudes of the stresses are very close to half their values for the same boxes but with simply supported ends.

(iii) As in simply supported cases, the most critical total transverse stress (σ_T) is induced at the edge of the

vertical web stiffeners at section (BA). However, the ratio σ_T / σ_o ranges in fixed end examples from 18% for example (7) to 31% for example (8). This ratio is close to half of that obtained for the same boxes but with simple supports.

6. PARAMETER STUDIES

6.1 GENERAL

In this chapter, the problem of torsion bending in the design of box girder bridges will be looked at in the following way: given a box bridge structure, subjected to an eccentrically distributed line load with unit eccentricity, i.e., eccentricity from the center equal to unit feet, what will be the maximum value of the longitudinal stress that should be added to the maximum longitudinal stress obtained by the conventional bending theory in which the structure is considered as centrically loaded? Also, what will be the order of magnitude of the transverse stresses that have been neglected in the design specifications?

In practice, a quick estimate of these secondary stresses is necessary during the preliminary design phase. Such an estimation will guide the designer to select quickly the best geometry of the structure and the number and locations of the diaphragms that ensure a safe and economic design.

In order to achieve this phase in bridge design, the

complete picture of the torsional behaviour of the structure should be understood, and the interaction of the various involved parameters should be clearly identified.

In this chapter, and based on the torsional study performed on the examples of the previous chapter, a parameter study is presented and graphs are plotted for the interaction between the variables. It should be emphasized that such a study is limited to single cell boxes of fixed or simply supported ends and with rigid diaphragms at the ends and at midspan. However, for boxes with different diaphragm locations and number, the designer should relate this study to the diaphragm study presented in Ref. (25). Also, for continuous girders, a fair understanding of the problem may be achieved by proper interpolation of the behaviour of fixed and simply supported ends.

A list of all the variables and parameters that might affect the torsional behaviour of a box bridge is shown in Table (1) for each example studied in Chapter 5. The variables considered are the length (L), the depth (d), the width (b), the moment of inertia of the bridge section about its neutral axis (I), the area enclosed by the walls of the box section (A), and the end conditions. The parameters shown are for the shape ratios α = a/d, L/b and L/d.

The percentage ratios of the maximum induced total longitudinal stress ($\tilde{\sigma}_L$) and transverse secondary stress ($\tilde{\sigma}_T$) to the reference stress σ_o have been recalculated from

Tables (3-a, b, c, d) for an eccentric uniform line load with unit eccentricity. These ratios are shown in Tables (4) and (5) for each example and for each of the four corner sections considered before.

6.2 LONGITUDINAL STRESS

The study that has been made on the effect of the parameters on the magnitude of the maximum secondary longitudinal stresses ($\tilde{\sigma}_L$) indicated that the percentage ratio $\tilde{\sigma}_L / \sigma_o$ is almost directly proportional to the parameter "K" which in fact includes the effect of the ratio of the longitudinal stiffness of the box to its torsional stiffness (I/A^2) and the effect of a parameter (L/b) which is an indication of shear lag effects.

$$K = \frac{I}{A^2 \, (L/b)^{2/3}} \qquad (6.1)$$

This has been demonstrated by the plot given in Fig. (6.1) for the stress ratio $\tilde{\sigma}_L / \sigma_o$ against K for the fixed and simply supported box examples considered. It can be seen that the relation can be very closely expressed by the equation of the straight line

$$\frac{\tilde{\sigma}_L}{\sigma_o} = 1.50 \cdot K - 4.5 \qquad (6.2)$$

In the above equation, and in order to simplify its form, the units of "A" and "I" which define the parameter "K" are chosen to be in ft and in^4 respectively.

The negative sign in equation (6.2) inherently means that for practical design purpose, the secondary longitudinal stresses can be neglected for values of K less than 3.0.

Although the accuracy of equation (6.2) is questionable outside the range of parameters used in the studied examples, it provides, however, a rational and physical understanding of the torsional behaviour of box bridges. For the purpose of demonstrating such a behaviour, equation (6.2) has been used to determine the magnitude of σ_L / σ_o for a wide range of the parameters I/A^2 and L/b. The results are shown in Figures (6.2) and (6.3). By studying the curves in these figures the following conclusions can be made:

(i) For constant ratio of I/A^2 the ratio σ_L / σ_o is almost linear, and is less than 10% for span to width ratio greater than 10, however, for smaller values of L/b the stress ratio starts to increase very rapidly.

(ii) By decreasing the ratio of I/A^2 the stress ratio is reduced. This reduction, however, is more significant for smaller values of L/b up to 10 and negligible for L/b more than 15.

6.3 TRANSVERSE STRESS

The maximum transverse torsion bending stress has been found to occur at section (BA) at the edge of the vertical web stiffeners. This stress is dominated by the transverse bending stress rather than in-plane stress. However, this bending

stress is largely dependent on the following factors:

(i) The geometry and stiffness of the web stiffeners. This has been changed in the examples according to design requirements.

(ii) The relative transverse stiffness of the web and the deck plate. However, the transverse stiffness of the deck is mainly governed by the stiffness of the cross beams. This stiffness has been changed in the examples with the change in the length of spans between the webs.

(iii) The ratio of span to depth L/d. This ratio has not been fixed in any two of the examples considered. This, therefore, adds more difficulty in inspecting the rest of the parameters involved in the problem.

In view of the above, it has been found impossible to perform a parameter study for the maximum transverse bending stress by using the results of the solved examples. However, the following comments can be made by studying the results presented in Table (5):

(i) The stress ratio σ_T / σ_o for the same bridge span is greater for cross sections of shallower shapes provided that the lateral wall stiffnesses of the box are the same.

(ii) The stress ratio σ_T / σ_o is most effectively reduced by decreasing the span to depth ratio L/d.

(iii) The stress ratio σ_T / σ_o in boxes with fixed ends is half that of simply supported boxes.

(iv) Except for very low L/b ratios, the transverse stress ratio σ_T / σ_o is always greater than the longitudinal

stress ratio $\grave{\sigma}_L / \sigma_o$.

(v) For long span bridges the percentage ratio of $\grave{\sigma}_T / \sigma_o$ did not exceed 3.9%, however, for short spans it increased up to 11.0%.

7. RECOMMENDATIONS TO ACCOUNT FOR TORSIONAL DEFORMATIONS IN BRIDGE DESIGN

It was thought advisable to describe these recommendations through an outline of a suggested design procedure for the particular type of bridge considered in this investigation. This procedure is summarized in the following steps:

(i) A very rough estimate of the bridge cross section is determined by the designer using his practical experience.

(ii) The parameter (k) is computed.

(iii) The deck is designed according to AISC (Ref. 41) as described in the design example given in Appendix C.

(iv) The bridge cross section is designed by the conventional means, as if it was a beam in flexure without twist. However, the live load plus impact are increased by a certain percentage to account for the longitudinal torsional bending stresses. This increase can be obtained by substituting the parameter (k) in the following equation derived from equation (6.2);

$$\text{percentage increase} = (1.5\,k - 4.5) \cdot e$$

where "e" is the eccentricity of the live load.

(v) Web stiffeners are proportioned for the shears corresponding to the reactions of the deck acting as a beam strip on undeflecting supports.

(vi) The stresses due to dead and live load are calculated using the established cross section and compared with the allowable values.

(vii) If the section is overstressed, the following is suggested to reduce the longitudinal torsional bending stresses:

(a) If the ratio of length of the bridge to the width of the bottom flange is less than 10, it is recommended that this width be increased.

(b) If the above ratio is more than 10, it is recommended the flange proportions be revised.

It should be emphasized here that the decrease in longitudinal stresses is not markedly changed if the number or stiffness of the diaphragms are increased.

(viii) It is necessary to repeat steps (ii) through (vii) only for substantial changes in the proportions of the cross section.

(ix) The peak transverse bending stress in the web stiffener is estimated by performing one run of the computer program considering live load on one side of the bridge. If the stiffeners are highly overstressed, it is strongly recommended that the number of interior diaphragms be increased. Two diaphragms at the third points are sufficient to reduce the stress to a small value. In order to avoid fatigue failure, special consideration should be given in the design of the weld at the junction between the web and top flange.

8. SUMMARY AND CONCLUSIONS

8.1 SUMMARY

A review of the theories dealing with the torsional behaviour of thin walled beams has been presented in Chapters 2 and 3. The applicability of such theories in the design of box girder bridges is investigated. They have been classified into two groups; (1) theories dealing with beams of non-deformable cross sections, (2) theories dealing with beams of deformable cross sections. In each group, solutions have been presented for particular problems of single cell box girders under torsional loading. Through these solutions, the effects of the loading conditions, shape of the box, length of girder, diaphragm stiffness and location on torsional bending stresses have been discussed and presented in many cases by curves. For some of these problems, comparisons have been made for solutions obtained by different theories, and their accuracy has been discussed.

Based on the three dimensional plate structure program

in Ref. (30), a finite element computer program is developed for analysing single cell orthotropic box girder bridges. The problem of preparing by hand the large amount of input information for the program is reduced to a simple matter of preparing very little basic input data on cards.

Another program is developed to interpret automatically the large amount of computer output for the specific type of box girders used in this investigation.

The finite element method of analysis, the development of the computer programs and the verification of their validity are presented in Chapter 4.

In Chapter 5, the finite element program is used to estimate for some chosen examples of single cell steel box girder bridges the longitudinal and transverse stresses which arise from torsional deformations. The examples are for different box shapes, lengths and end conditions. The torsional behaviour of these boxes are explained and discussed in detail.

A parameter study based on the torsional study performed on the above mentioned examples is given in Chapter 6. The percentage ratio of the maximum secondary longitudinal stresses ($\tilde{\sigma}_L$) and the reference bending stress (σ_o) is found to be related to a new parameter (k) by a simple straight line relationship (equation 6.2).

In Chapter 7 and through a suggested design procedure,

recommendations are given to account for the torsional deformation in bridge design.

8.2 CONCLUSIONS

8.2.1 COMPUTER PROGRAM

The computer program developed in this study is a powerful tool for investigating any problem that may face the designers in the analysis of box girder bridges. It can be used for arbitrary loading and boundary conditions. It can also treat the cases of varying dimensional and natural properties throughout the structure. It has, however, the disadvantages that it involves the solution of a very large system of equations for structures of the complexity of multicell box girder bridges. The size of this problem is large even for present day computers, in terms of storage and computer time required for the solution. In addition, the accuracy of the program is dependent on the fineness of the subdivisions used in dividing the structure into finite elements.

It is expected, however, by the continuous development of fast digital computers of large storage capacity, that it may be more practical to use the program as a direct method for the elastic analysis of a specific bridge under a given loading or temperature changes. In this case the program may eventually be used to replace the present semi-empirical methods used in analysing complex bridge systems. It may also be used as an aid in studying the effect of different parameters on certain

internal forces or load distribution properties. This will provide a means for developing improved simplified analysis procedures similar to those presently being used for design. An example of the latter application is demonstrated in the parameter study presented in Section 6.2 which leads to the simplified formula for evaluating the secondary longitudinal stresses developed in a single cell box due to eccentric line loads.

8.2.2 BEHAVIOUR OF SINGLE CELL BOX GIRDER BRIDGES UNDER UNIFORM TORSIONAL LOAD

Analyses of single cell box bridges typical of those used in highway bridges show that torsional deformations give rise to substantial longitudinal and transverse stresses which have been completely ignored in the conventional design. These stresses become more important for bridges with a high ratio of live load to dead load, with more eccentric loads, with wide and short structures and with bridges of smaller I/A^2 ratio.

The torsional bending stresses can be effectively reduced by introducing intermediate diaphragms. The reduction, especially in the longitudinal stresses, is insensitive to practical variations of diaphragm stiffness.

For the specific types of problem studied in the present investigation the following is a summary of the most important remarks and conclusions that can be made on the torsional bending stresses:

(a) Longitudinal Stresses

(i) The longitudinal stresses are maximum at midspan in the case of simply supported ends, and at the ends in the case of fixed ends. They are almost equal in magnitude in both cases and they occur at the corner sections of the bottom flange.

(ii) The use of theories that neglect the longitudinal bending stiffness of the wall elements of the girder (e.g. Wlassow's theory) may lead to inaccurate results in short span bridges. In some of the examples considered, the bending stress was about 35% of the total maximum longitudinal stress. This was at the corner sections of the top flange since it is heavily stiffened in the longitudinal direction.

(iii) The maximum longitudinal stress ($\bar{\sigma}_L$) increases with the parameter (k).

(iv) It is expected that smaller values of longitudinal stresses would be produced if the line load was placed between webs rather than over the webs. In the former case the load has a chance to distribute longitudinally before it is picked up by the web; while in the latter case, the effect of shear lag tends to produce a concentration of stress at the web. It is necessary to differentiate between this kind of stress concentration and the local stress concentration due to point loading.

(b) Transverse Stresses

(i) The maximum transverse stresses (σ_T) occur at the free edge of the vertical web stiffeners at their connection

with the top flange.

(ii) The stress σ_T is dominated by the bending stress part, and is reduced approximately 50% by changing the end conditions from simple supports to fixed supports.

(iii) The transverse stress is a function of the geometry of the vertical stiffeners and increases with shallower box shapes and larger span to depth ratios.

(iv) The magnitude of σ_T may reach a sizable value, and undergo full reversal as lanes on alternate sides of the bridge are loaded. The high potential number of cycles of such load reversal suggests a special consideration in the design of the weld at the junction of web stiffener to top flange where fatigue failure may occur.

8.3 RECOMMENDATIONS FOR FURTHER STUDY

(a) Finite Element Program

There are several possible modifications which could be incorporated into the program. Some of these modifications are for better accuracy, others which appear desirable because they would improve the usefulness or flexibility of the program or reduce the computing time. These modifications are summarized below:

(i) The coupling action between in-plane and bending deformations can be included in the analysis by the replacement of the in-plane elasticity matrix ($\bar{\underline{D}}_p''$) and the bending elasticity matrix ($\bar{\underline{D}}_b$) by the total elasticity matrix ($\bar{\underline{D}}$) derived in Chapter 4.

(ii) Modification of the program can be made to include structural elements in which the direction of orthotropy does not coincide with the structural axes.

(iii) Modification of the structural idealization program can be made to include bridges of different geometrical shapes (trapezoidal, multicell, ...).

(iv) It is believed that the capacity of the program cannot be materially improved at the moment unless a link system is used in the program. This may need basic modifications in the procedure of formulating the program.

(v) Further improvement can easily be added to the interpretation program to represent the results graphically by means of an automatic plotter.

(b) Torsional Study

The computer programs used in this investigation can be used to perform parameter studies for reinforced concrete bridges or for steel bridges of reinforced concrete deck subjected to torsional loading.

Further examples of the type used in this investigation but with different ranges of parameters could be solved to confirm the parameter study made for the longitudinal stresses ($\tilde{\sigma}_L$), and to complete the data necessary to perform another parameter study for the transverse stresses ($\tilde{\sigma}_T$).

It is possible to modify the program to perform a torsional study of multicell box girders using the present capacity of

computers. This can be achieved in two steps; (1) A coarse mesh of finite element idealization for the whole structure is used to obtain an approximate solution for the nodal displacements and stresses in the elements, (2) at locations where more accurate results are required, a solution for this particular part of the structure is obtained by refining its mesh, applying the external nodal forces within this part and imposing the nodal displacements at its boundary which were obtained from the first solution.

Further study is suggested to investigate the effect of torsional bending stresses on buckling consideration in the design of box girder elements, especially the webs.

TABLE (1)

Variables and Parameters Included in the Studied Examples

Example No.	End Condition	Variables					Parameters				
		Length (L)	Width (b)	Depth (d)	Moment of Inertia (I)	Area (A)	$\alpha=\frac{b}{d}$	$\frac{L}{b}$	$\frac{L}{d}$	$\frac{I}{A^2}$	$K=\frac{I}{A^2}\cdot\frac{1}{(L/b)^{2/3}}$
		feet	feet	feet	in^4	ft^2	-	-	-	-	-
1	Simple Supports	200	24	8	839,300	192	3	8.3	25	22.8	5.55
2		200	24	12	1,969,200	288	2	8.3	16.6	23.8	5.78
3		80	24	8	705,200	192	3	3.3	10.0	19.2	8.62
4		80	12	4	82,750	48	3	6.6	20.	35.9	10.4
5		80	12	6	199,550	72	2	6.6	13.3	38.4	11.0
6	Fixed Supports	200	24	8	839,300	192	3	8.3	25.	22.8	5.55
7		200	24	12	1,969,200	288	2	8.3	16.6	23.8	5.78
8		80	12	4	82,750	48	3	6.6	20.0	35.9	10.4

TABLE 2

COMPARISON BETWEEN FINITE ELEMENT SOLUTION AND THE THEORETICAL SOLUTIONS FOR THE DEFLECTION AND STRESSES AT THE CENTER OF AN ORTHOTROPIC PLATE LOADED WITH 1 KIP AT THE CENTER

Author	Method of Solution		Deflection in	Stresses at Top of Deck Plate p.s.i		Stresses at Bottom of Stiffeners p.s.i.	
				σ_x	σ_y	σ_x	σ_y
Clifton (Oct. 1963) Ref. (36)	Exact	Single Series	0.004505	-230	-163	+1092	+1059
		Double Series	0.004503	-227	-163	+1073	+1055
	Approx.	Single Series	0.004257	-280	-220	+ 999	+ 937
		% Error	-5.5	+27.1	+35.1	- 9.1	-11.6
Hudson (Oct. 1968) (Ref. 37)	Descrete Element Analysis		0.004234	-218	-121	+1030	+ 782
	% Error		-5.9	-3.96	25.2	3.96	25.2
	Finite Element Analysis		0.004880	-212	-171	+ 990	+1160
	%Error		+8.3	5.5	4.9	-7.75	+9.95

TABLE 3.a

STRESSES IN THE STUDIED EXAMPLES AT SECTION AD

Example No.	Stress	End Condition	% (Max. -ive Stress) / σ_o		% (Max. +ive Stress) / σ_o		% Max. Bending Stress / σ_o	% Max. Plain Stress / σ_o	Max. Plain Stress / Max. Bending Stress
			Value %	Location x/L =	Value %	Location x/L =			
1	Longitudinal Stresses	Simple Supports	27	0.5	20	0.23	2	23	11.5
2			30	0.5	27	0.22	2	28	14
3			44	0.5	60	0.23	1	60	60
4			38	0.5	31	0.20	1	37	37
5			37	0.5	31	0.20	1	36	36
6		Fixed Support	26	0.0	11	0.30	1	25	25
7			28	0.0	12	0.29	1	27	27
8			38	0.0	18	0.30	1	38	38
1	Transverse Stresses	Simple Support	4	0.21	5	0.21	4	1	0.25
2			5	0.50	3	0.21	4	5	1.25
3			9	0.5	7	0.18	3	9	3.0
4			7	0.5	8	0.22	7	7	1.0
5			8	0.5	6	0.22	5	8	1.8
6		Fixed Support	11	0.0	3	0.25	2	11	5.5
7			8	0.0	3	0.25	2	8	4.0
8			13	0.0	5	0.25	3	13	4.3

TABLE 3.b

STRESSES IN THE STUDIED EXAMPLES AT SECTION AB

Example No.	Stress	End Condition	% (Max. -ive Stress) / σ_o		% (Max. +ive Stress) / σ_o		% Max. Bending Stress / σ_o	% Max. Plain Stress / σ_o	Max. Plain Stress / Max. Bending Stress
			Value %	Location x/L =	Value %	Location x/L =			
1	Longitudinal Stresses	Simple Supports	27	0.5	20	0.23	2	23	11.5
2			30	0.5	27	0.22	2	28	14
3			44	0.5	60	0.23	1	60	60
4			38	0.5	31	0.20	1	37	37
5			37	0.5	31	0.20	1	36	36
6		Fixed Support	26	0.0	11	0.30	1	25	25
7			28	0.0	12	0.29	1	27	27
8			38	0.0	18	0.30	1	38	38
1	Transverse Stresses	Simple Support	5	0.5	3	0.20	4	5	1.25
2			3	0.5	3	0.22	1	3	3.0
3			3	0.5	16	0.20	3	14	4.7
4			7	0.5	4	0.20	7	7	1.0
5			7	0.5	8	0.20	5	7	1.4
6		Fixed Support	11	0.0	3	0.25	2	11	5.5
7			9	0.0	4	0.25	1	9	9.0
8			11	0.0	3	0.25	2	11	5.5

TABLE 3.c

STRESSES IN THE STUDIED EXAMPLES AT SECTION BA

Example No.	Stress	End Condition	% (Max. -ive Stress) / σ_o		% (Max. +ive Stress) / σ_o		% Max. Bending Stress / σ_o	% Max. Plain Stress / σ_o	Max. Plain Stress / Max. Bending Stress
			Value %	Location x/L =	Value %	Location x/L =			
1	Longitudinal Stresses	Simple Supports	17	0.20	27	0.50	2	25	12.5
2			18	0.20	27	0.50	2	25	12.5
3			45	0.22	36	0.50	1	44	44
4			24	0.22	31	0.50	1	30	30
5			23	0.20	35	0.50	1	34	34
6		Fixed Support	11	0.25	28	0.0	1	27	27
7			11	0.25	28	0.0	1	27	27
8			13	0.25	33	0.0	1	32	32
1	Transverse Stresses	Simple Support	6	0.25	47	0.22	49	6	1/8.2
2			6	0.25	38	0.22	41	6	1/6.85
3			16	0.25	25	0.22	40	14	1/2.85
4			10	0.25	66	0.22	70	3	1/23.5
5			8	0.25	32	0.22	40	5	1/8.0
6		Fixed Support	4	0.25	21	0.25	23	7	0.3
7			4	0.25	18	0.25	20	7	0.35
8			6	0.25	31	0.25	35	8	0.23

TABLE 3.d

STRESSES IN THE STUDIED EXAMPLES AT SECTION BC

Example No.	Stress	End Condition	% (Max. -ive Stress) / σ_o		% (Max. +ive Stress) / σ_o		% Max. Bending Stress / σ_o	% Max. Plain Stress / σ_o	Max. Plain Stress / Max. Bending Stress
			Value %	Location X/L =	Value %	Location X/L =			
1	Longitudinal Stresses	Simple Supports	18	0.20	25	0.5	7	24	3.40
2			18	0.20	27	0.5	4	25	6.25
3			41	0.20	27	0.5	17	37	2.20
4			25	0.20	30	0.5	17	25	1.48
5			24	0.20	33	0.5	14	28	2.00
6		Fixed Support	11	0.25	25	0.0	8	24	3.00
7			10	0.25	28	0.0	2	27	13.50
8			6	0.25	37	0.0	25	28	1.12
1	Transverse Stresses	Simple Support	1	0.20	2	0.2	1	1	1.00
2			2	0.20	6	0.2	6	2	0.33
3			3	0.20	3	0.5	1	3	3.00
4			1	0.20	2	0.5	1	2	2.00
5			1	0.20	2	0.5	1	2	2.00
6		Fixed Support	1	0.20	7	0.0	1	7	7.00
7			1	0.20	5	0.0	3	5	1.66
8			1	0.20	4	0.0	2	4	2.00

TABLE 4

VALUES OF THE PERCENTAGE RATIO $\bar{\sigma}_L/\sigma_o$ OBTAINED FROM

THE STUDIED EXAMPLES FOR UNIT ECCENTRIC LINE LOAD

End Conditions	Example No.	Max. Longitudinal Sec. Str. $\bar{\sigma}_L$ for Unit Eccentricity / σ_o × 100			
		Sections			
		AD	AB	BA	BC
Simple Supports	1	2.25	2.25	2.25	2.10
	2	2.50	2.50	2.25	2.25
	3	5.00	5.00	3.75	3.41
	4	6.35	6.35	5.20	5.00
	5	6.15	6.15	5.80	5.50
Fixed Supports	6	2.16	2.16	2.34	2.10
	7	2.35	2.35	2.34	2.34
	8	6.30	6.30	5.50	6.15

TABLE 5

VALUES OF THE PERCENTAGE RATIO σ_T/σ_o OBTAINED FROM

THE STUDIED EXAMPLES FOR UNIT ECCENTRIC LINE LOAD

End Conditions	Example No.	Max. Transverse Sec. Str. σ_T for Unit Eccentricity / σ_o × 100			
		Sections			
		AD	AB	BA	BC
Simple Supports	1	0.415	0.42	3.90	0.16
	2	0.415	0.25	3.15	0.50
	3	0.750	1.32	2.10	0.25
	4	1.330	1.16	11.00	0.33
	5	1.330	1.16	5.30	0.33
Fixed Supports	6	0.920	0.92	1.75	0.58
	7	0.660	0.75	1.50	0.42
	8	2.150	1.83	5.20	0.66

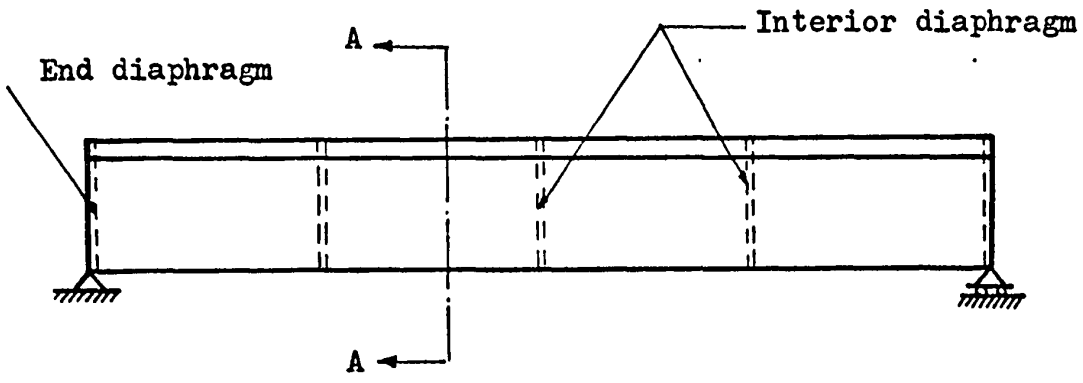

(a) SIDE ELEVATION

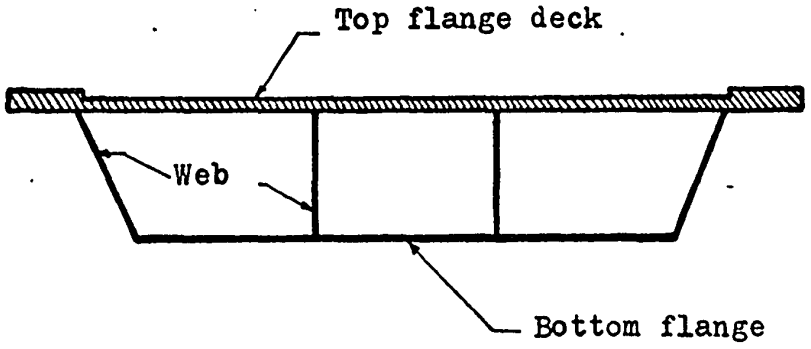

(b) CROSS-SECTION A-A

FIG. (1.1)

TYPICAL BOX GIRDER BRIDGE

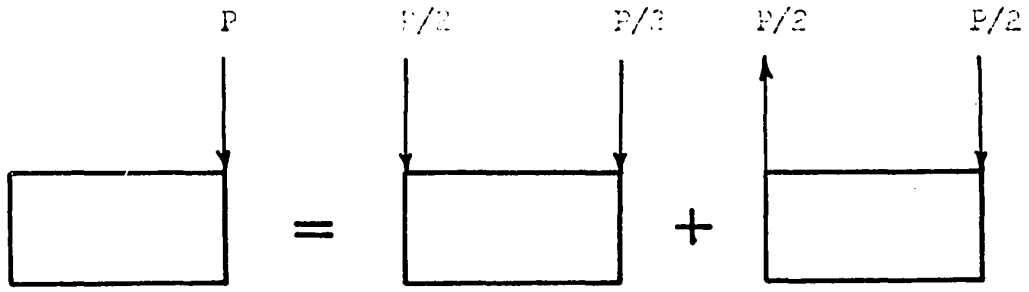

FIG. (1.2)

EQUIVALENT SYSTEMS FOR ECCENTRIC LOAD

FIG.(1.7-a)

DIAGONAL DEFORMATION

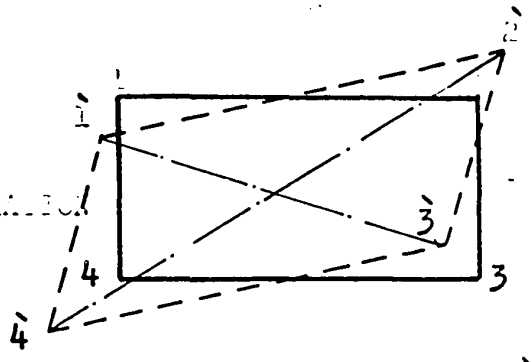

FIG.(1.7-b)

WALL DEFORMATION

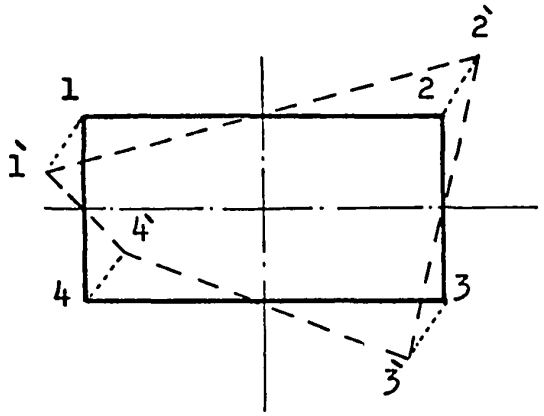

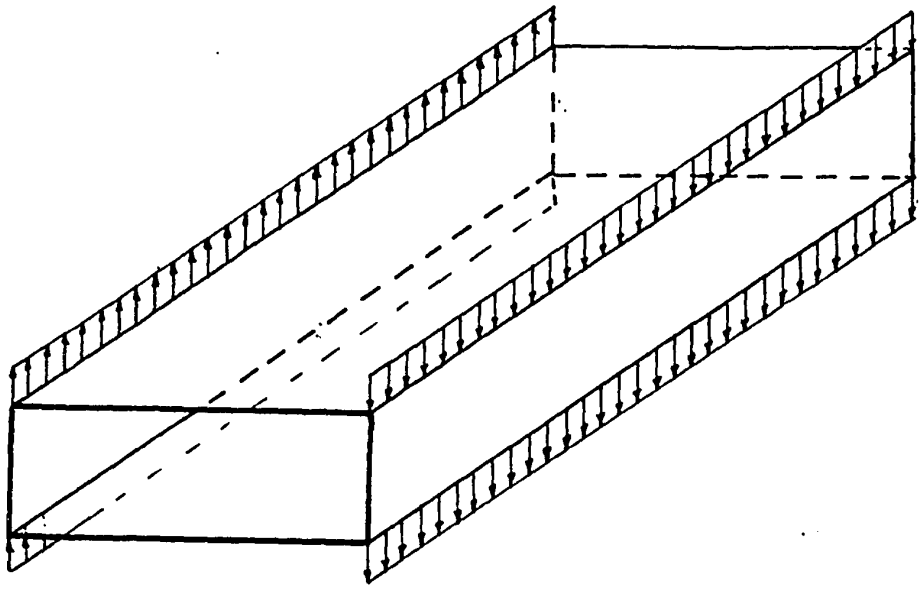

FIG. (1.4)

LOADING ARRANGEMENT

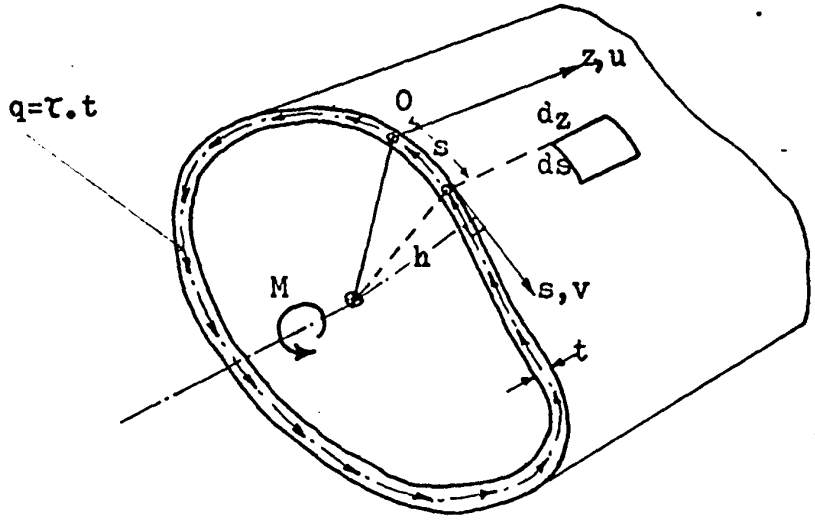

FIG. (2.1)

IN-PLANE DISPLACEMENTS OF A POINT

DUE TO TWISTING OF THE SECTION

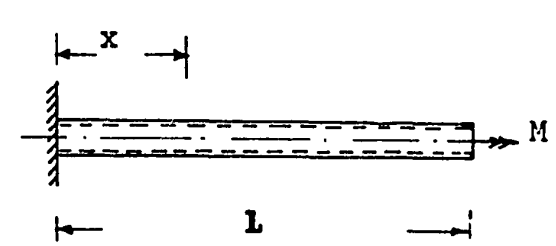

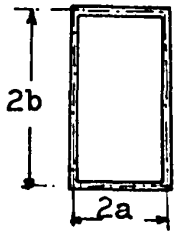

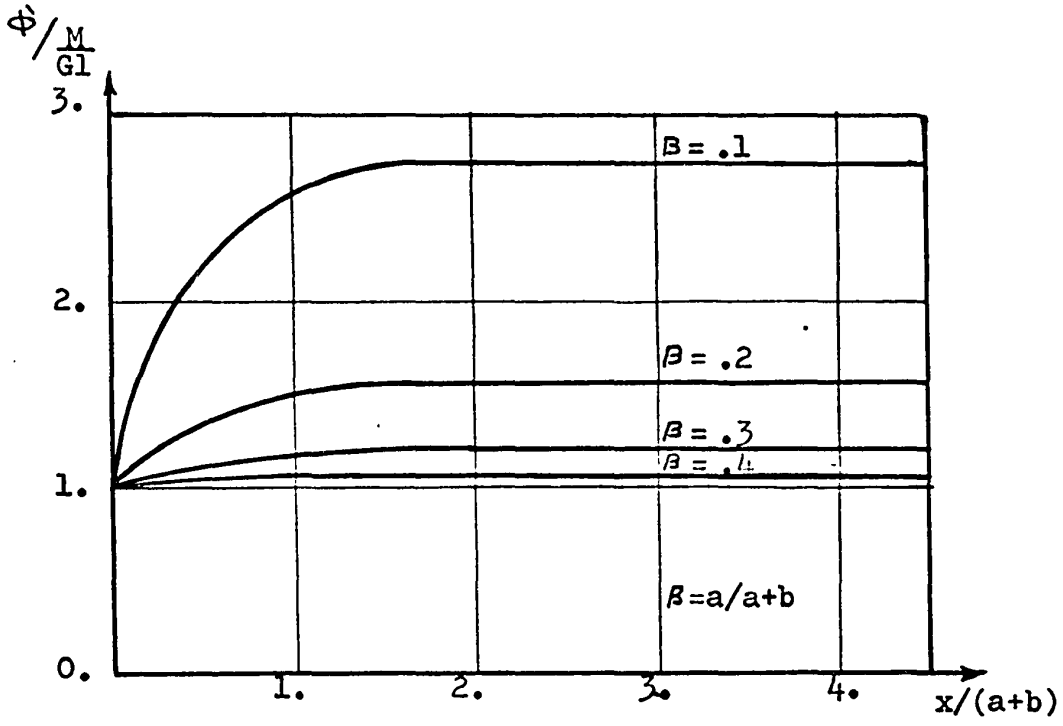

FIG.(3.1)

THE RATE OF TWIST AT VARIOUS

DISTANCES FROM THE RESTRAINED END.

(Karman & Chien)

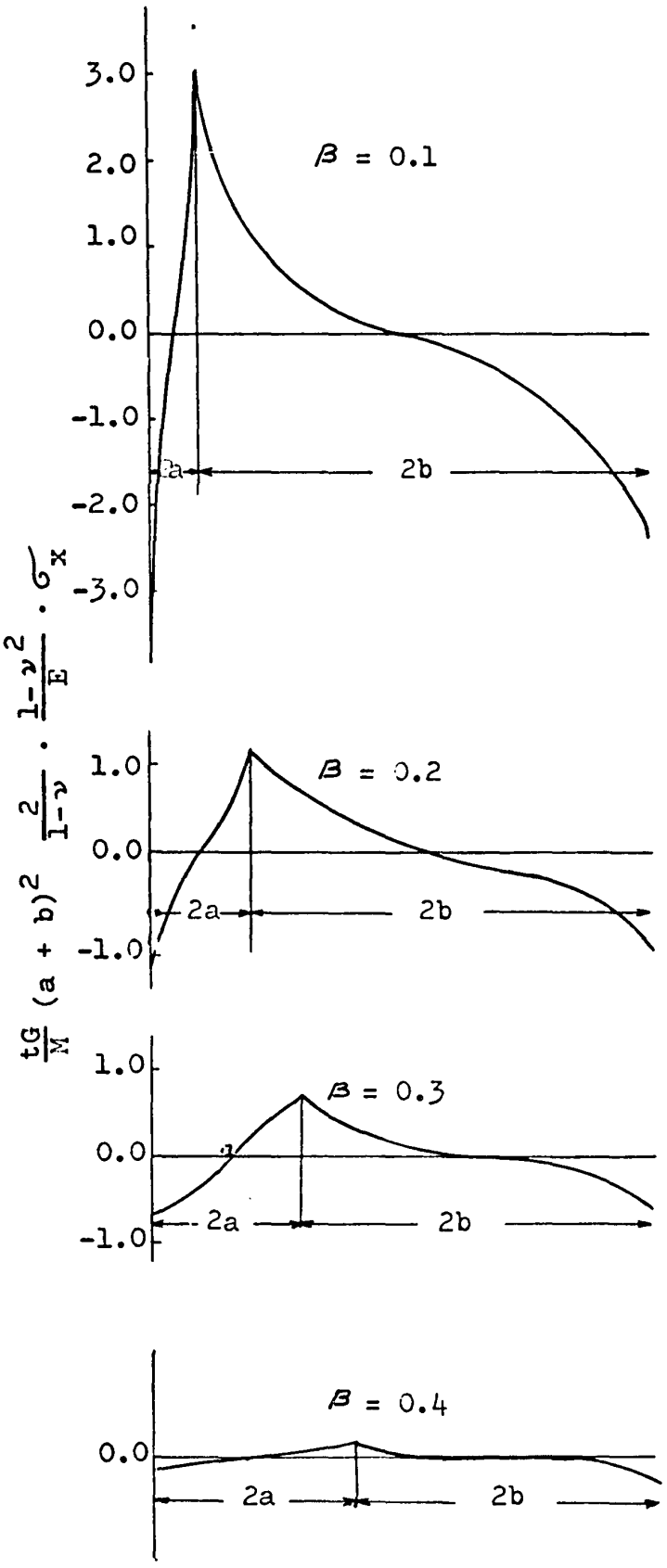

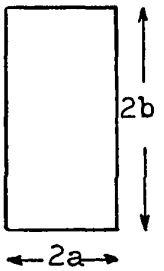

Fig. (3.2)
Circumferential distribution of axial stress at the fixed end.

(Karman & Chien)

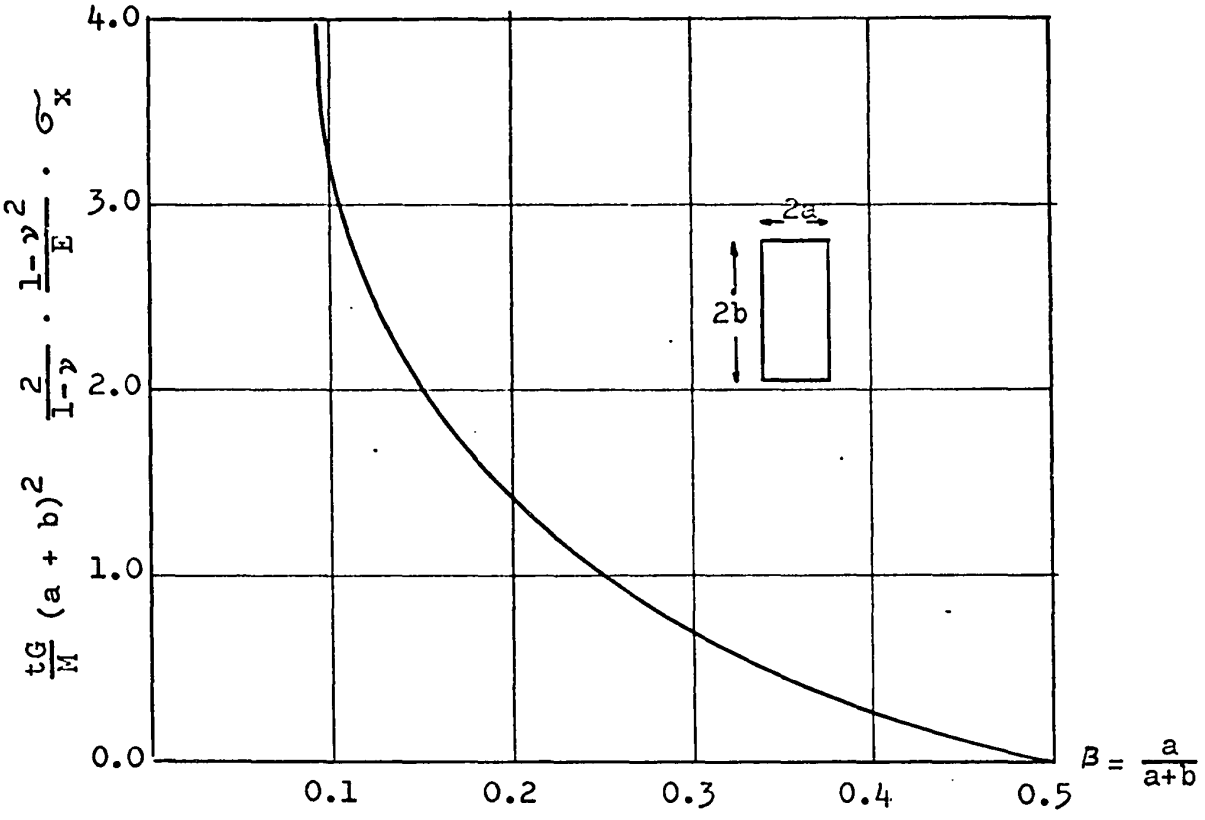

Fig. (3.3)

Maximum Axial Stress at the Corner for
Various Rectangular Thin-Walled Sections.

FIG.(3.4)

COMPARISON BETWEEN THE TWO APPROXIMATE THEORIES OF UMANSKY&PANOVKO

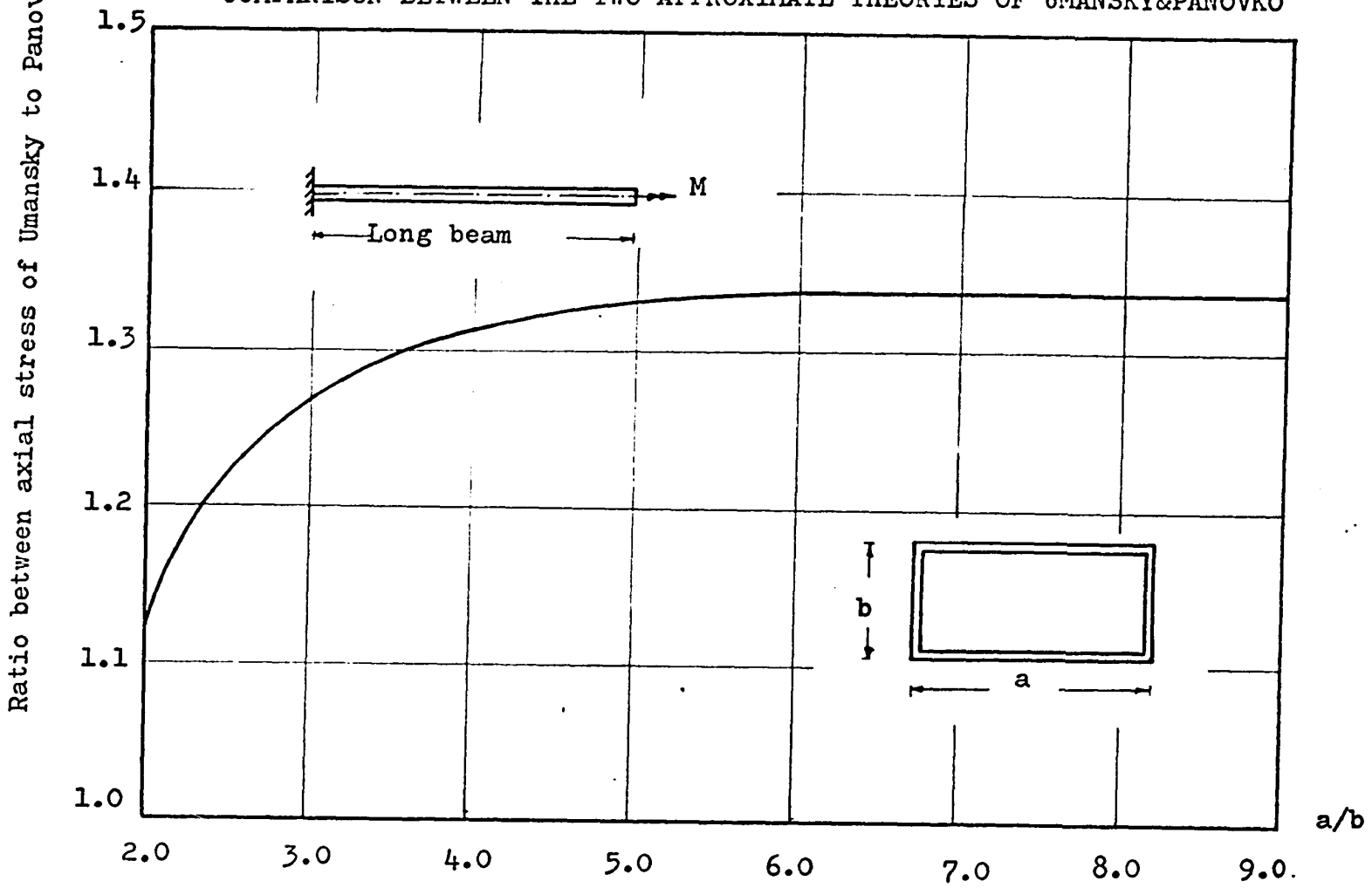

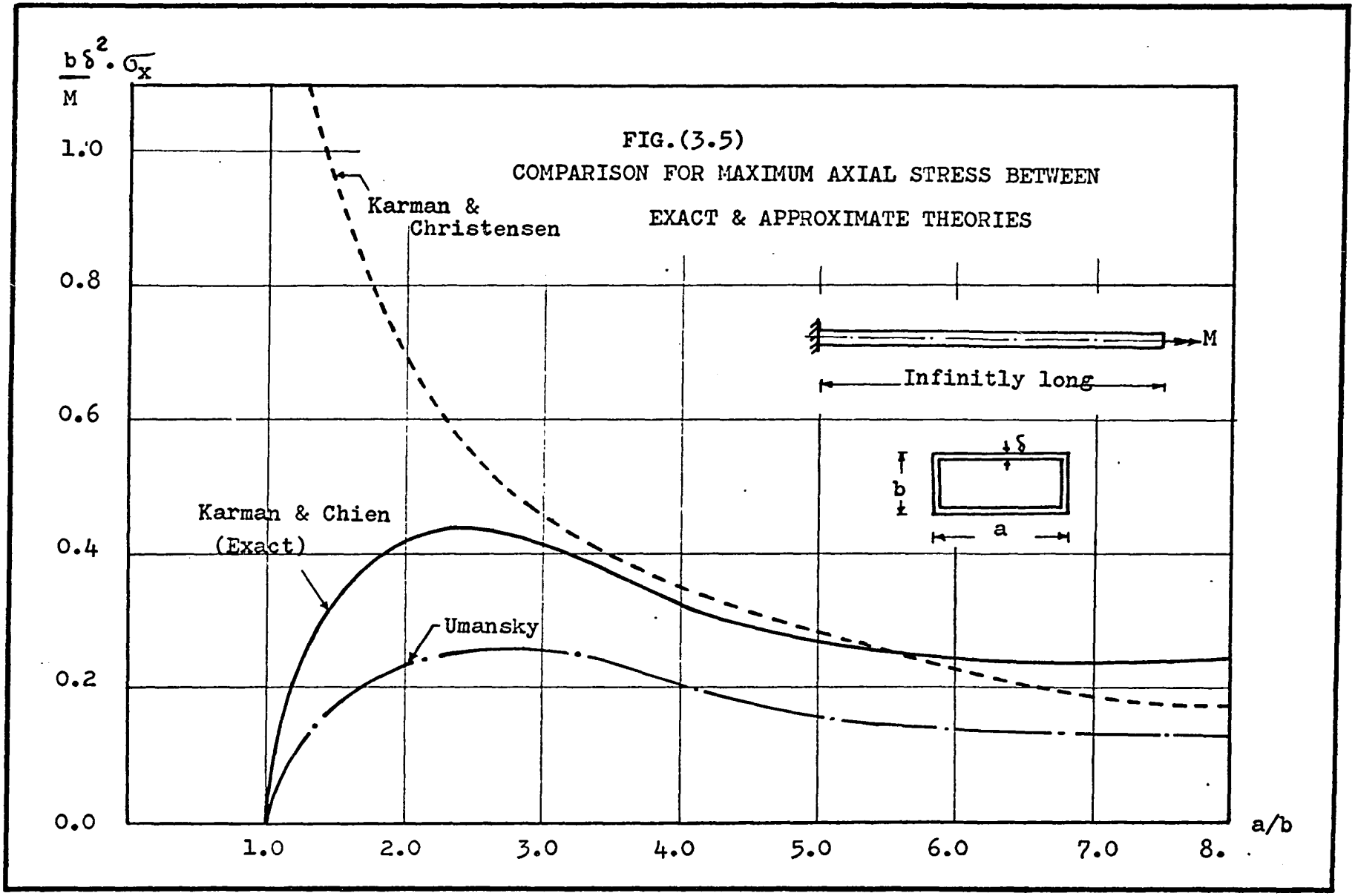

FIG.(3.5)

COMPARISON FOR MAXIMUM AXIAL STRESS BETWEEN

EXACT & APPROXIMATE THEORIES

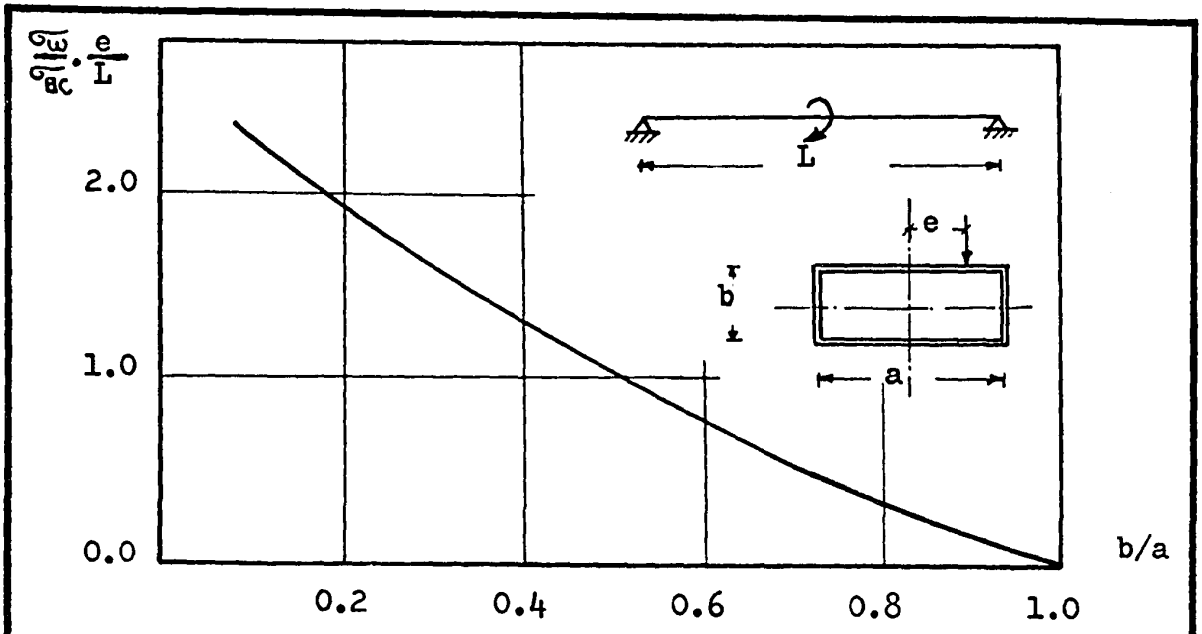

FIG.(3.6)

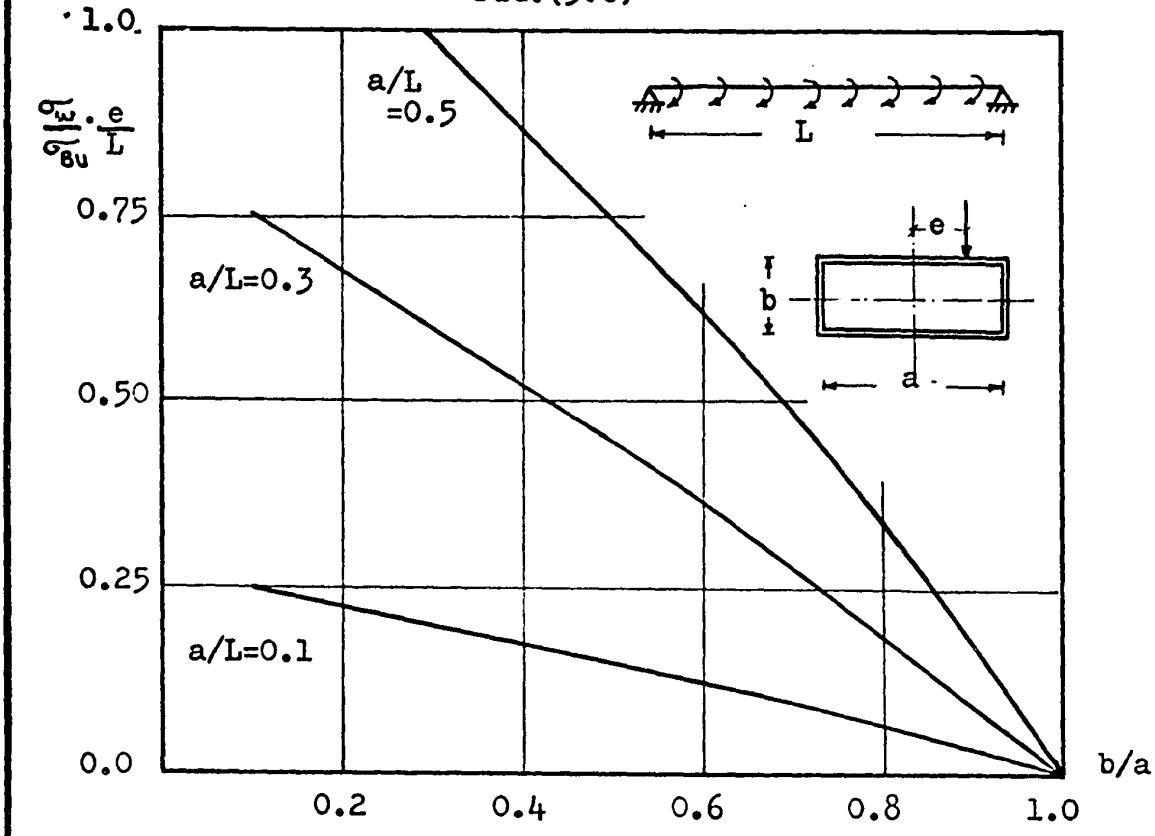

FIG.(3.7)

EFFECT OF SHAPE RATIO ON RATIO OF AXIAL STRESS DUE TO TORSION BENDINDING TO FLEXURE STRESS, FOR BEAMS OF NON-DEFORMABLE SECTIONS

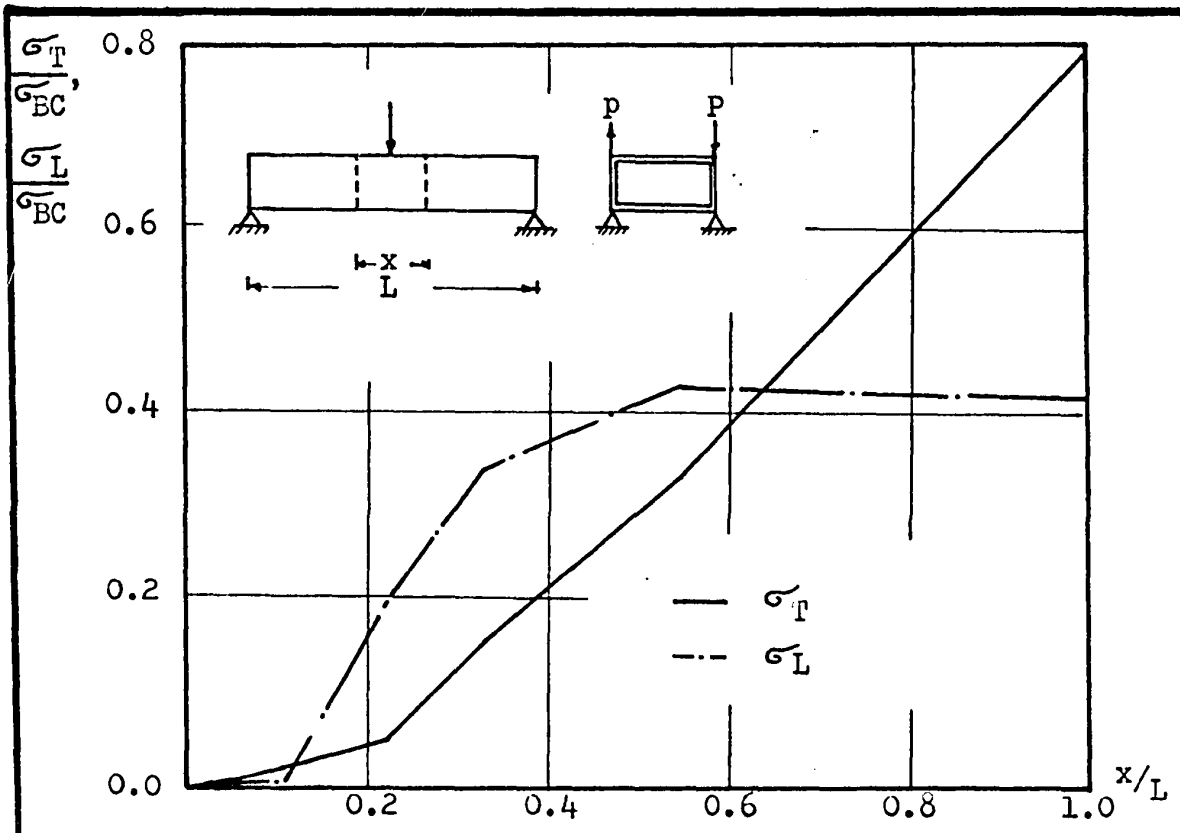

FIG. (3.8)

EFFECT OF DIAPHRAGM LOCATION ON σ_L and σ_T

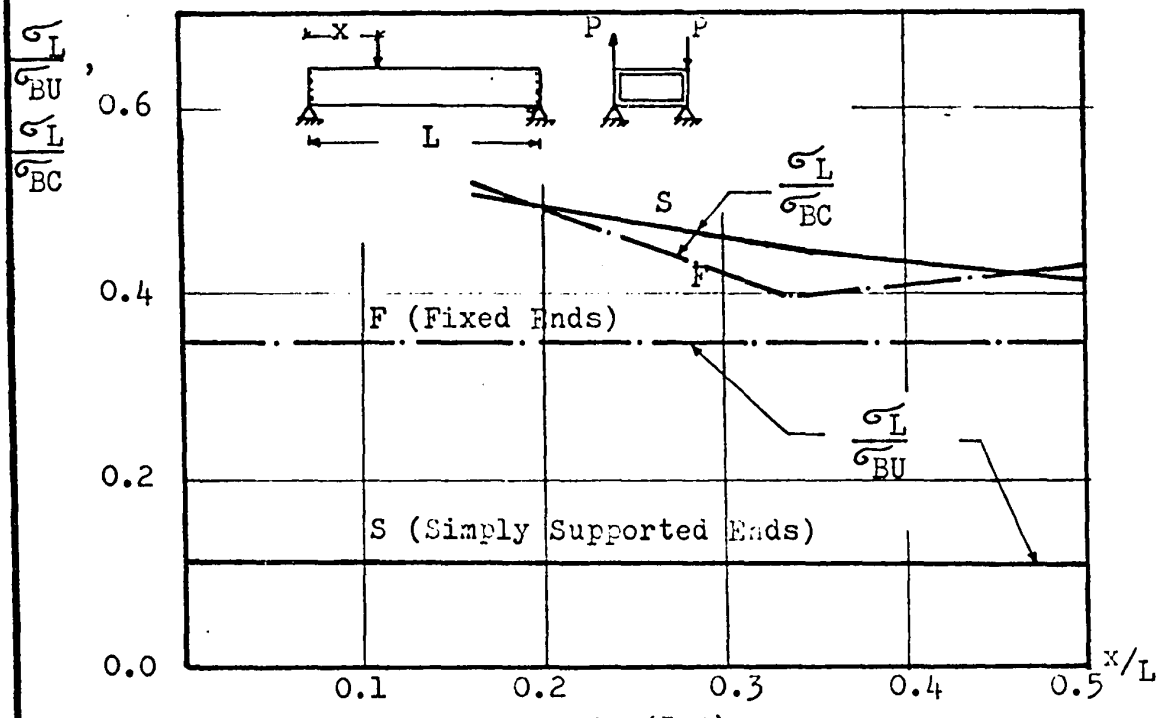

FIG. (3.9)

EFFECT OF LOADING AND END CONDITIONS ON MAX. LONGITUDINAL STRESS σ_L

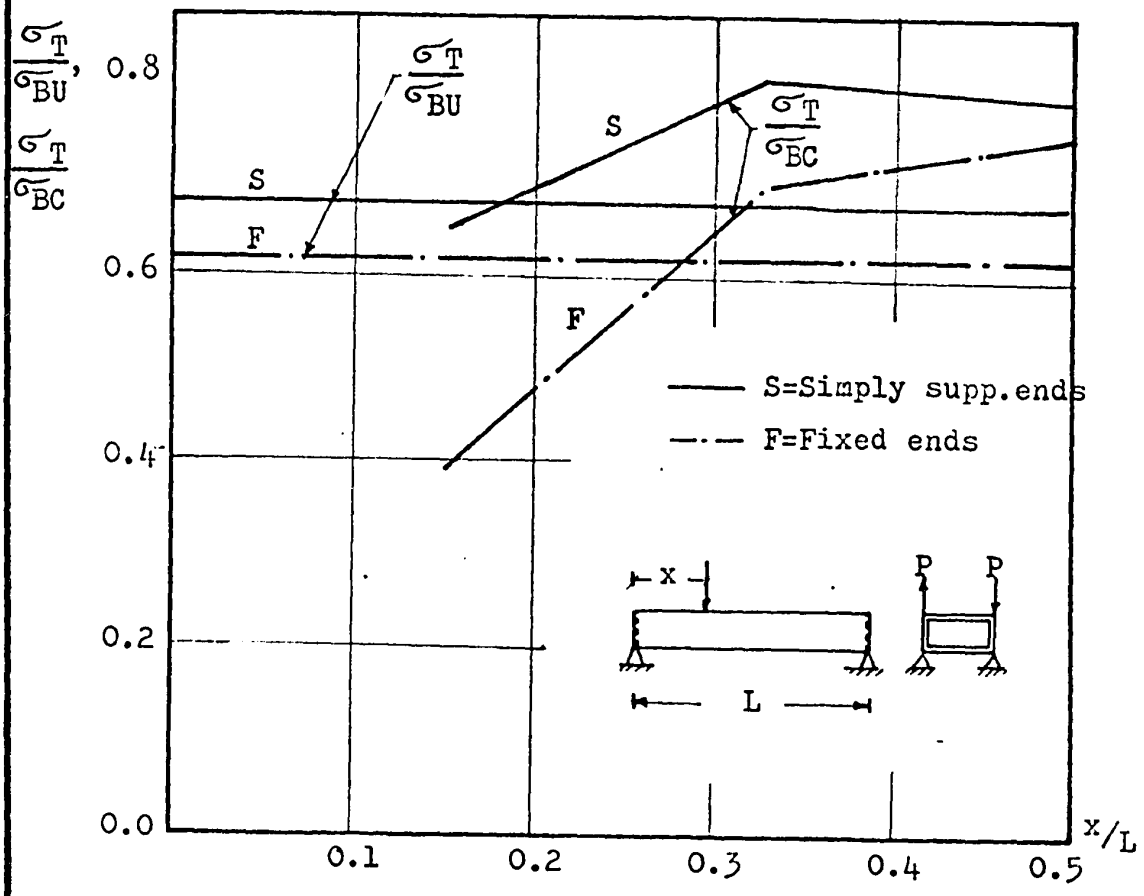

FIG. (3.10)

EFFECT OF LOADING AND END CONDITIONS ON MAXIMUM TRANSVERSE STRESS σ_T

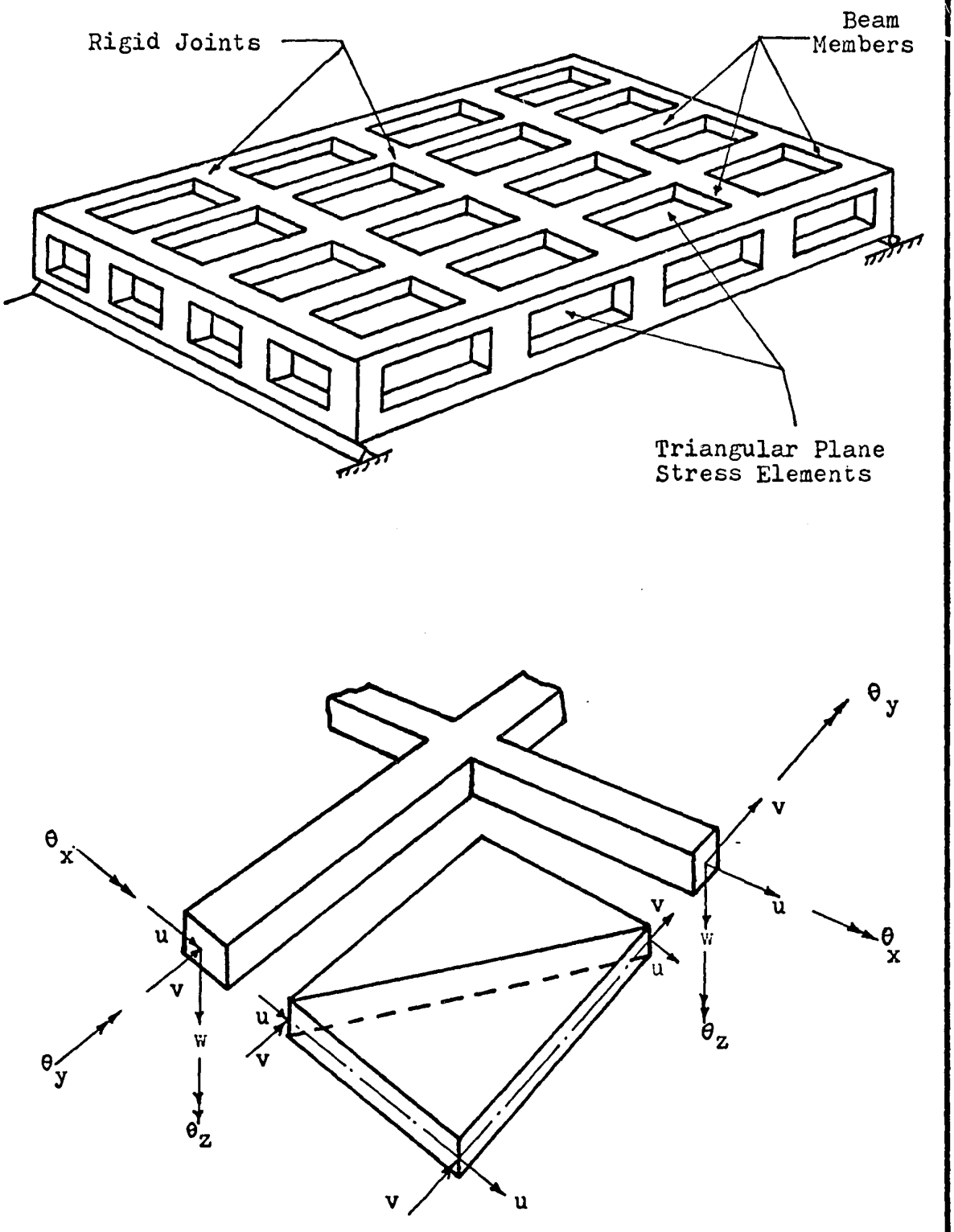

FIG. (4.1)

IDEALIZATION OF A BOX GIRDER BRIDGE BY EQUIVALENT GRIDWORK AND PLANE STRESS TRIANGULAR ELEMENTS

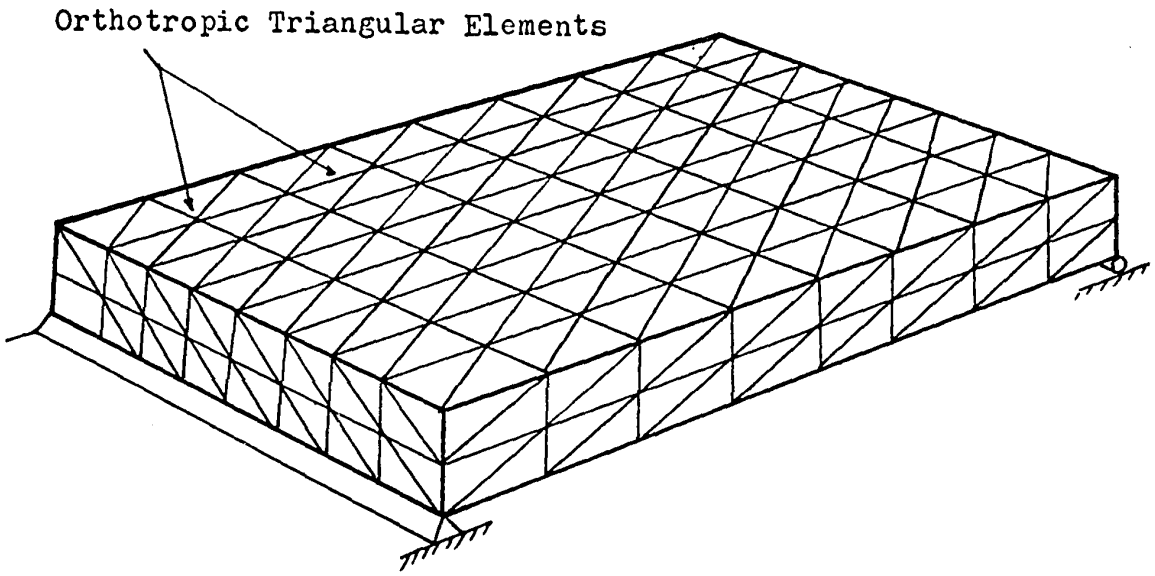

FIG. (4.2)
IDEALIZATION OF A BOX GIRDER BRIDGE BY EQUIVALENT ORTHOTROPIC TRIANGULAR ELEMENTS

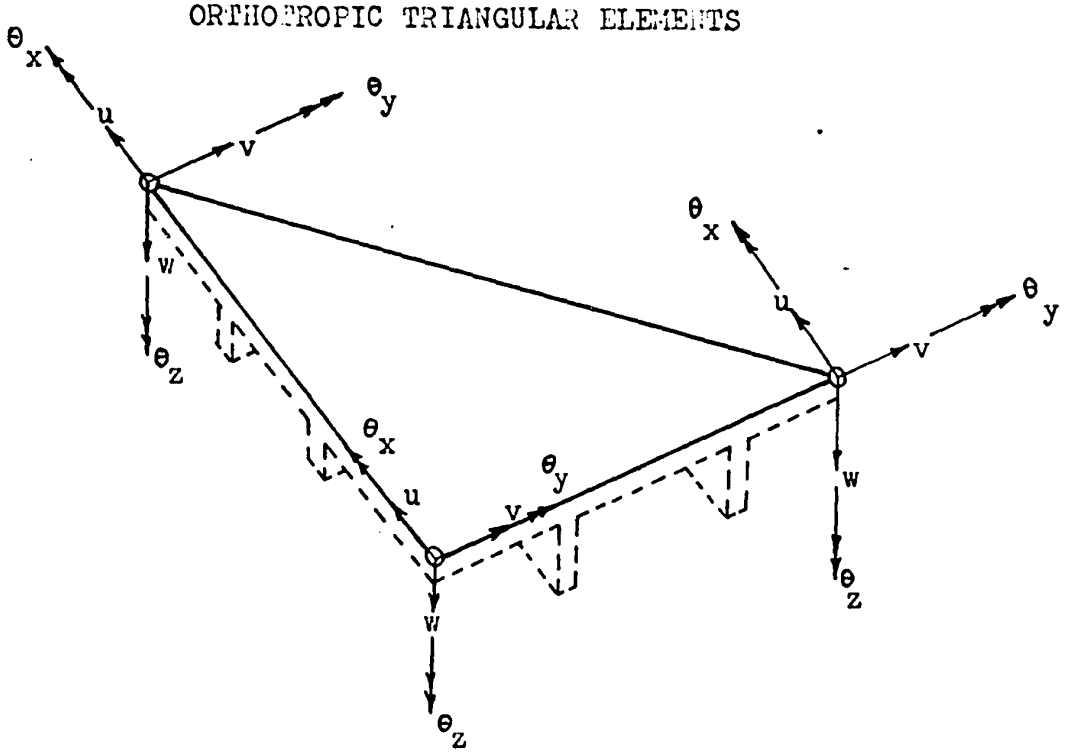

FIG. (4.3)
ORTHOTROPIC PLATE ELEMENT

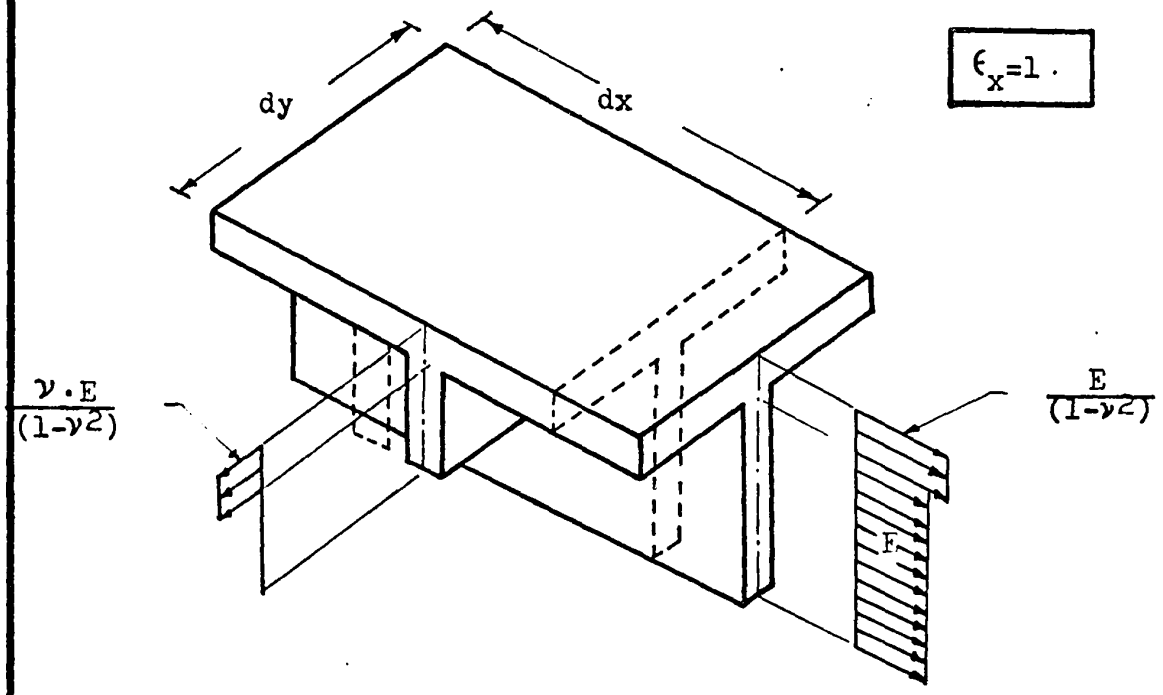

FIG. (4.4)
STRESSES IN AN ORTHOTROPIC ELEMENT DUE TO UNIT AXIAL STRAIN IN THE X-DIRECTION .

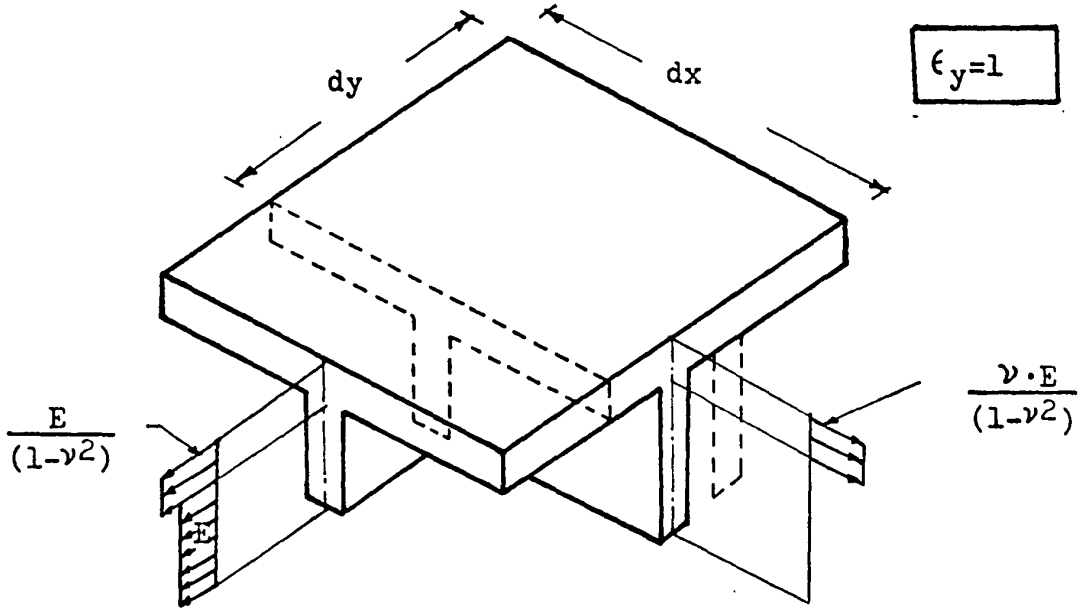

FIG. (4.5)
STRESSES IN AN ORTHOTROPIC ELEMENT DUE TO UNIT AXIAL STRAIN IN THE Y-DIRECTION

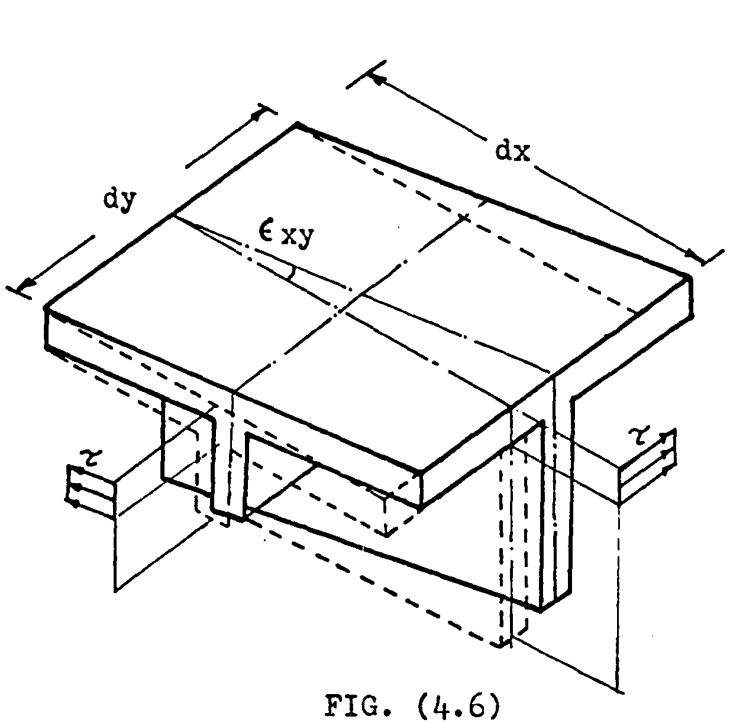

FIG. (4.6)

STRESSES IN AN ORTHOTROPIC ELEMENT DUE TO UNIT IN-PLANE SHEAR STRAIN

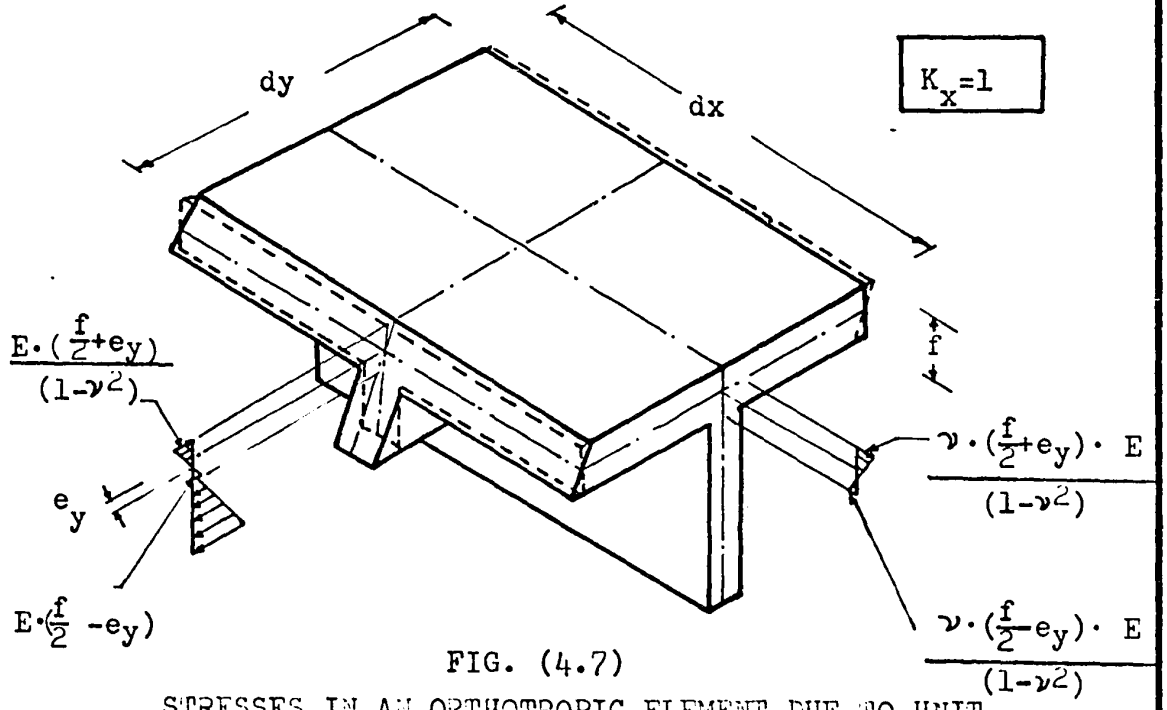

FIG. (4.7)

STRESSES IN AN ORTHOTROPIC ELEMENT DUE TO UNIT CURVATURE IN THE Y-DIRECTION

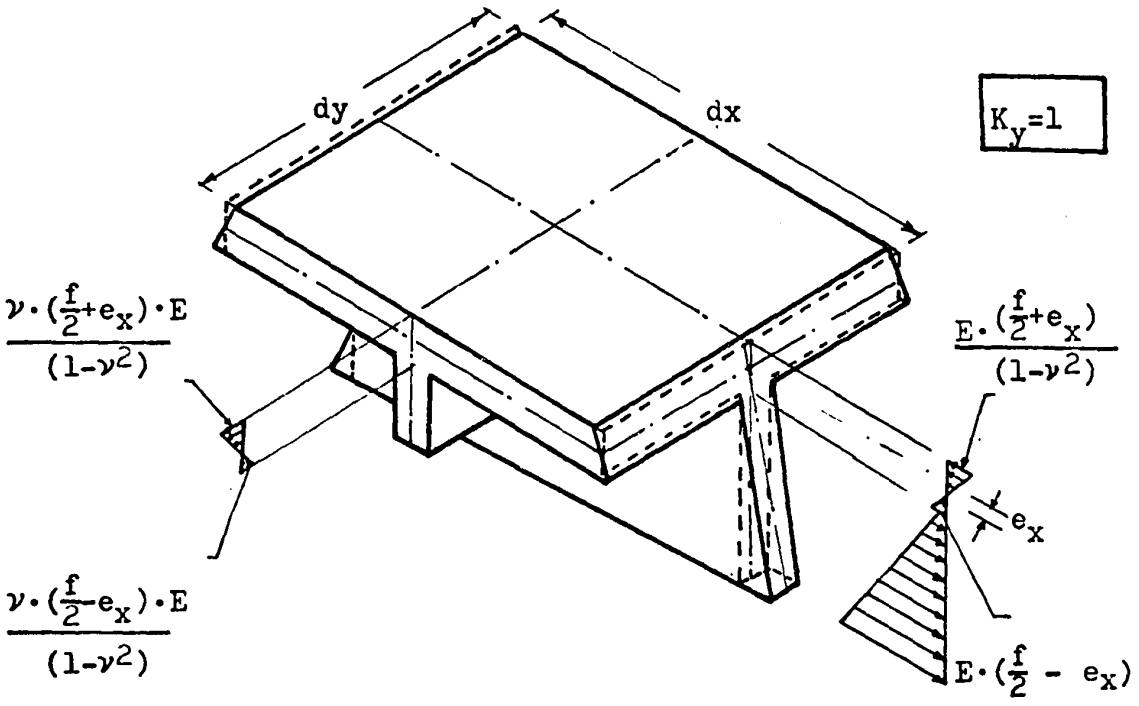

FIG. (4.8)

STRESSES IN AN ORTHOTROPIC ELEMENT DUE TO UNIT CURVATURE IN THE X-DIRECTION

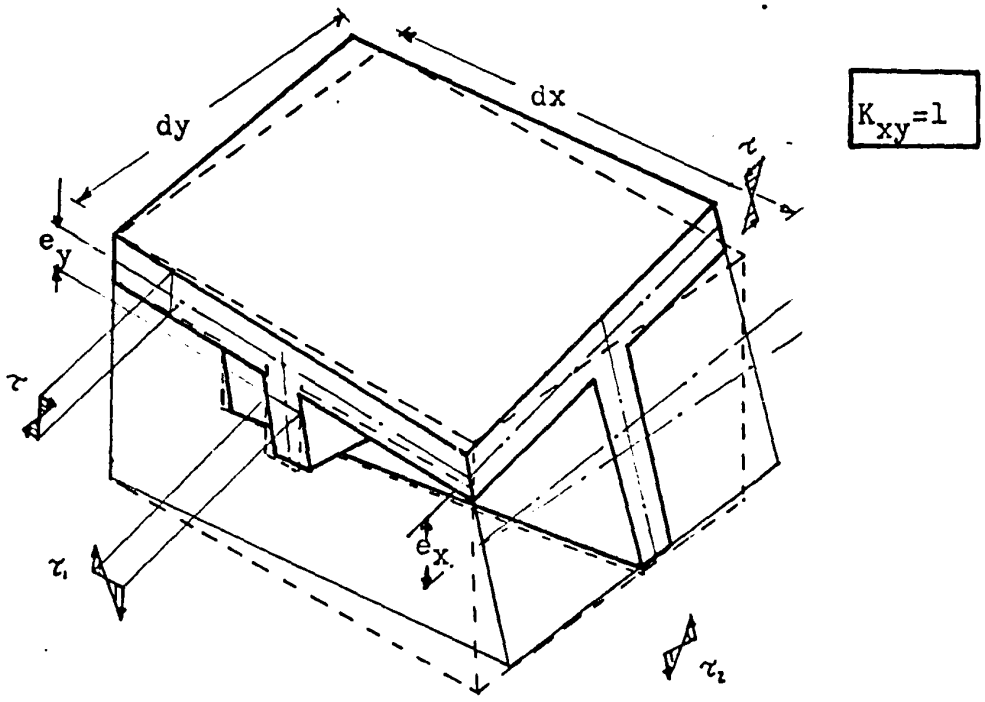

FIG. (4.9)

STRESSES IN AN ORTHOTROPIC ELEMENT DUE TO UNIT TORSIONAL STRAIN

Fig. (4.10)

FORM OF SUBDIVISIONS USED IN THE IDEALIZATION PROGRAM

Length	A_1	A_2	A_2	A_1
No. of Divisions	K_1	K_2	K_2	K_1
Size of Mesh	$\frac{A_1}{K_1}$	$\frac{A_2}{K_2}$	$\frac{A_2}{K_2}$	$\frac{A_1}{K_1}$

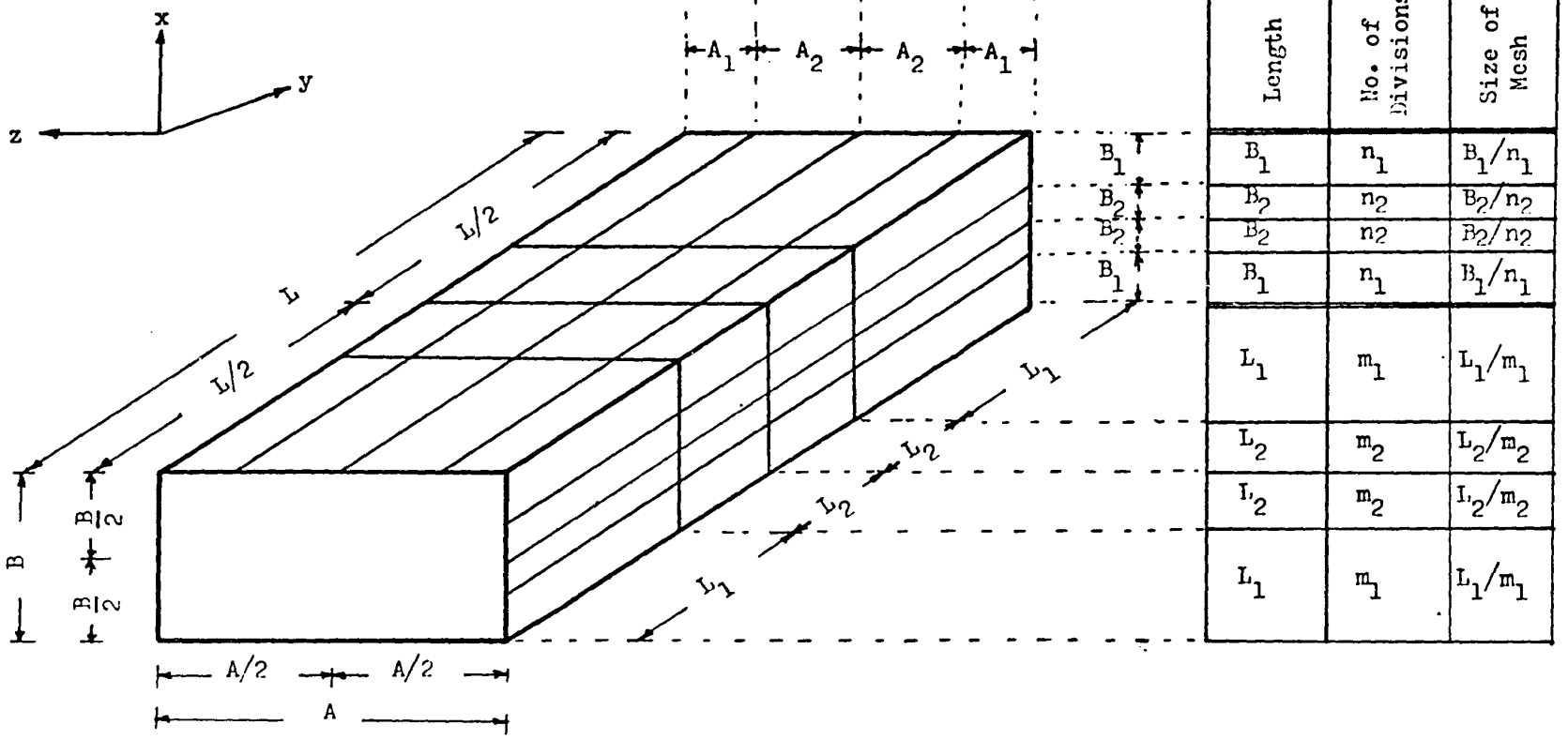

Length	No. of Divisions	Size of Mesh
B_1	n_1	B_1/n_1
B_2	n_2	B_2/n_2
B_2	n_2	B_2/n_2
B_1	n_1	B_1/n_1
L_1	m_1	L_1/m_1
L_2	m_2	L_2/m_2
L_2	m_2	L_2/m_2
L_1	m_1	L_1/m_1

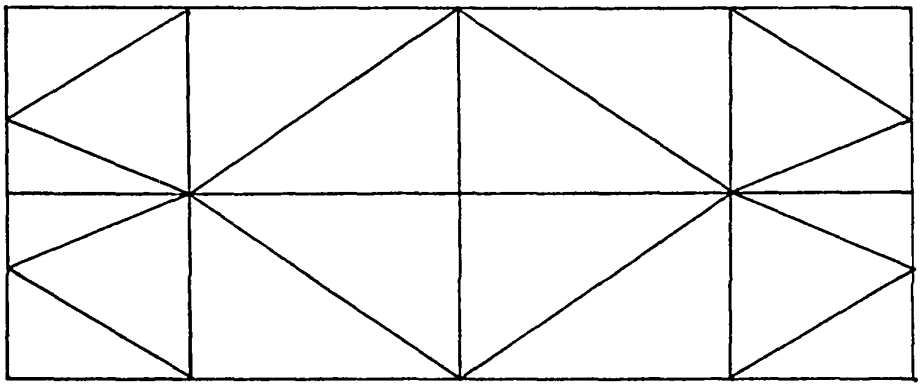

FIG. (4.11)

FORM OF SUBDIVISIONS USED IN IDEALIZING THE PLATE DIAPHRAGMS

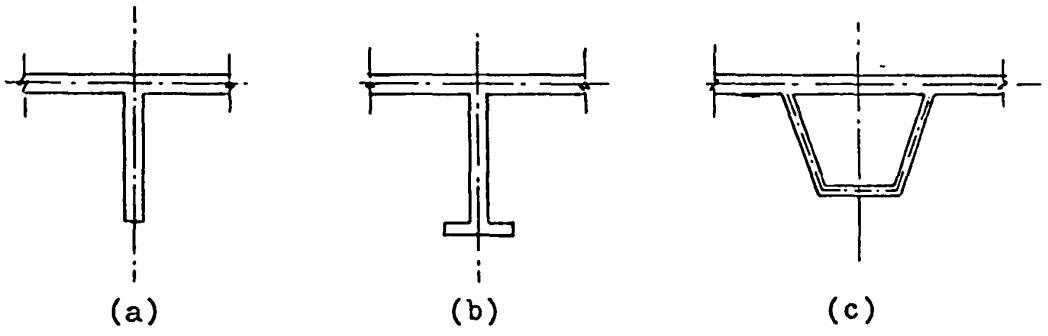

FIG. (4.12)

GEOMETRY OF THE STIFFENERS WHICH CAN BE USED IN THE PROGRAM

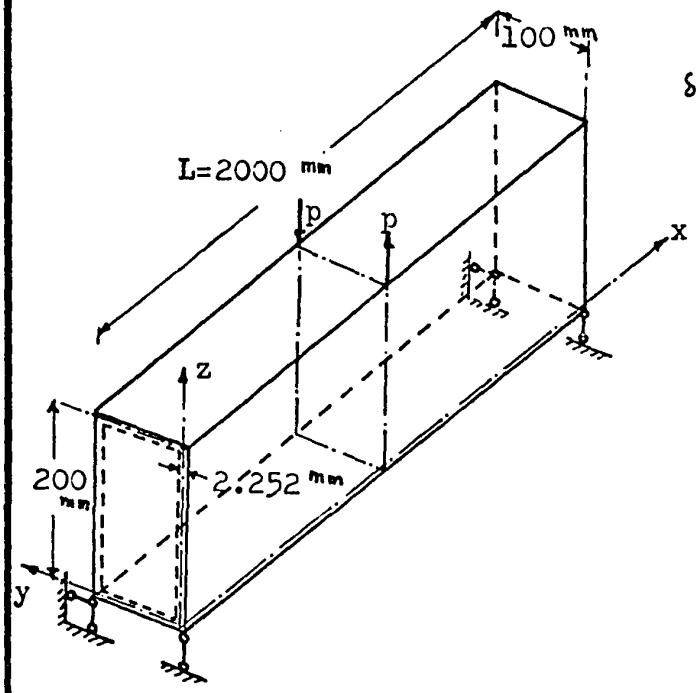

FIG. (4.13)
ISOTROPIC BOX GIRDER MODEL

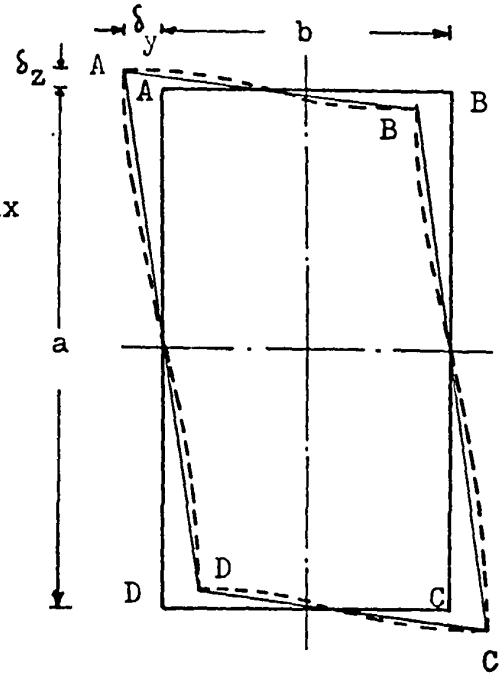

FIG. (4.14)
DISTORTIONAL DEFORMATIONS OF THE MODEL CROSS SECTIONS

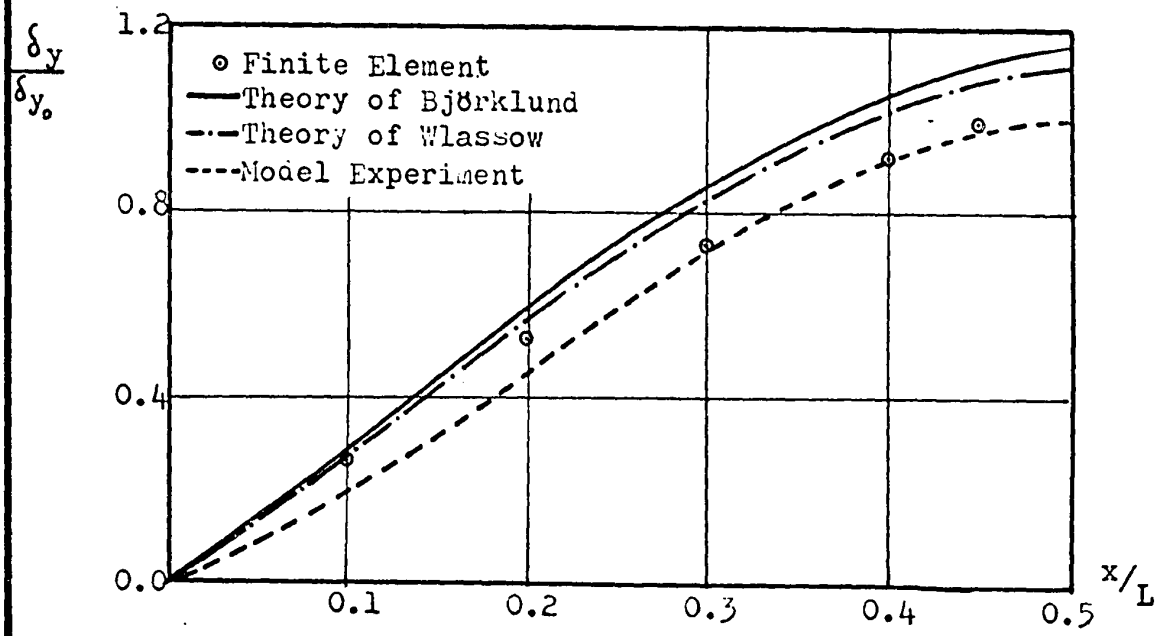

FIG. (4.15)
VARIATION OF DISTORTIONAL DEFORMATION (δ_y) ALONG $\frac{1}{2}$ THE SPAN

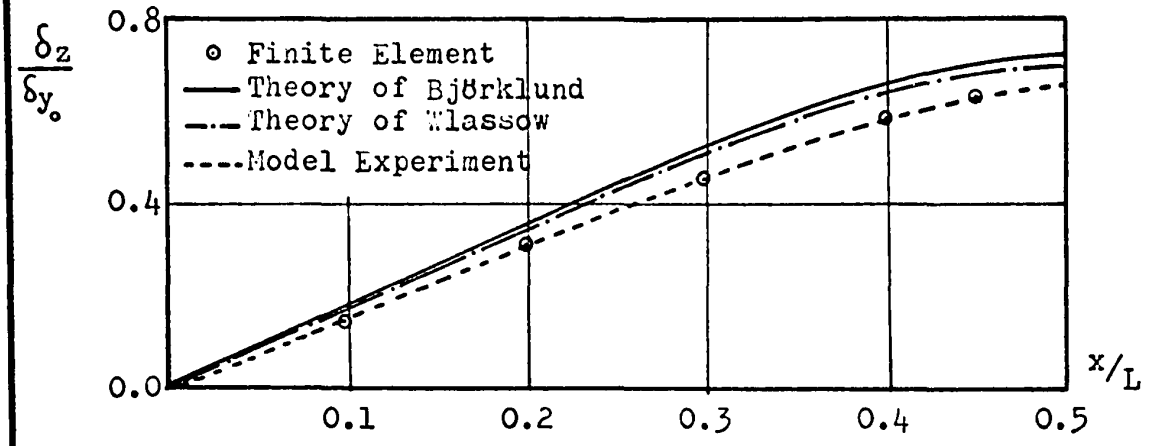

FIG. (4.16)

VARIATION OF DISTORTIONAL DEFORMATION (δ_z) ALONG $\frac{1}{2}$ THE SPAN

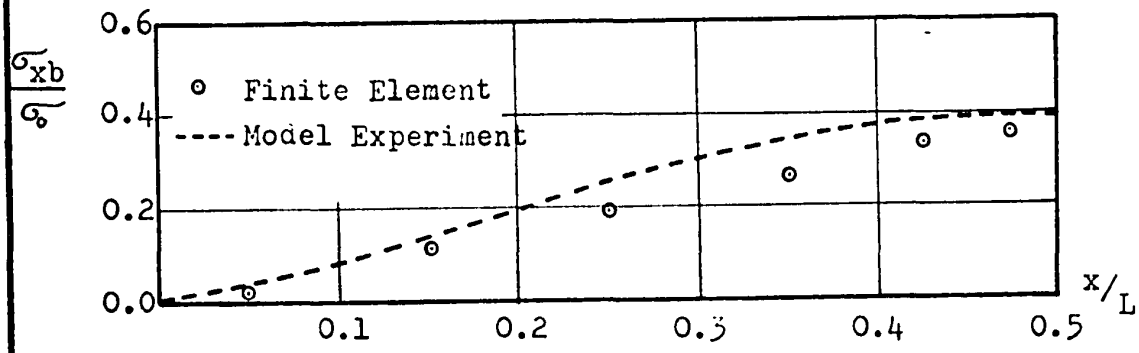

FIG. (4.17)

VARIATION OF LONGITUDINAL BENDING STRESS σ_{xb} ALONG $\frac{1}{2}$ THE SPAN

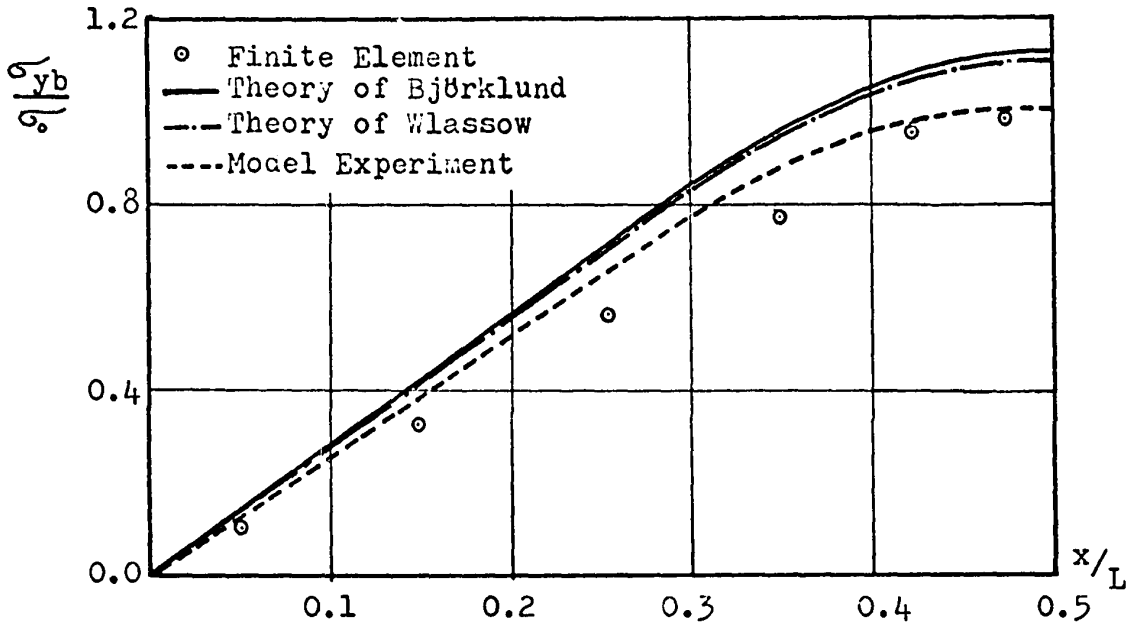

FIG. (4.18)

VARIATION OF THE TRANSVERSE BENDING STRESS σ_{zb} & σ_{yb} ALONG ½ THE SPAN

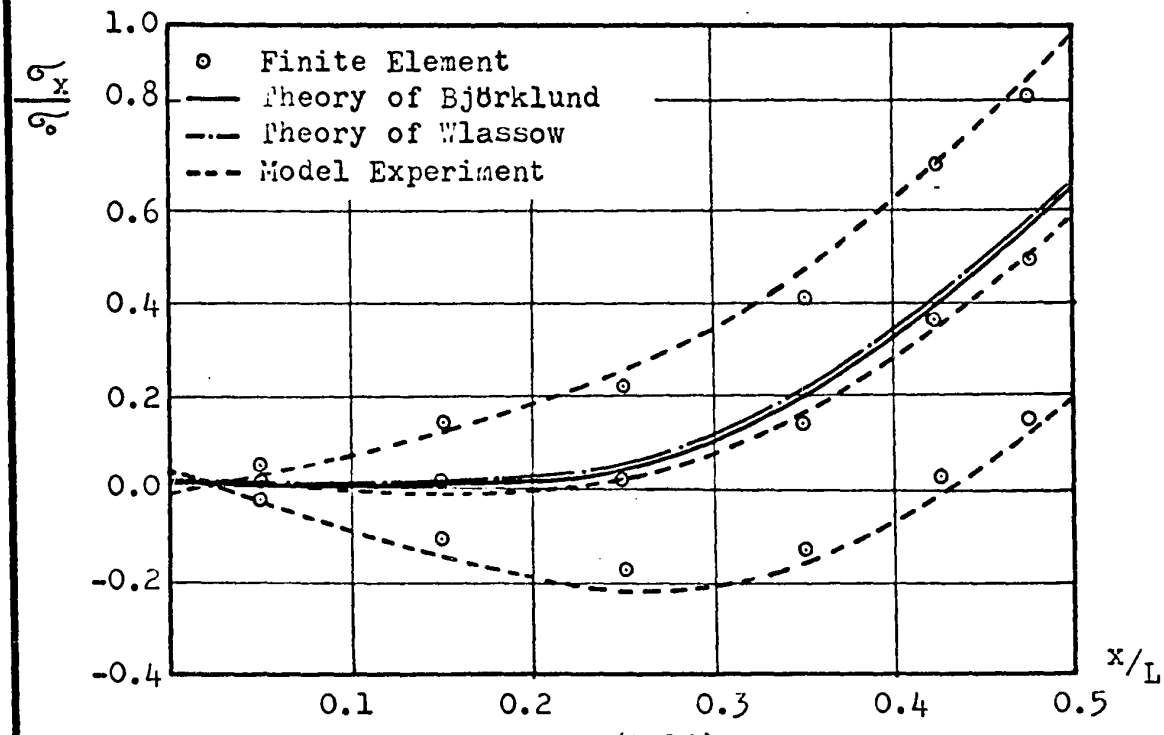

FIG. (4.19)

VARIATION ALONG ½ THE SPAN OF THE LONGITUDINAL STRESSES AT TOP, MIDDLE AND BOTTOM OF THE PLATE

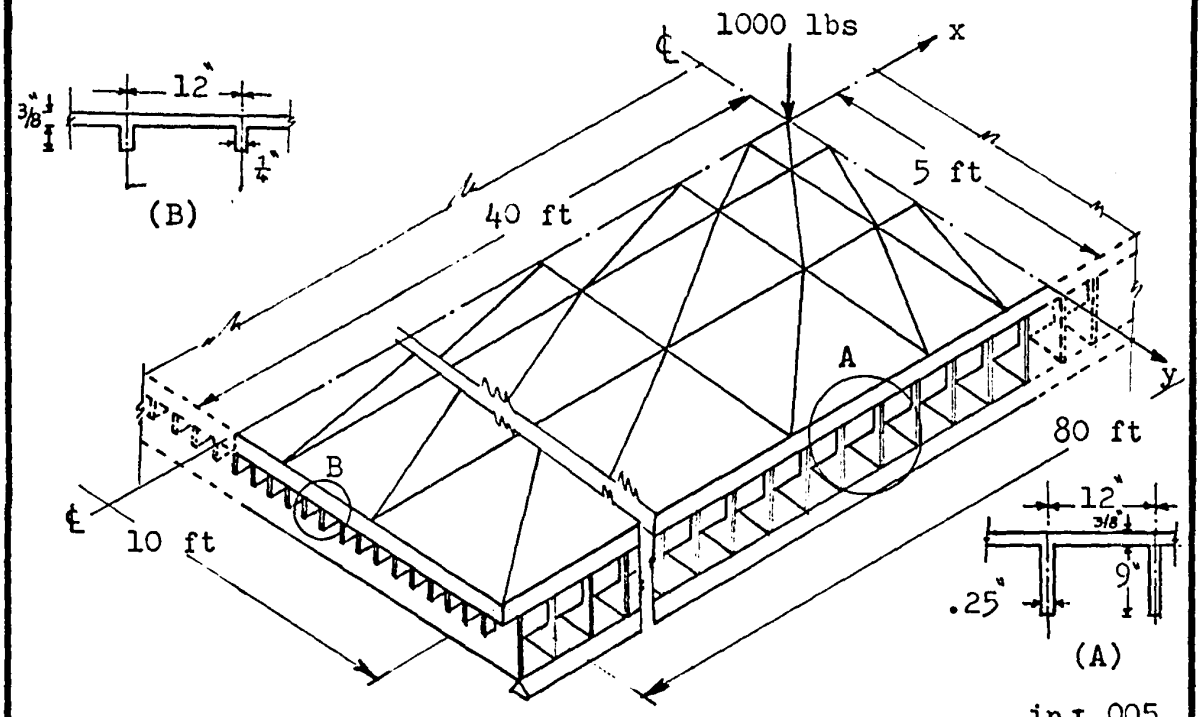

FIG. (4.20)
ORTHOTROPIC PLATE WITH 1-KIP
AT THE CENTER

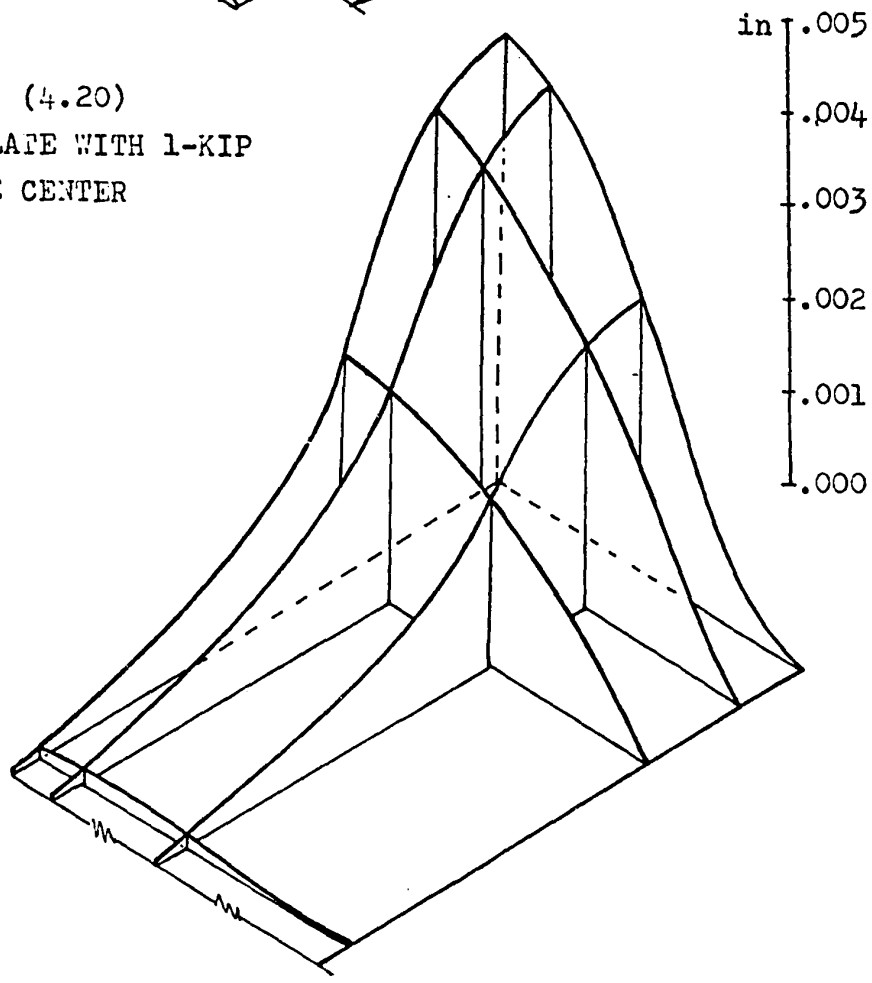

FIG. (4.21)
INFLUENCE SURFACE FOR THE VERTICAL DEFLECTION

FIG. (4.22)
INFLUENCE SURFACE FOR THE STRESS δ_y AT TOP OF THE DECK PLATE

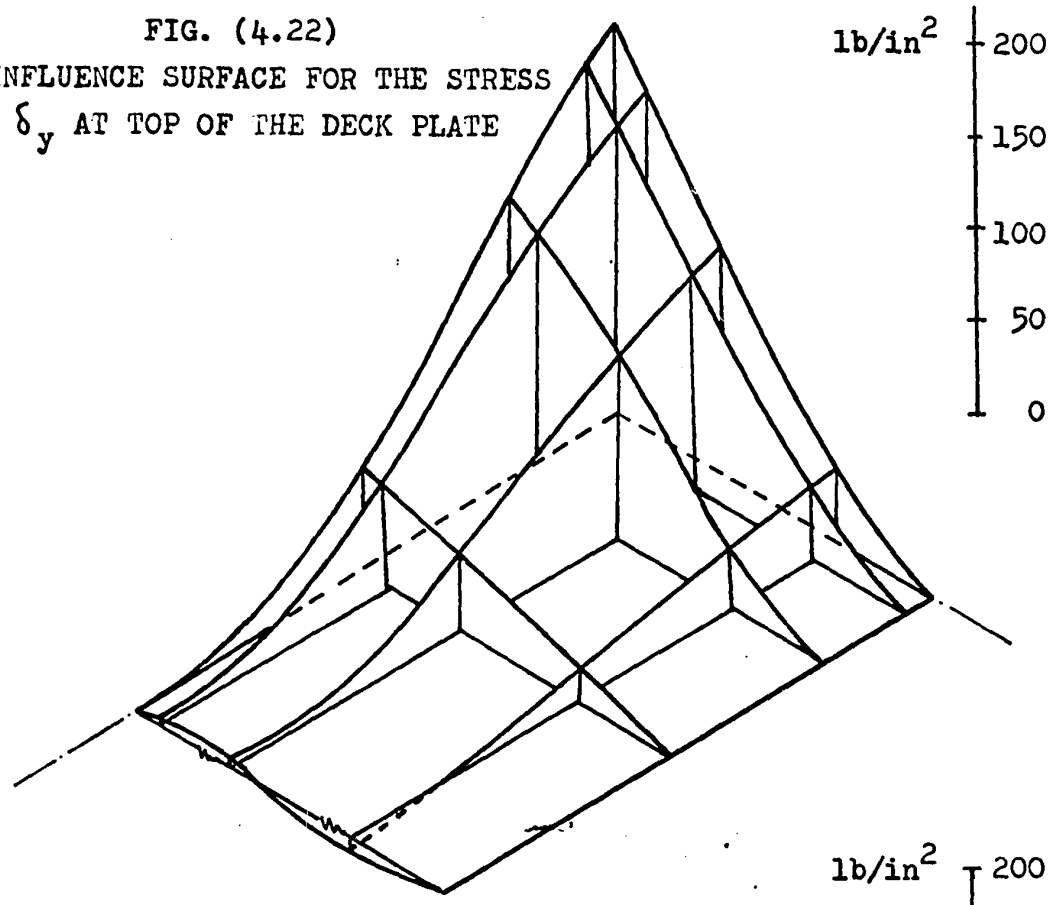

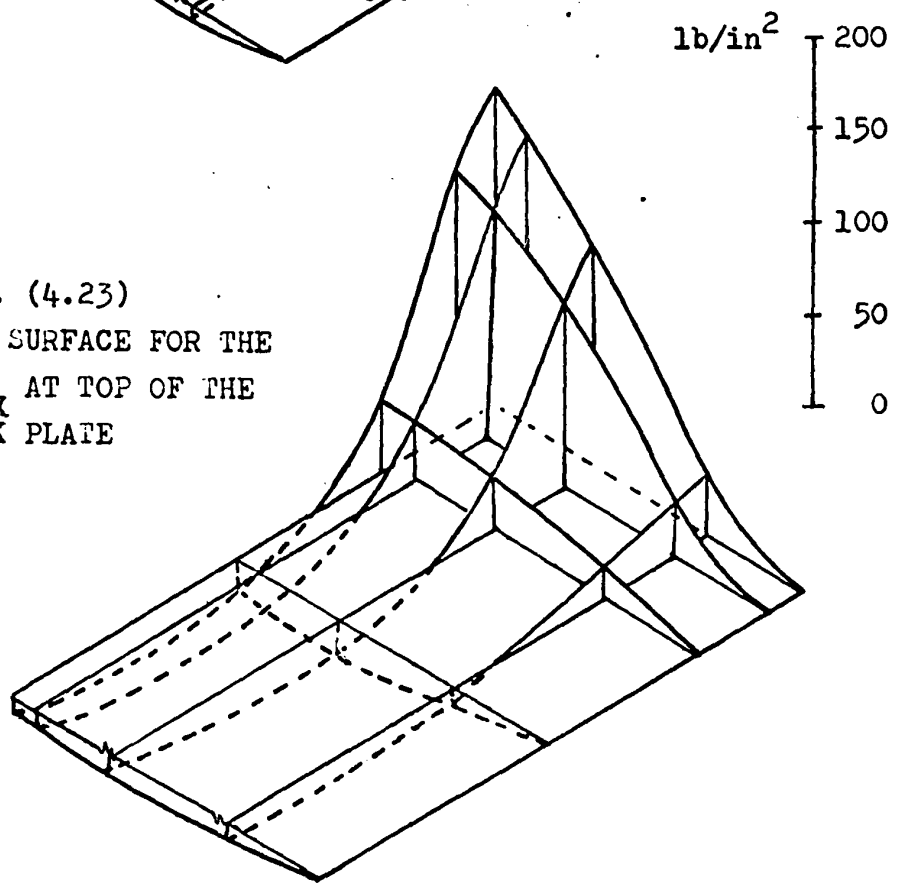

FIG. (4.23)
INFLUENCE SURFACE FOR THE STRESS σ_x AT TOP OF THE DECK PLATE

RIBS

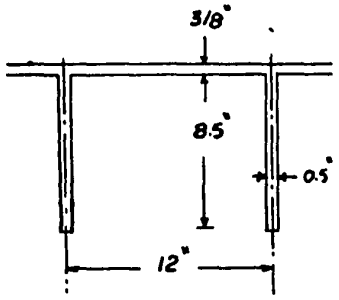

TYPE (A)

FLOOR BEAMS

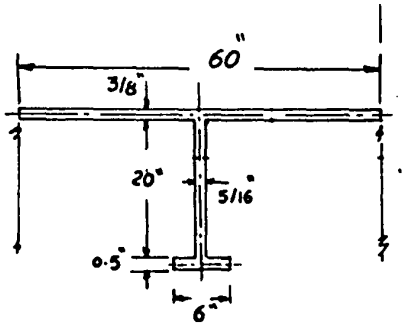

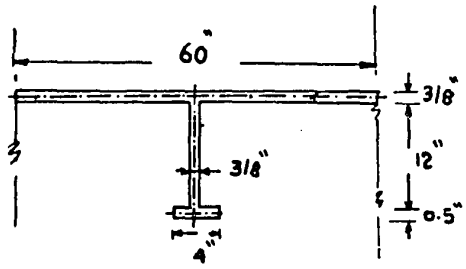

TYPE(B)

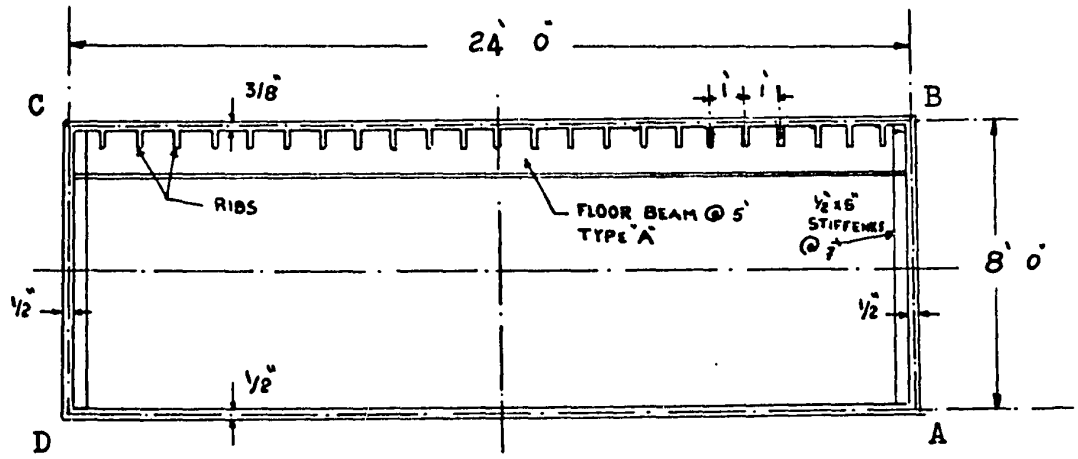

FIG. (5.1)

DETAILED CROSS - SECTION OF THE BRIDGES IN EXAMPLES (1) AND (6)

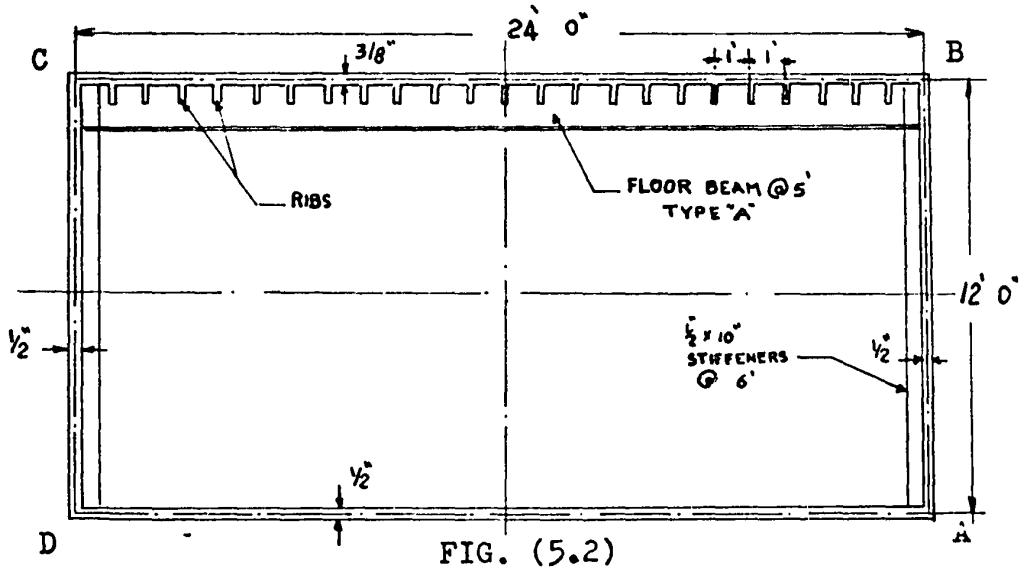

FIG. (5.2)

DETAILED CROSS - SECTION OF THE BRIDGES IN EXAMPLES (2) AND (7)

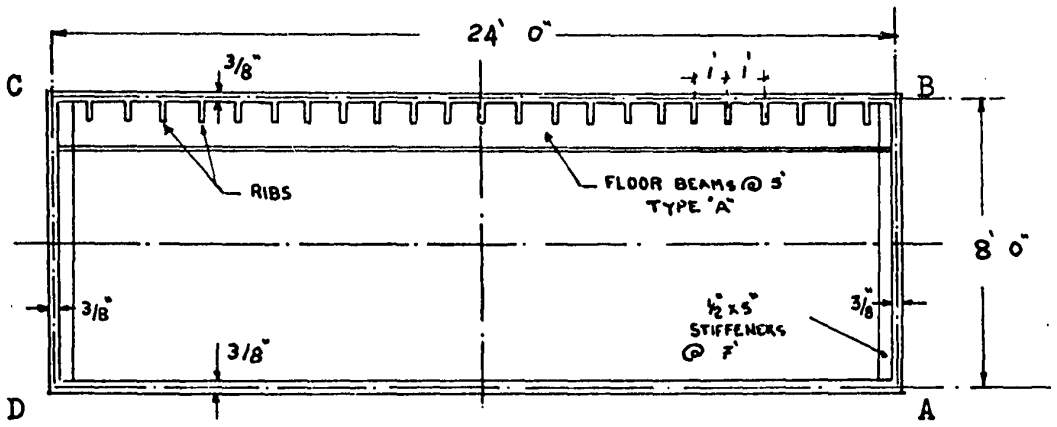

FIG. (5.3)

DETAILED CROSS-SECTION OF THE BRIDGE IN EXAMPLE (3)

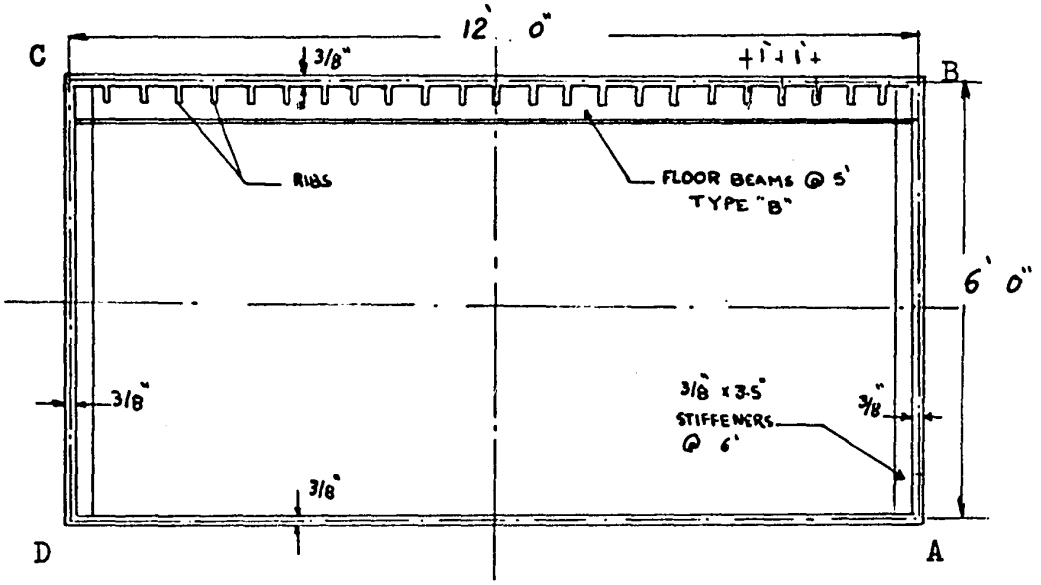

FIG. (5.4)

DETAILED CROSS-SECTION OF THE BRIDGE IN EXAMPLE (5)

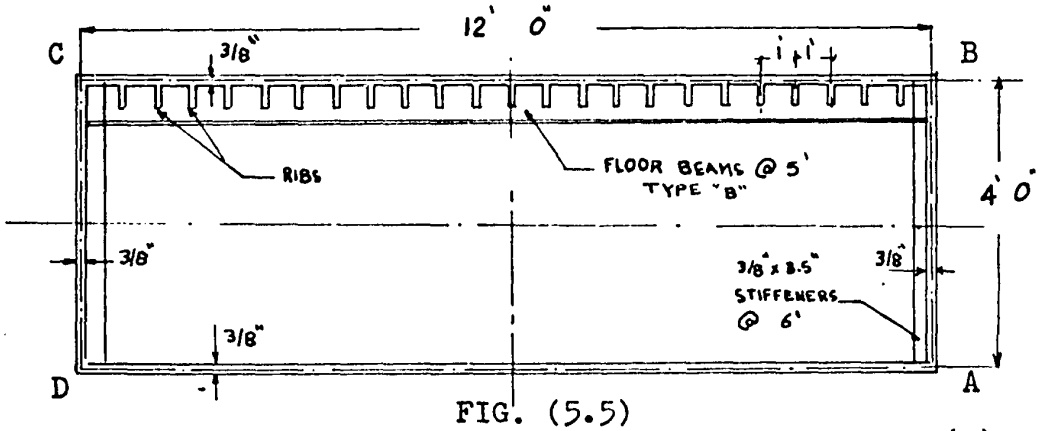

FIG. (5.5)

DETAILED CROSS-SECTION OF THE BRIDGES IN EXAMPLES (4) AND (8)

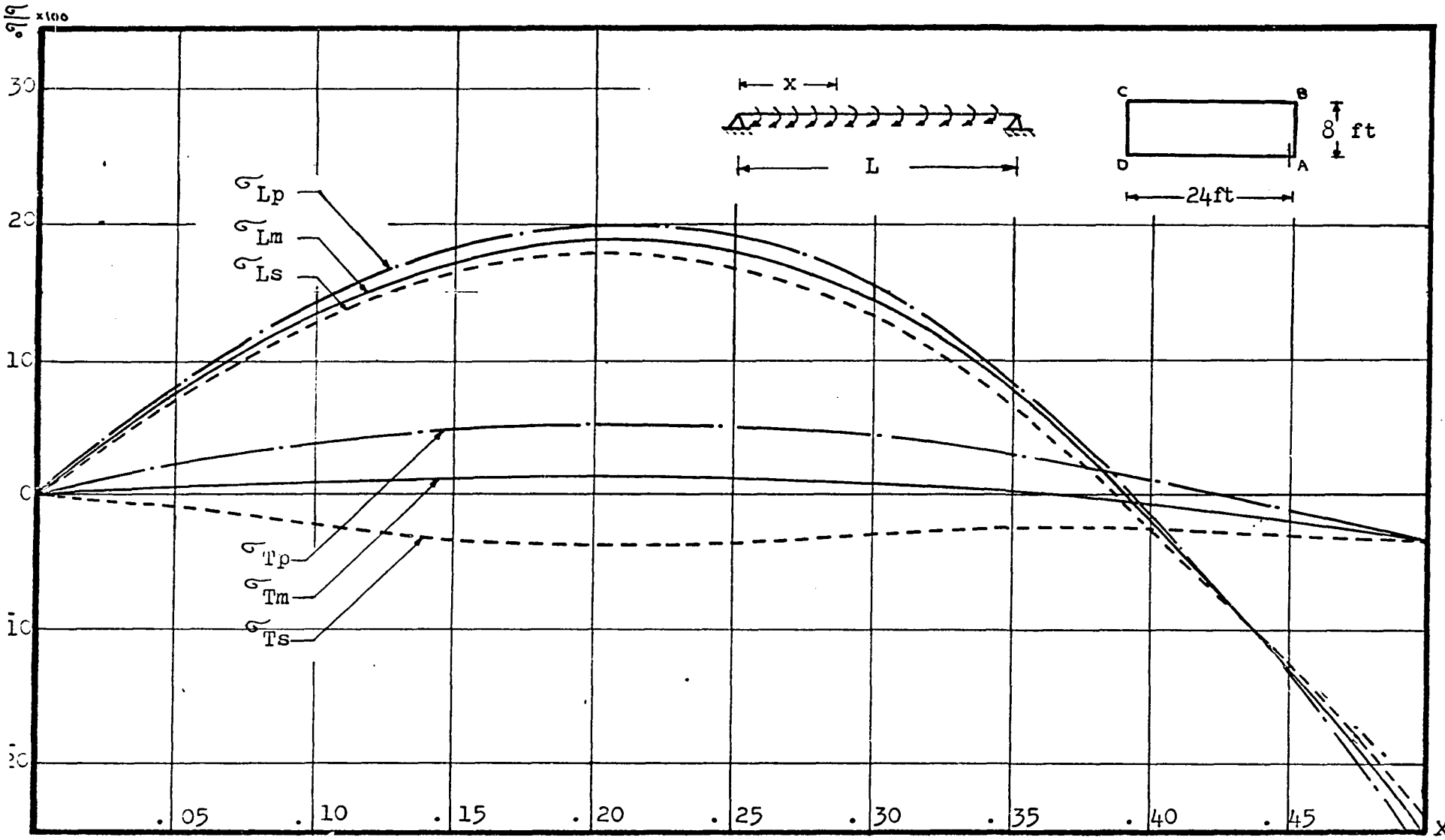

FIG. (5.6)
VARIATION OF STRESSES ALONG THE SPAN IN EXAMPLE (1)
AT SECTION AD

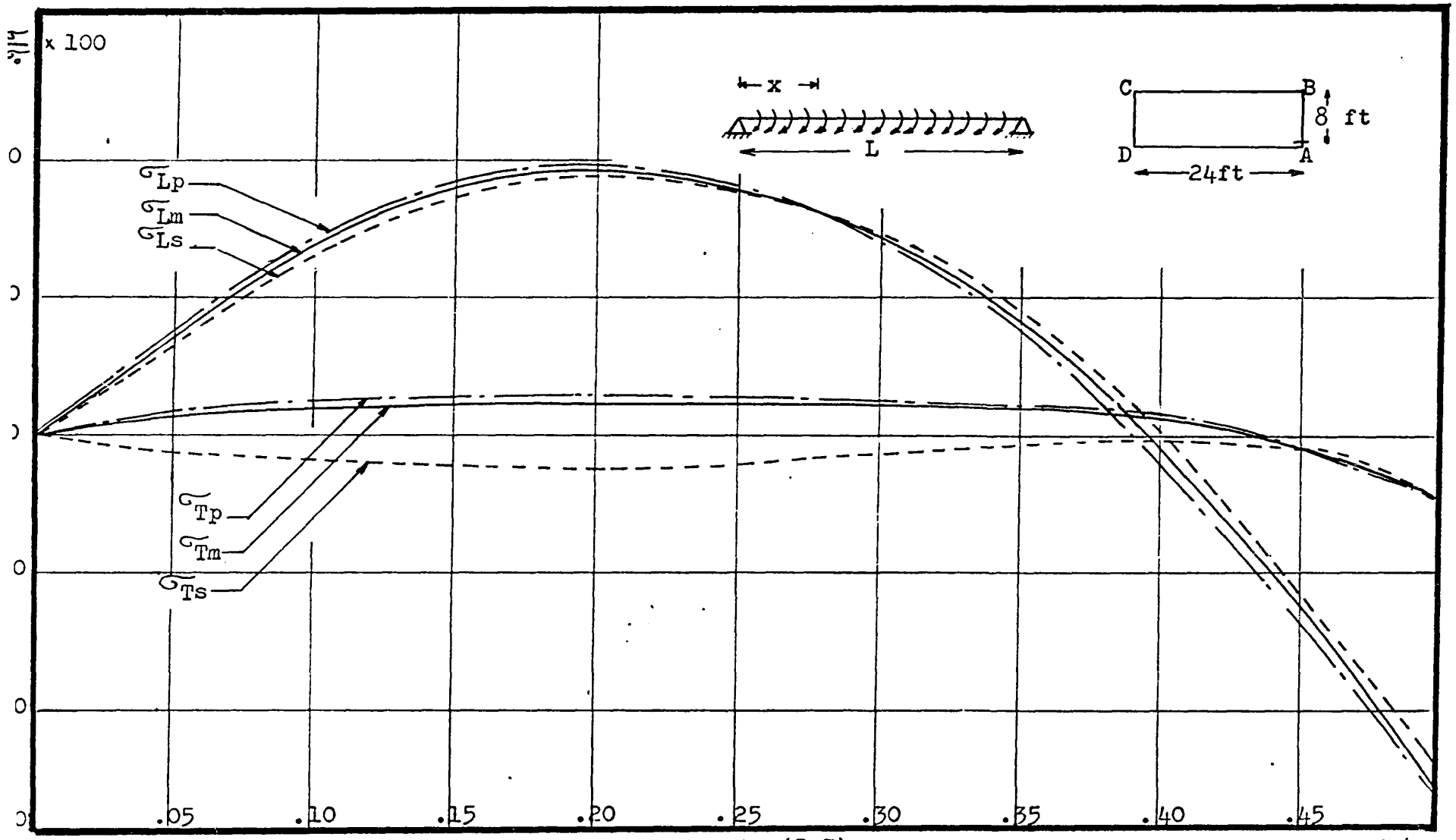

FIG. (5.7)
VARIATION OF STRESSES ALONG THE SPAN IN EXAMPLE (1)
AT SECTION AB

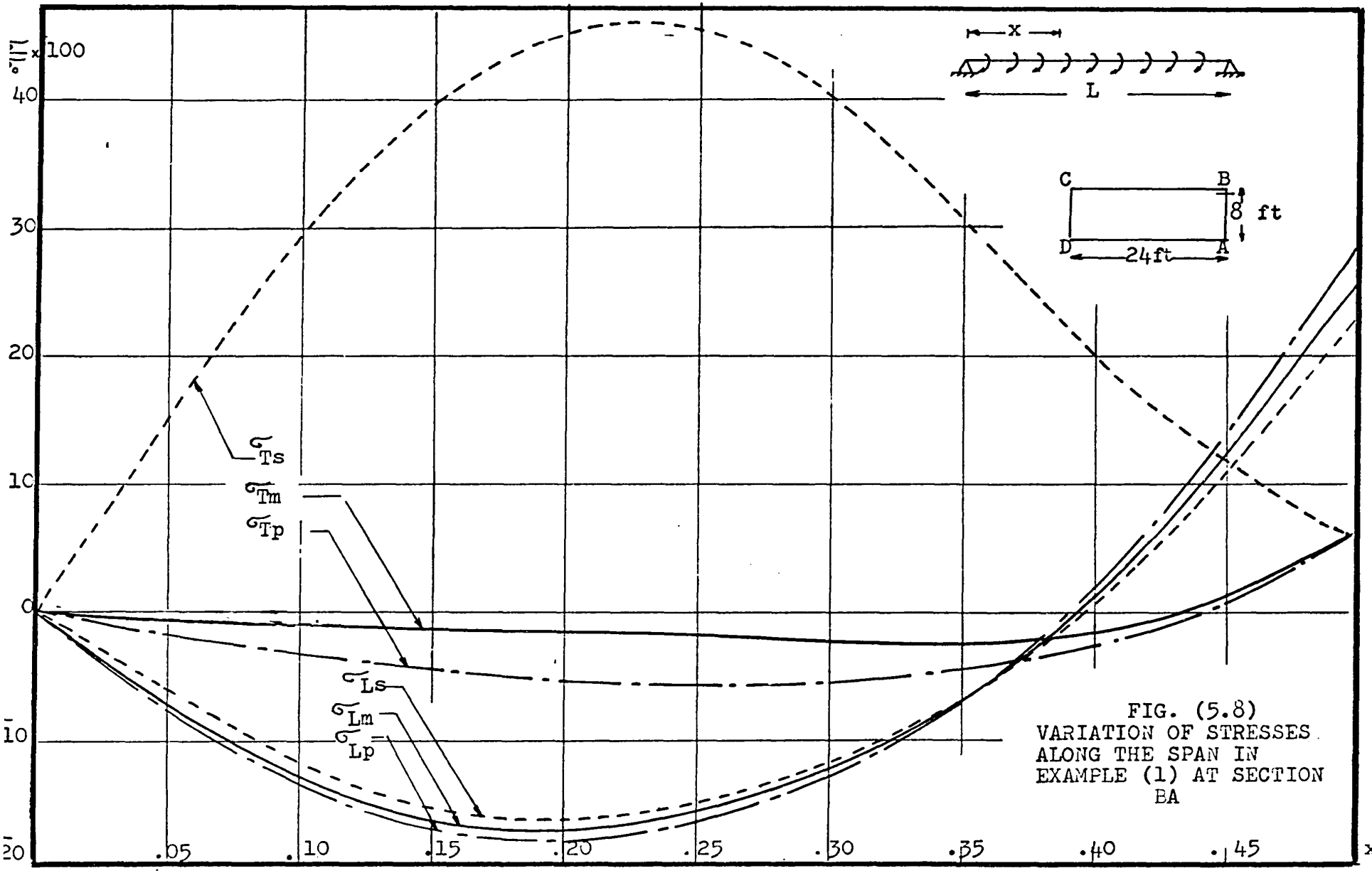

FIG. (5.8)
VARIATION OF STRESSES ALONG THE SPAN IN EXAMPLE (1) AT SECTION BA

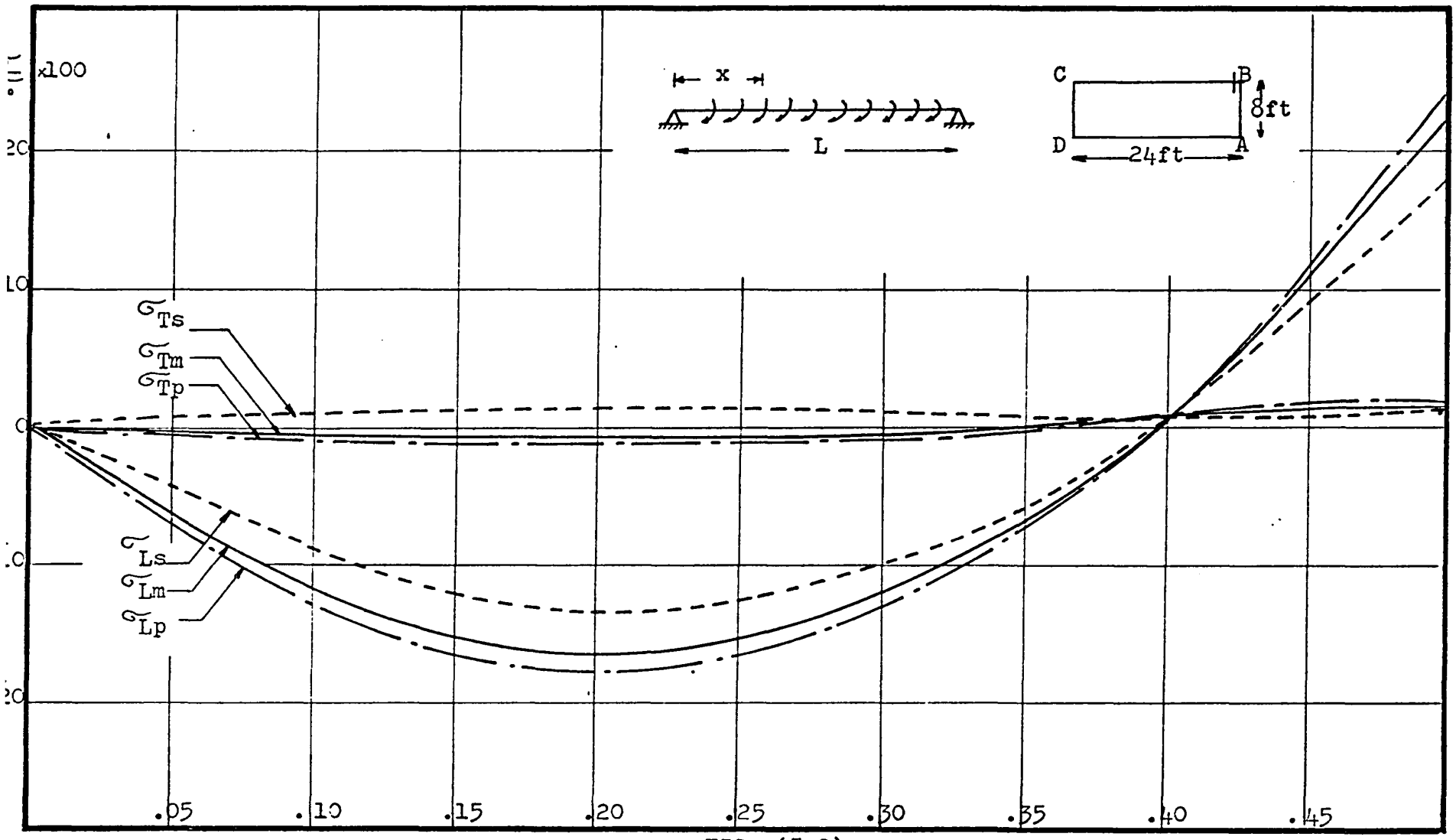

FIG. (5.9)
VARIATION OF STRESSES ALONG THE SPAN IN EXAMPLE (1)
AT SECTION BC

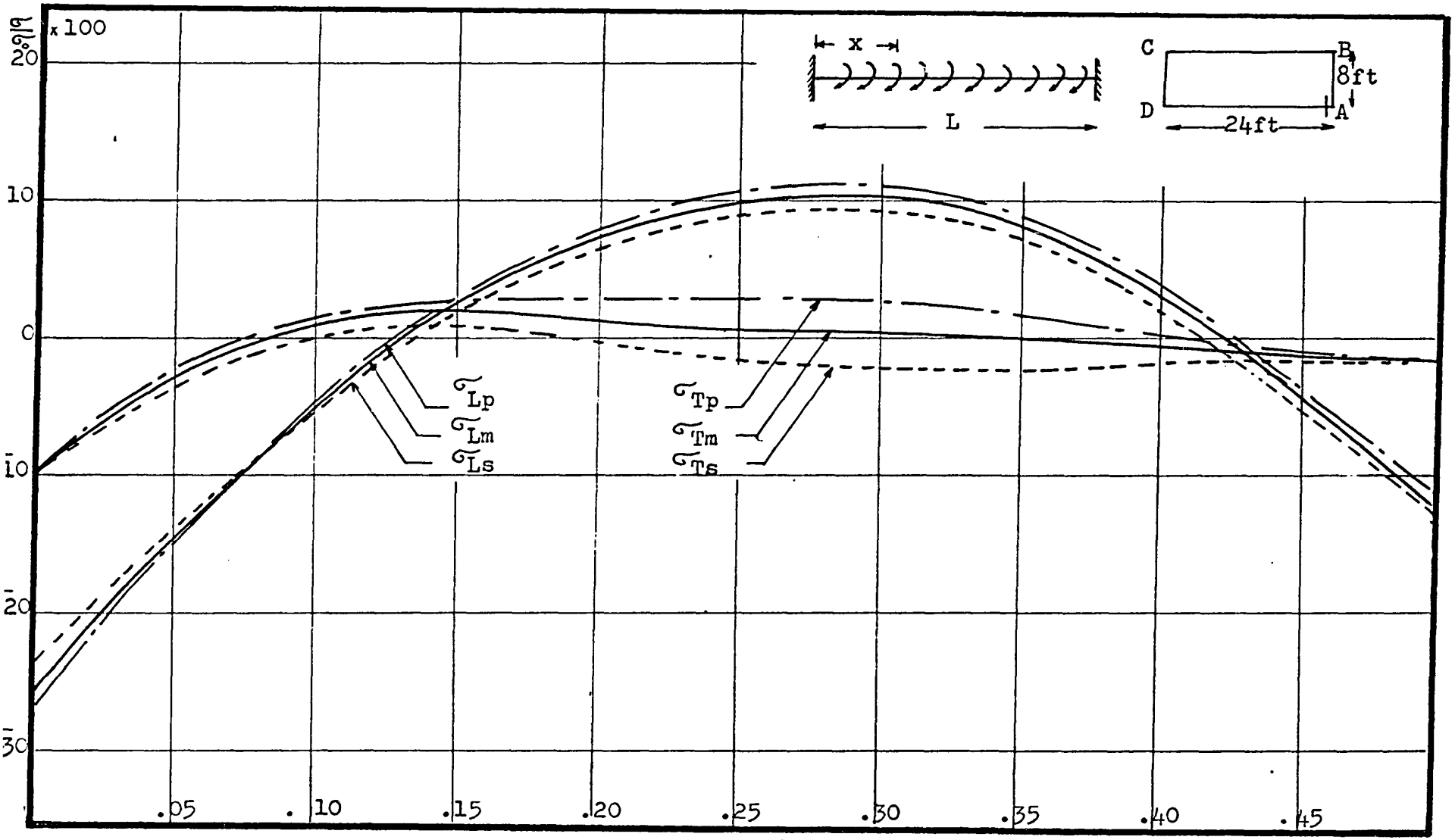

FIG. (5.10)
VARIATION OF STRESSES ALONG THE SPAN IN EXAMPLE (6)
AT SECTION AD

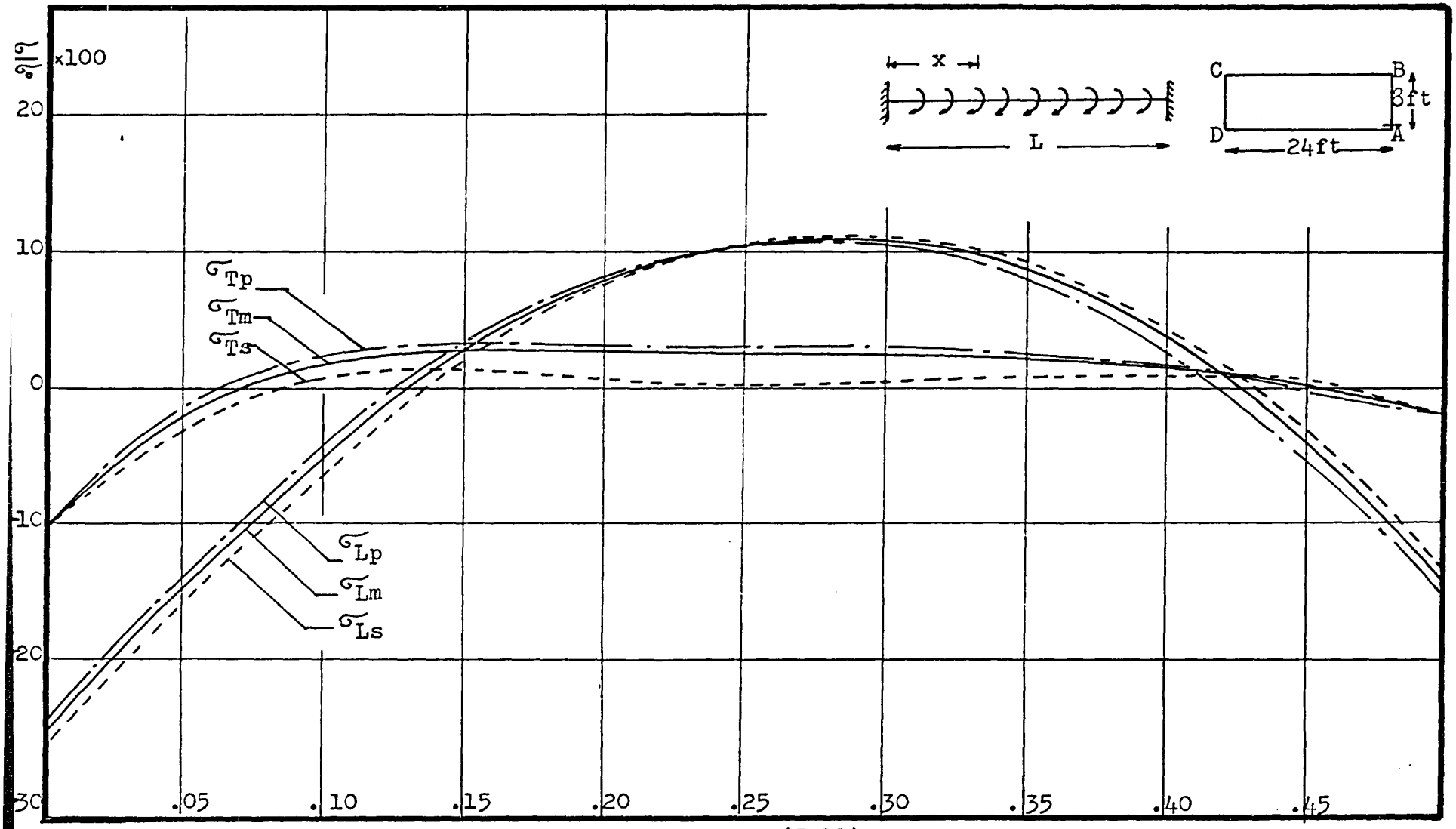

FIG. (5.11)
VARIATION OF STRESSES ALONG THE SPAN IN EXAMPLE (6)
AT SECTION AB

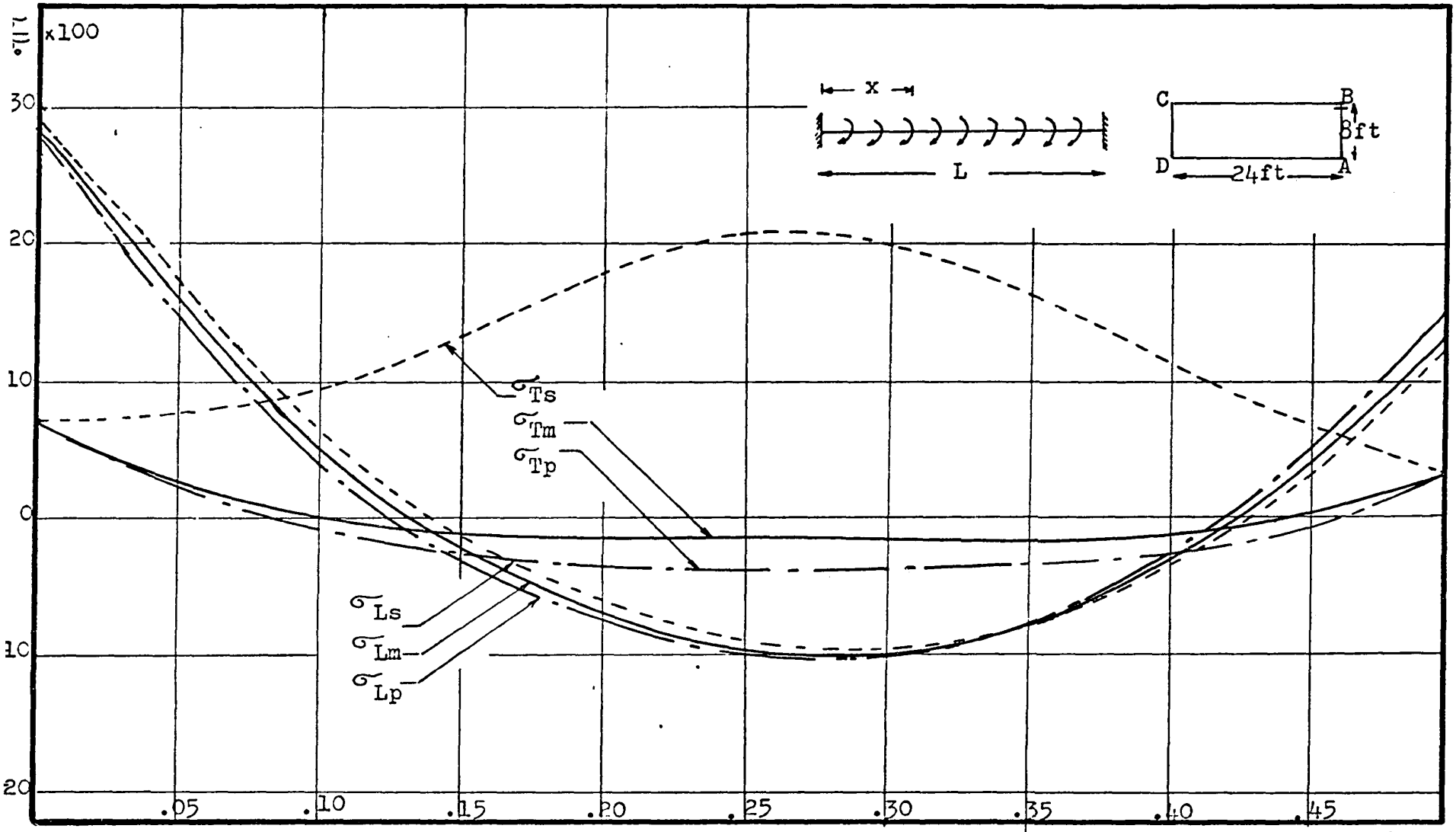

FIG. (5.12)
VARIATION OF STRESSES ALONG THE SPAN IN EXAMPLE (6)
AT SECTION BA

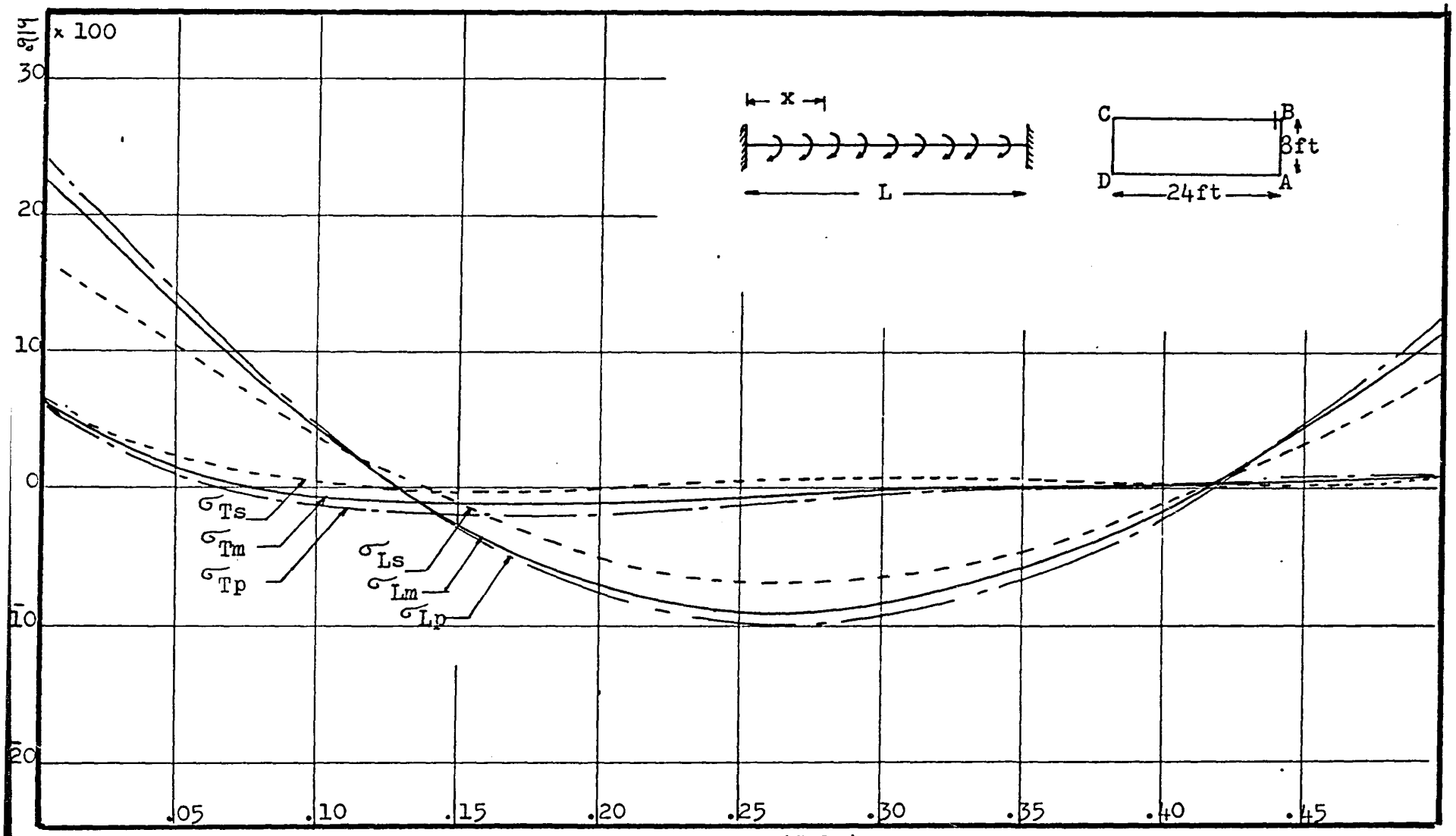

FIG. (5.13)
VARIATION OF STRESSES ALONG THE SPAN IN EXAMPLE (6)
AT SECTION BC

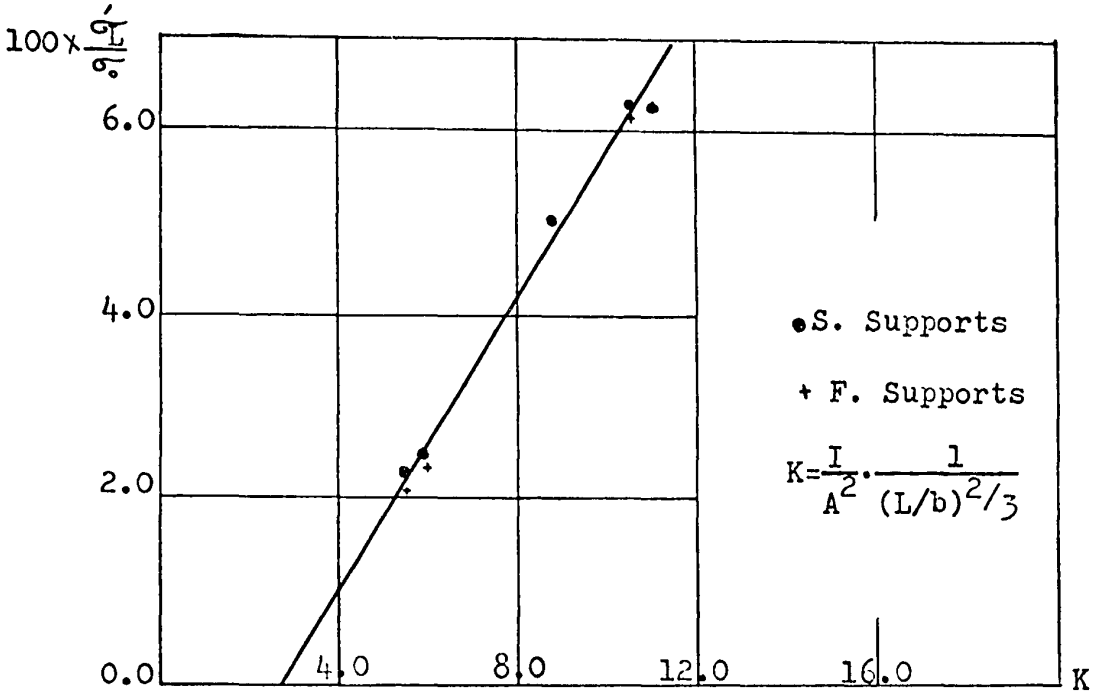

FIG. (6.1)

RELATION BETWEEN THE PARAMETER "K" AND THE PERCENTAGE RATIO OF σ'_L/σ_0 OBTAINED FROM THE EXAMPLES STUDIED

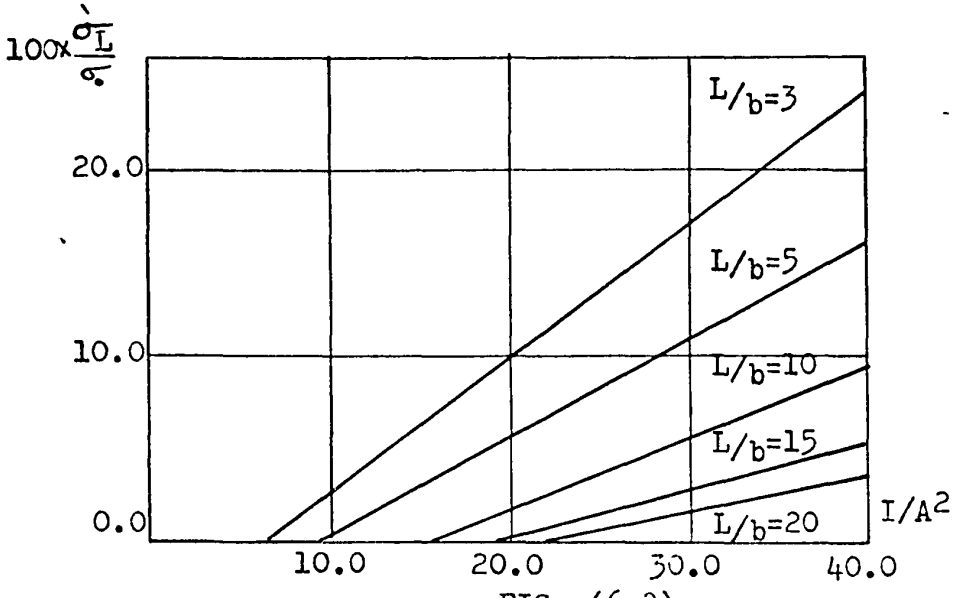

FIG. (6.2)

RELATION BETWEEN THE PERCENTAGE RATIO OF σ'_L/σ_0 AND I/A^2 FOR VARIOUS VALUES OF L/b

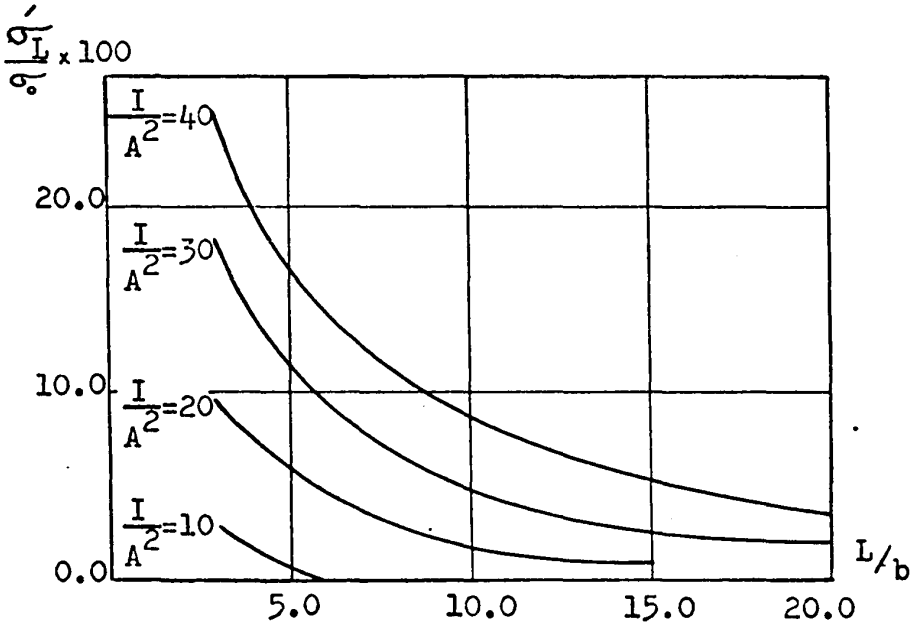

FIG. (6.3)

RELATION BETWEEN THE PERCENTAGE RATIO OF σ'_L/σ_o AND L/b FOR VARIOUS VALUES OF I/A^2

Macro-flow chart showing the integration of the programs used to analyse box girder bridges.

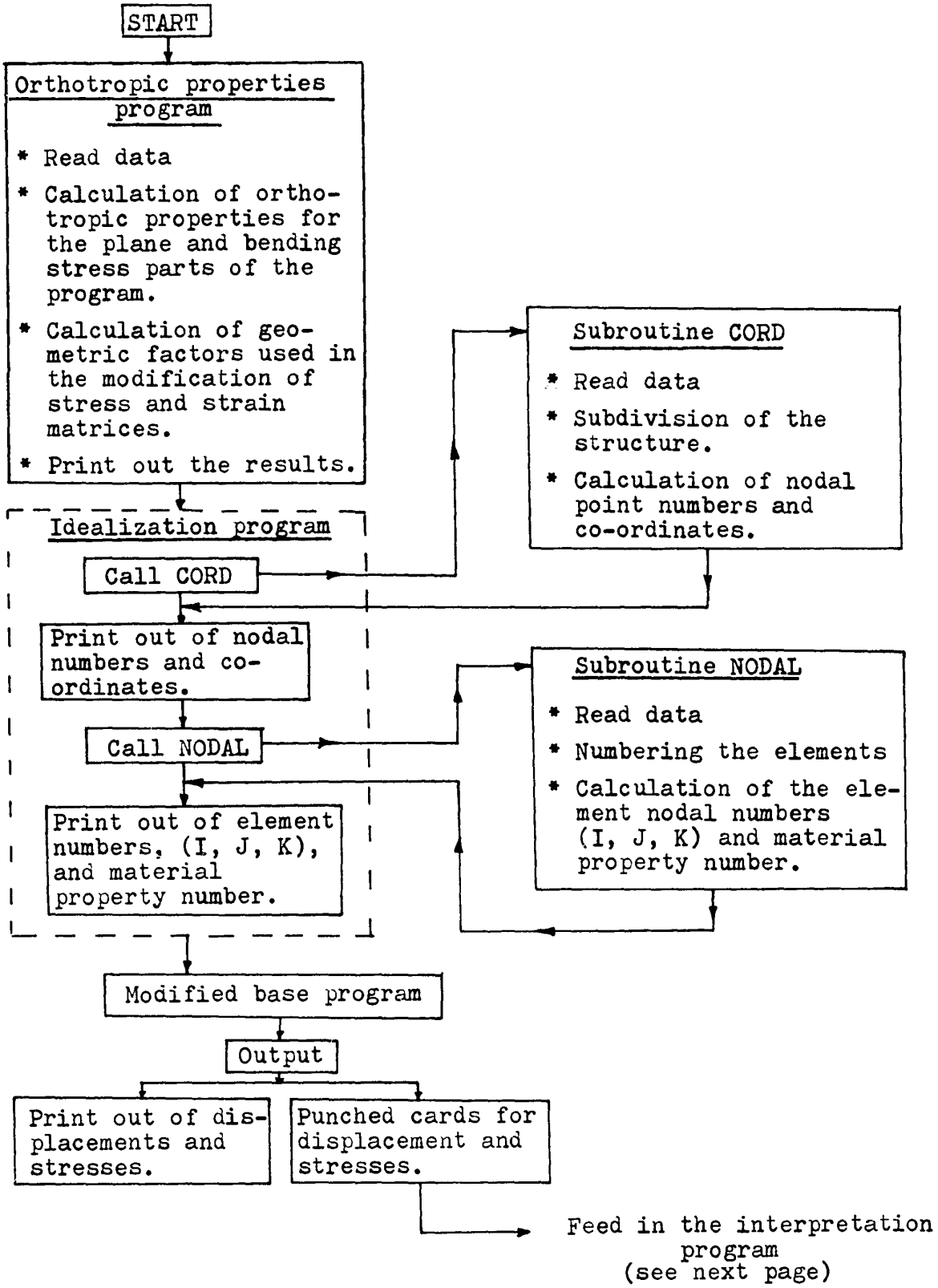

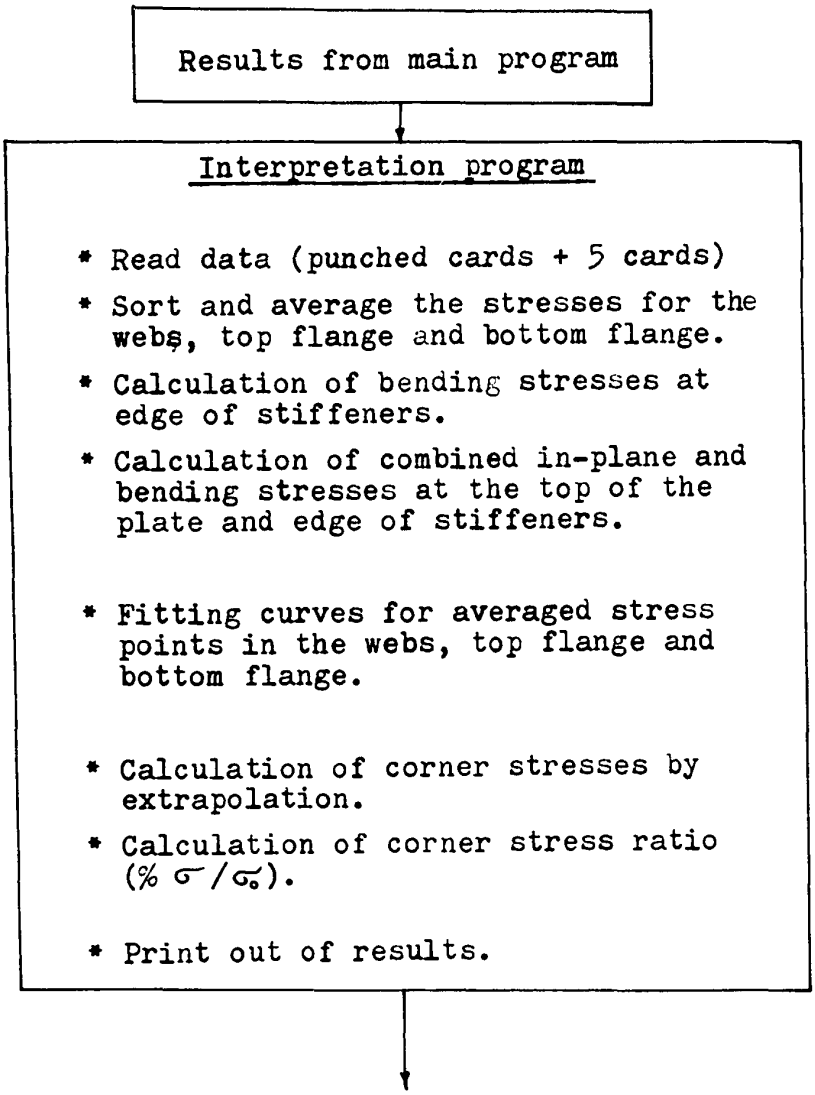

Drawing of stress distribution curves.

Appendix B

Comparison between 3-D finite element method and other theories in the solution of shear lag problem.

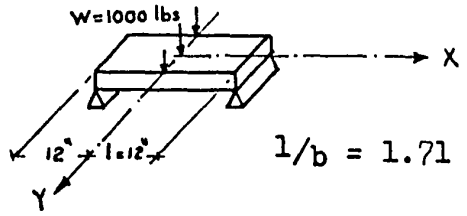

——— Orthotropic plate theory. △ Experimental results.

– – – – Finite elements (Pl.Str.) ⊗ 3-D finite elements.

—.— Stiffener-sheet theory.

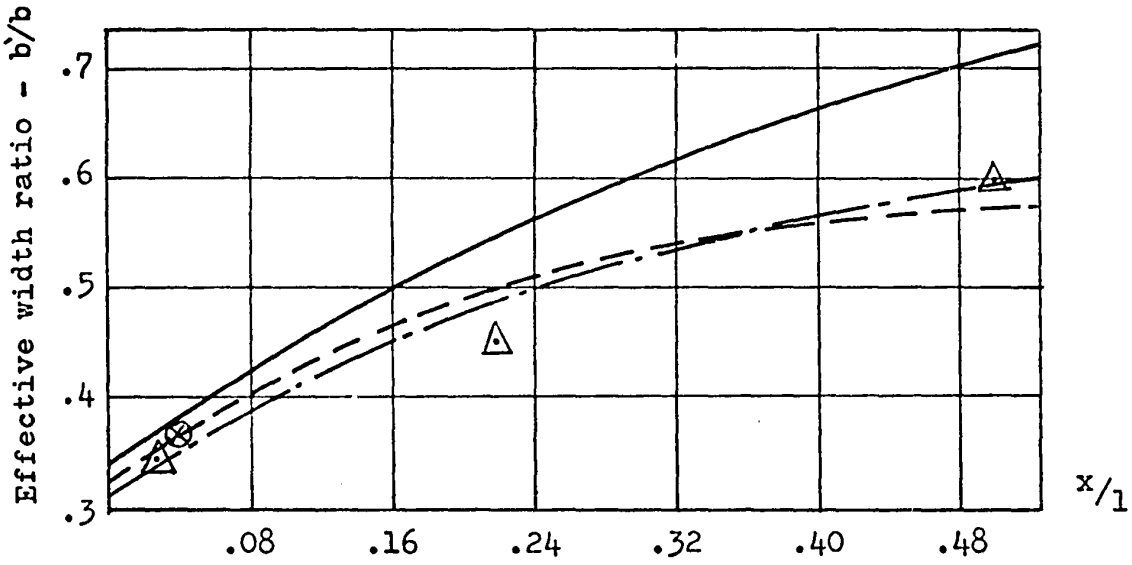

LARGE STIFFENERS

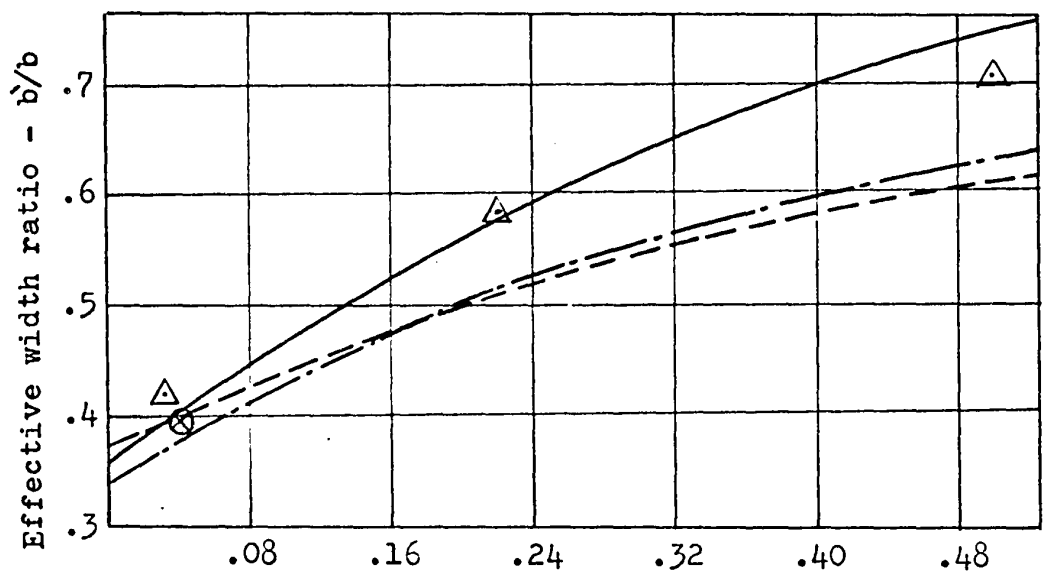

SMALL STIFFENERS

APPENDIX "C"

DESIGN EXAMPLE OF BOX GIRDER BRIDGE

Span = 200 ft Width = 24 ft Depth = 8 ft

End conditions: Simply supported

Material : A-36 Steel E = 29,000 ksi ν = 0.30 f_y = 36 ksi

Live load : Standard ASSHO H 20-44

DESIGN PROCEDURE

(A) DESIGN OF THE DECK: The procedure and notations given by AISC manual (Ref. 41) are applied here.

(A.1) CHOICE OF DECK PLATE THICKNESS

Rib spacing = 12 in Design pressure for 12,000 lbs wheel = P = 59 psi

The deck plate thickness $t_p \geqslant 0.007 \times 12 \times \sqrt[3]{59} = 0.328$ in

Choose t_p = 3/8 in

Spacing of cross beams is chosen = 5 ft.

(A.2) SECTION PROPERTIES

(A.2.1) LONGITUDINAL RIBS

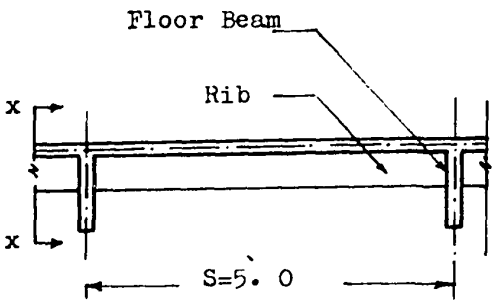

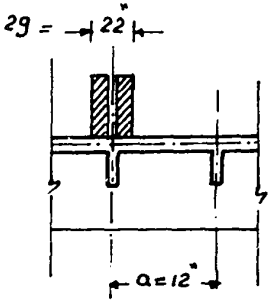

Sec. (x-x)

Wheel width = $2g = 22"$

$\frac{2g}{a} = \frac{22}{12} = 1.83$

Using chart (2) case 1

$\therefore$ Effective rib spacing = $a_0^* = (\frac{a^*_0}{a}) \cdot a = 17.6"$

Effective rib span = $S_1 = 0.7\ S = 42.0"$

Intering chart (1) with $\frac{a^*_0}{S_1} = \frac{17.6}{42} = 0.42$ the effective width of the deck acting

with the rib = $0.8 \times 17.6 = 14.0"$

Consider a rib of dimensions $8.5" \times 0.5"$ (Fig. C-1)

$y` = 1.982"$ $y = 2.17"$

Moment of inertia $I`_R = 72.0\ in^4$

Section modulus at top of plate = $S`_{RT} = 33.4\ in^3$

Section modulus at bottom of rib = $S`_{RB} = 10.72\ in^3$

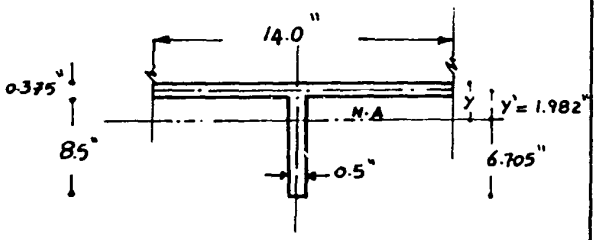

Fig. (C-1)

The values of I_R and S_R are recalculated for the computation of the effect of floor flexibility by considering $a = 1.1\,a = 13.2"$.

The corresponding values are $I_R = 70.7\ in^4$, $S_{RT} = 31.5\ in^3$ $S_{RB} = 10.7\ in^3$

(A.2.2) FLOOR BEAMS

Assuming the effective spacing $S^* = S = 60"$ and entering Chart (1) with

$\frac{S^*}{l} = \frac{60}{24 \times 12} = 0.193$ we get the effective width of plate acting with the floor beam

$S_e = 60"$

Consider the cross section shown in (Fig. C-2)

$y' = 3.94"$

Moment of inertia $I_F = 1620\ in^4$

Section modulus at top of plate $I_{FT} = 394\ in^3$

Section modulus at bottom of beam = $I_{FB} = 97\ in^3$

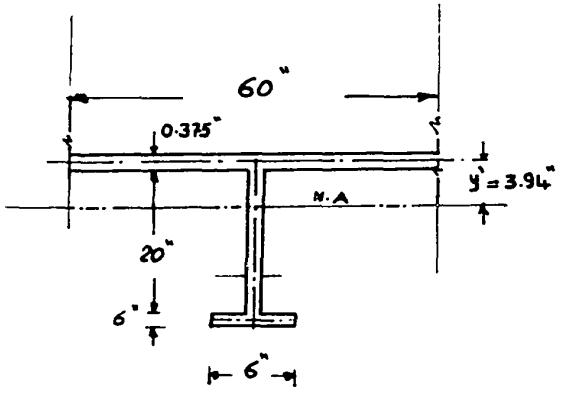

Fig. (C-2)

(A.3) RELATIVE RIGIDITY COEFFICIENTS

$$\gamma = \frac{l^4 \cdot I_R}{a \cdot S^3 \cdot \pi^4 \cdot I_F} = \frac{(24\times12)^4\ 70.7}{12(60)^3 \times \pi^4 \times 1620} = 1.19$$

$$\gamma' = \frac{t_p^3}{10.92\ I'_R} \cdot \frac{S_2^4}{a^3 \pi^4} = \frac{(0.375)^3}{10.92\times72} \cdot \frac{(0.81\times60)^4}{(12)^3 \cdot \pi^4} = 0.0024$$

Since γ' is less than 0.006 no correction of the effect of deck plate rigiuity is needed in the calculation of bending moment.

(A.4) ELASTIC STABILITY OF RIBS

$\frac{t_R}{h} = \frac{0.5}{8.5} = \frac{1}{17}$ K = 1.0 (See the manual, Appendix II, II.1.3.1.1)

f_i = Ideal buckling stress = $(26{,}200) \times (1.0)(\frac{1}{17})^2$ = 90.7 ksi

Since $f_i > f_y$ the critical buckling stress can be found by entering Curve 1, Fig. II.2

(Manual) with $f_y/f_i = 36/90.7 = 0.4$

$\therefore f_{cr}/f_y = 0.96$ $\quad f_{cr} = 0.96 \times 36 = 34.6$ ksi with factor of safety = 1.5

The allowable comp. stress = 34.6/1.5 = 23.10 ksi

The actual max. comp. stress = 17.03 ksi (see Table C.1) O.K

(A.5) DESIGN BY CHARTS FOR AASHO LOADS

Following the same procedure described in Section 11.2.3 of the manual, the results are found as follows:

(A.5.1) BENDING MOMENT IN A SYSTEM WITH RIGID FLOOR BEAMS

(A.5.1.1) LIVE LOAD MOMENT IN RIBS

At midspan	Loading "a"	$M_{RC} = 7.10$ K.ft
	Loading "a_1"	$M_{RC} = 7.10$ K.ft
At support	Loading "d"	$M_{RS} = -5.55$ K.ft

(A.5.1.2) LIVE LOAD MOMENT IN FLOOR BEAMS

The max. bending are found to be:

Loading "A" M = 308 K.ft

Loading "B" M = 324 K.ft

(A.5.2) DEAD LOAD MOMENTS

Ribs

Weight of:

2" Asphalt	=	20.0
3/8" Deck plate	=	15.3
½"x8½" Ribs	=	11.8
TOTAL	=	47.1 Plf

MOMENTS IN RIB

MIDSPAN MOMENT = $\frac{0.0471 \times 25}{24}$ = 0.05 K.ft

SUPPORT MOMENT = $\frac{0.0471 \times 25}{12}$ = 0.10 K.ft

Floor Beams

Weight of:

Asphalt, plate and ribs	=	235.5 Plf
Floor beam	=	32.5 Plf
TOTAL	=	268.0 Plf

Span Moment = $\frac{0.268 \times 24^2}{8}$ = 19.20 K.ft

(A.5.3) EFFECT OF FLOOR BEAM FLEXIBILITY

(A.5.3.1) ADDITIONAL BENDING MOMENT IN RIBS

(a) Positive moment increment:

Loading "a" $\Delta M_{RC} = 1.92$ K.ft

"a_1" $\Delta M_{RC} = 1.00$ K.ft

"h" $\Delta M_{RC} = 2.70$ K.ft

→ Total moment increment is for loading (a+h)
$\Delta M_{RC} = \underline{4.62}$ K.ft

(b) Negative moment reduction:

The reduction is computed for loading "d" and using Chart 24

$$\Delta M_{RS} = \underline{2.15} \text{ K.ft}$$

(A.5.3.2) BENDING MOMENT RELIEF IN FLOOR BEAMS

Using Charts 30 and 32 for $\gamma = 1.19$ $S = 5.0$ Loading "B" , the reduction is found to be $= \Delta M_F = \underline{210}$ K.ft

(A.6) STRESSES IN THE DECK WHEN CONSIDERED AS THE FLANGE OF THE MAIN GIRDER

The max. stresses in this case will be obtained in Section (B.4).

(B) DESIGN OF MAIN BOX GIRDER (Fig. A.3)

The thickness of the web plate $t = \frac{D\sqrt{f_b}}{23000}$ (ASSHO, Clause 1.7.71), with depth of web $D = 96$ in , and assuming compressive bending stress $\simeq$ 16.0 ksi, the web thickness $t = \frac{1}{2}$ in.

The bottom flange thickness is assumed $\frac{1}{2}$".

(B.1) LOADING

(a) LIVE LOAD: The standard ASSHO loading HS.20-44

(b) DEAD LOAD

2" asphalt	=	480 plf
3/8" deck plate	=	366 "
longitudinal ribs	=	333 "
floor beams	=	149 "
½" web plates	=	325 "
½" bottom flange	=	490 "
diaphragms and web stiffeners,..	=	107 "
Total D.L	=	2250 plf

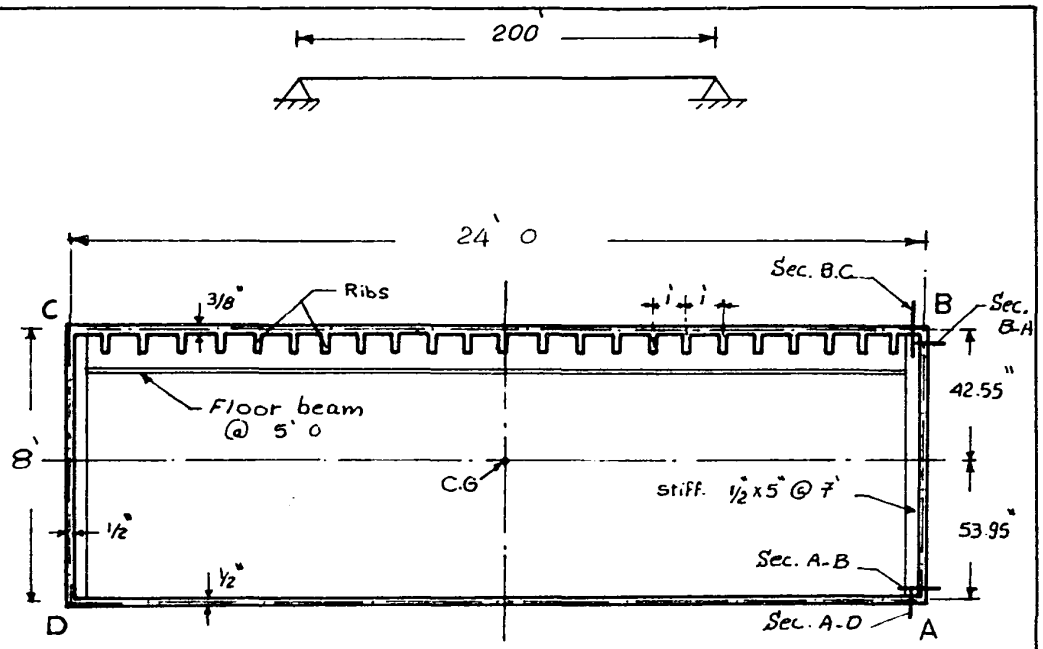

Fig. (C.3)

(B.2) MAXIMUM BENDING MOMENTS

The max. B.M. is at midspan

(a) B.M. due to D.L.: $M_{D.L} = \frac{2.25 \times (200)^2}{8} = \underline{11250}$ K.ft

(b) B.M. due to L.L.: Impact factor $= \frac{50}{L + 125} = \frac{50}{200 + 125} + 100 = 1.155$

From ASSHO Page 299, For L = 200 and using impact factor = 1.155 the bending moment

due to L.L $M_{L.L} = 4100 \times 2 \times 1.155 = \underline{9500}$ K.ft

DESIGN BENDING MOMENT $M = M_{D.L} + M_{L.L} = 11250 + 9500 = \underline{20750}$ K.ft

(B.3) MAXIMUM SHEARING FORCE:

The max. S.F. is at the supports

(a) Max. S.F. due to D.L. : $S_{D.L} = \frac{2.25 \times 200}{2} = \underline{225}$ KIP

(b) Max. S.F. due to L.L. : (See ASSHO page 299), for span = 200' and impact factor = 1.155 $S_{L.L} = 90 \times 2 \times 1.155 = \underline{205}$ KIP

Design shearing force for each web = $\frac{225+205}{2} = \underline{215}$ KIP

(B.4) SECTION PROPERTIES

Area of the section = 446 in^2

Distance from top flange to C.G. of section = 42.55 in)
Distance from bottom flange to C.G. of section = 53.95 in) (See Fig. C.3)

Moment of inertia of the section = 839300 in^4

(B.5) STRESSES DUE TO MAIN SYSTEM

Stress at top of deck plate $= -\frac{20750 \times 12 \times 42.55}{839300} = -\underline{12.70}$ KSI

Stress at bottom of deck plate $= -\frac{20750 \times 12 \times 34.125}{839300} = -\underline{10.00}$ KSI

Stress at bottom flange $= +\frac{20750 \times 12 \times 53.95}{839300} = +\underline{16.10}$ KSI

Allowable stress = 20.0 KSI

(C) SUMMARY OF MOMENTS AND STRESSES IN TOP FLANGE

The results obtained in Section A and B are listed in the following Table. It can be seen that the stress did not exceed f_{all} = 20.0 KSI.

TABLE C.1

Location		Loading	Bending Moment K.ft		Section Modulus in^3		Stress KSI		
					Top	Bottom	Top	Bottom	
Ribs	(1)	L.L. Rigid System		7.10	33.4	10.72	- 2.55	7.90	
	(2)	L.L. Effect of Floor Flexibility	4.62						
	(3)	D.L. Superimposed	0.05						
	(4)	Total (2) + (3)	4.67		31.5	10.70	- 1.78	5.20	
	(5)	Total System (A)					- 4.33	13.10	
	(6)	Total System (B)					-12.70	-10.00	
	(7)	Total Stress					-17.03		o.k.
Floor Beams	(1)	D.L.		19.20	394.0	97.00			
	(2)	L.L. Rigid Floor		324.00					
	(3)	L.L. Effect of Floor Flexibility		-210.00					
		TOTAL		133.20			- 4.15	16.50	o.k.

(D) DESIGN OF WEB PLATE

The avarage shear stress $f_v = \frac{215000}{96 \times 0.5} = 4450$ psi

The distance between transverse stiff. $d = \frac{11{,}000\ t}{\sqrt{f_v}} = \frac{11000 \times 0.5}{\sqrt{4450}} = 83.9"$

The dimensions of the transverse stiffeners are chosen 5.0" x 0.5" and spaced every 7' 0.

(These dimensions satisfy the requirements of AASHO (Clause 1.7.72)).

REFERENCES

1	Oden, J.T.	"Mechanics of Elastic Structures", 1967 McGraw Hill Book Co.
2	Ebner, H.	"Torsional Stress in Box Beams with Closed Sections Partially Restrained against Warping" NACA TM744, 1934.
3	Ebner, H. & Köller, H.	"Calculation of Load Distribution in Stiffened Cylindrical Shells" NACA TM866, 1938.
4	Umansky, A.A.	"Bending and Torsion of Thin-Walled Aircraft Structures" Oborongiz, Moscow, 1939.
5	Karman, Th.V. & Christensen, N.B.	"Methods of Analysis for Torsion with Variable Twist" Journal of Aeronautical Science, 1944, P. 110.
6	Karman, Th.V. & Chien, W.Z.	"Torsion with Variable Twist" Journal of Aeronautical Science, 1946, P. 503.
7	Adadurov, R.A.	"Strain and Deformations in a Cylindrical Shell Stiffened by Transverse Membranes" Doklady Akad. Nauk SSSR, Vol. 62, No. 2, P. 183.
8	Benscotter, S.U.	"A Theory of Torsion Bending in Multicell Beams" Journal of Applied Mechanics, 1954, P. 25.
9	Umansky, A.A.	"Chapter IV in the Handbook (Mashines-toyenye)" Vol. 1, Moscow, 1948, P. 347.
10	Benscotter, S.U.	"Secondary Stresses in Thin-Walled Beams with Closed Cross-Sections" NACA TN 2529, 1951.
11	Dshanelidze, G.J. & Panovko, J.G.	"Statics of Elastic Thin-Walled Members" GTTL Moscow, 1948.
12	Heilig, R.	"Beitrag zur Theorie der Kastenträger Beliebiger Querschnittsform" Stahlbau, 1962, No. 4, P. 128.

13	Dabrowski, R.	"Torsion Bending of Thin-Walled Members with Non-Deformable Closed Cross Section" Report of the School of Engineering, Columbia University, Sept. 1963.
14	Reissner, E.	"Neuere Probleme aus der Flugzeugstatik" Zeitschrift f. Flugtechnik u. Motorluftfahrt, 1962, P. 384; 1927, P. 153.
15	Ebner, H.	"Die Beanspruchung Dünnwandiger Kastenträger auf Drillung bei behinderter Querschnittswölbung z. Flugtech. Motorluft, 1933, 24 (24), 684-692.
16	Argyris, J.H.	"Energy Theorems and Structural Analysis Part I and II" Butterworths, London, 1960.
17	Resenger, F.	"Der Dünnwandige Kastenträger" Stahlbau-Verlag, Köln, 1959.
18	Richmund, B.	"Twisting of Thin-Walled Box Girders" Proc. Instn. Civ. Engrs., 1966, 33. (April) 659-675.
19	Dalton, D.C. & Richmond, B.	"Twisting of Thin-Walled Box Girders of Trapezoidal Cross Section" Proc. Instn. Civ. Engrs. January 1968.
20	Wlassow, W.S.	"Raschet Tonkostennikh Prismaticheskikh Obolochek, Prikladga Matamatika i Mekhanika, 8, 5, (1946) Amerikanische Übersetzung. Computation of Thin-Walled Prismatic Shells, NACA TM1234 (1969), S. 1-51.
21	Björklund, A.	"Beräkning av Symmetrisk Ladbalk Utsatt för Vridning" Unveröffentlichter Interner Bericht Nr. T-16 Staatliche Wasserkraftverwaltung, Stockholm, 1959.
22	Goldberg, J.E. & Leve, M.L.	"Theory of Prismatic Folded Plates Structures" IABSE, Zürich, Switzerland, No. 87, 1957, P.P. 59 - 86.
23	De Fries-Skene & Scordelis, A.C.	"Direct Stiffness Solution for Folded Plates", Journal of the Structural Division, Asce, Vol. 90, No. ST 4. Proc. Paper 3994, August 1966, PP. 15. 47.

24 Wright, R.N. Abdel-Samad, S.R. & Robinson, A.R. "BEF Analogy for Analysis of Box Girders" Journal of the Structural Division, Asce., Vol. 96, No. ST 4, Proc. Paper 5394, August 1967, P. 165.

25 Abdel-Samad, S.R. "Analysis of Multicell Box Girders with Diaphragms" Thesis Presented to the University of Illinois at Urbana, Ill, in Feb. 1967, in Partial Fulfilment of the Requirements for the Degree of Doctor of Philosophy in Civil Engineering.

26 Zienkiewicz, O.E. "The Finite Element Method of Structural and Continuum Mechanics" McGraw Hill (1967).

27 Clough, R.W. & Johnson, C.P. "A Finite Element Approximation for the Analysis of Thin Shells" Int. J. Solid Structures 1968 Vol. 4 P.P. 43 to 60.

28 Clough, R.W. & Tocher, J.L. "Finite Element Stiffness Matrices for the Analysis of Plate Bending" Proc. Conf. Matrix Methods in Structural Mechanics, Airforce Institute of Technology, Ohio, October 1965.

29 Carr, A.J. "The Analysis of Three Dimensional Structures Using a High Speed Digital Computer" (Report), University of California, Department of Civil Engineering.

30 Mehrota, B.L. Mufti, A.A. & Redwood, R.G. "A Program for the Analysis of Three Dimensional Plate Structures" McGill University, Structural Mechanics Series, Report No. 5, Sept. 1968.

31 Mehrota, B.L. Mufti, A.A. "A Modified Torcher's Function for the Analysis of Three Dimensional Plate and Shell Structures" McGill University, Structural Mechanics Series, Report No. 8, November 1968.

32 Fam, A.R.M. "Finite Element Program for the Analysis of Single Cell Box Girder Bridges" Report No. 13 Structural Mechanics Series, Department of Civil Engineering and Applied Mechanics, McGill University, 1969.

33 Griencke, E. "Die Grundgleichungen für die Orthotrope Platte mit Exzentrischen Steifen" Der Stahlbau Vol. 24, 1955, P 128.

34 Klöppel, E.M. "Systematische Ableitung der Differential Gleichungen für Ebene Anisotrope Flächentragwerke" Der Stahlbau, Feb. 1960, P. 42.

35 Peck, J.E.L. "Polynomial Curve Fitting, with Constraints" University of Alberta, Calgary.

36 Clifton, Rodney J. "Analysis of Orthotropic Plate Bridges" Journal of Structural Division, ASCE, Vol. 89, No. ST5, Proc. Paper 3675, Oct., 1963, pp. 133-171.

37 Hudson, R.W. & Matlock, H. "Discrete-Element Analysis for Discontinuous Plates" Journal of Structural Division, ASCE, Oct., 1968.

38 Malcolm, D.J. "Shear Lag in Stiffened Wide Flanged Box Girders" Master Thesis, April 1969, Department of Civil Engineering, McGill University.

39 Florin, G. "Vergleich verschiedener Theorien für den auf Verdrehung beanspruchten Kastenträger ohne Querschnittsaussteifung an der Lasteinleitungsstelle an Hand eines Modellversuchs" Der Stahlbau, Feb. 1963, P. 51.

40 Scordelis, A.C. "Analysis of Simply Supported Box Girder Bridges" Report No. SESM-66-17, College of Engineering Office of Research Services, University of California, Oct. 1966.

41 AISC "Design Manual for Orthotropic Steel Plate Deck Bridges" The American Institute of Steel Construction, New York, 1963.

42 AASHO "Standard Specifications for Highway Bridges" The American Association of State Highway Officials, Washington, 1965.